SYNTHESIS, CHARACTERIZATION OF ZEOLITES AND METAL COMPLEX IMMOBILIZED MESOPOROUS ALUMINA FOR ACYLATION, ALKYLATION AND OXIDATION REACTIONS

A THESIS

SUBMITTED TO THE

UNIVERSITY OF PUNE

FOR THE DEGREE OF

DOCTOR OF PHILOSOPHY

(CHEMISTRY)

BY

VANDANA. D. CHAUBE

CATALYSIS DIVISION
NATIONAL CHEMICAL LABORATORY
PUNE- 411 008
INDIA

SEPTEMBER 2005

DEDICATED TO

MY

DADY, MUMMY, AMMA, PAPA

&

HUSBAND

DECLARATION BY RESEARCH GUIDE

Certified that the work incorporated in the thesis entitled: **"Synthesis Charaterization of Zeolites and Metal Complex Immobilized Mesoporous Alumina for Acylation, Alkylation and Oxidation Reactions",** submitted by **Mrs. V. D. Chaube,** for the Degree of ***Doctor of Philosophy,*** was carried out by the candidate under my supervision at Catalysis Division, National Chemical Laboratory, Pune 411 008, India. Material that has been obtained from other sources is duly acknowledged in the thesis.

Dr. Anand Pal Singh
(Research Supervisor)

DECLARATION BY THE CANDIDATE

I hereby declare that the thesis entitled **"Synthesis Charaterization of Zeolites and Metal Complex Immobilized Mesoporous Alumina for Acylation, Alkylation and Oxidation Reactions"**, submitted for the Degree of ***Doctor of Philosophy*** to the University of Pune, has been carried out by me at Catalysis Division, National Chemical Laboratory, Pune 411 008, India, under the supervision of **Dr. Anand Pal Singh**. The work is original and has not been submitted in part or full by me for any other degree or diploma to this or any other University.

V.D. Chaube

Acknowledgement

I wish to express deep sense of gratitude to my research supervisor, **Dr. A. P. Singh** for his valuable guidance and encouragement during the course of the present study.

I am thankful to Dr. Rajiv Kumar, Head of the Catalysis Division, Dr. S. Sivasanker, former Head of the Catalysis Division, NCL, for provoding division facilities.

I am greatful to scientific non-scientific staff members of the Catalysis Division, Centre for Material Characterization and Microanalysis for all their help in characterizing catalysts, discussion and useful suggestions.

I always had a learning inspiration from my lab mates: Sushama ,Venkatesan, Chidambaram, Shylesh , Surendran, Shrikant, Selva, Shainaz, Jino, Shanskrity and Neelu. Their co-operation, splendid suggestions and encouragement made this thesis a possible one.

I am also thankful to my numerous friends: Dr. Mukherjee, Dr. Patra, Dr. Mandal, Dr. Anirban, Amit, Senapati, Sachin, Sonu, Pranjal, Mahesh, Sharada, Priti, Raina, Dr.Rajesh Pandey, Dr.Tressa, Smitha, Surekha, Dhanshree, Kala raj, Biju, Yogesh, Samsun, for their everlasting prayer and charming company.

I am obliged to my parents, husband, brothers, sister-in-law, my friends and other family members for their love, unfailing support, tremendous patience, sacrifice and encouragement they have shown in their own way during my long period of studies. They have been a constant source of strength and inspiration for me.

Finally my thanks are due to Council of Scientific and Industrial Research, New Delhi, India for granting Senior Research Fellowship and Dr. S. Sivaram, Director, NCL, Pune for allowing me to carry out my research work and extending all possible infrastructural facilities at NCL, and permitting me to summit the present work in the form of thesis.

(Vandana. D. Chaube)

CONTENTS

Chapter 1. Introduction

Chapter 2. Synthesis modification and characterization of catalysts

Chapter 3. Acylation reactions of aromatics

Chapter 4. Alkylation reaction of benzene

Chapter 5. Mesoporous alumina and modified mesoporous alumina

Chapter 6. Summary and conclusions

LIST OF FIGURES

LIST OF TABLES

CHAPTER 1

INTRODUCTION

1.1. INTRODUCTION

Zeolites are hydrated, microporous aluminosilicates which are constructed from TO_4 tetrahedral (T= tetrahedral atom, e.g., Si, Al); each apical oxygen is shared with an adjacent tetrahedra. The crystallographic unit cell of the zeolites may be represented by the general formula: [1]

$$M_{x/n}\,[(AlO_2)_x\,(SiO_2)y]\,zH_2O$$

Consequently the crystalline framework has net negative charge due the presence of alumina tetrahedral, which must be compensated by associated cations, e.g., Na^+, NH_4^+ K^+, Ca^{2+}, H^+ etc. z is the number of the water molecules and x + y represents total number of tetrahedral in the unit cell of zeolites. In general, the ratio ($y/x > 1$) controls the acidity and to a lesser extent, the morphology of zeolites.

1.2. CLASSIFICATIONS AND NOMENCLATURE

Several attempts have been made to classify families of zeolites on the basis of their morphological characteristics [1,4], crystal structure [1,2,5], chemical composition [1,2,6], effective pore diameter [1,3,7] and natural occurrence [1,2]. On the basis of the morphology, zeolites are classified as fibrous, lamellar and those having framework structure. Structural classification of zeolites has been proposed depending on the difference in secondary building units. With the addition of new synthetic and natural zeolites, they are grouped into ten classes: Analcime, Natrolite, Chabazite, Philpsite, Heulandite, Mordenite, Faujasite, Laumonite, Pentasil and Clantharate. Based on their chemical compositions, zeolites are classified as low silica zeolites, medium silica zeolites, high silica zeolites and silicates Table (1.1). Zeolites are also classified based on their pore size, namely small, medium, large and extra-large pore zeolites (Table 1.2).

TABLE 1.1. CLASSIFICATION OF ZEOLITES BASED ON CHEMICAL COMPOSITION

Group	SiO_2/Al_2O_3	Example
Low Silica	1 to 3	Sodalite, A, X
Intermediate Silica	4 to 10	L, Mordenite, Omega
High Silica	10 to several thousands	ZMS-5, EU-1
Silicalite	∞ (No Alumina)	Silicatite-1, Silicalite-2

TABLE 1.2. CLASSIFICATION OF ZEOLITES BASED ON PORE SIZE

Group	No. of Tetrahedral in pore opening	Max. free diameter (Å)	Example
Small	6 and 8	4.3	Erionite, SAPO-34, CaA
Medium	10	6.3	ZSM-5. ZSM-48
Large	12	7.5	Y, Beta, ZSM-12, Faujasites, Mordenite, $AlPO_4$-5
Extra-Large	18	~12	VPI-5, JDF-20, $AlPO_4$-8, Cloverite
Mesoporous	--	15- 100	MCM-41
Macroporous	--	>500	

The nomenclatures of the zeolites were haphazard until the IUPAC commission published certain guidelines for their nomenclature [8]. Barrer and his co-workers identified products of their synthesis as A, B, C, and so on. Scientist of Union Carbide

also used alphabetical nomenclature. Mobile Oil Corporation used Greek alphabets such as Beta, Omega. The IUPAC nomenclature system is based their framework density and number of T atom per thousand Å, irrespective of their composition, distribution of T-atoms, cell dimensions or symmetry parameters. This does not contain numbers and characters other than capital Roman letters. e.g., MFI stands for ZSM-5, MEL stands for ZSM-11, MTW stands for ZSM-12 and AEL stands for $AlPO_4$-11 structures.

1.3. SYNTHESIS OF ZEOLITES

The era of synthetic zeolites began with the pioneering work by Barrer on their synthesis and adsorption. [2] The formation of zeolites is a nucleation-controlled process occurring from inhomogeneous hydrogels in the temperature range of 348–523 K [7]. Zeolites are synthesized hyrothermally by the combination of cations (both organic and inorganic), a source of silicon, a source of aluminium and water. Silicon sources normally used include: Sodium Silicate, Silica Sol, Silica Gel, Fumed Silica and tetraethyl orthosilicate. Aluminium sources include: Sodium Aluminate, Aluminium Sulphate and Aluminium Nitrate.

The measure factors, which influence the structure of the zeolites, are hydrothermal synthesis temperature and time. The silica to alumina ratio determines the elemental framework composition of the crystalline product. Various other factors suggest OH^- concentration, water concentration, cations (both organic and inorganic) and the anion influences the synthesis. In addition, there are history-dependent factors such as aging period, stirrer, and order of the mixing which may also influence the structure of the final product. The first step in the synthesis of zeolites involves the dissolution or depolymerisation of aluminium and silicon to form aluminate and silicates anions. These

species are the brought together to form gel by the condensation and/or polymerization reactions. The different steps occurring during the crystallization process of the zeolites have been discussed in detail by Sand [9]. The stabilization of the zeolites crystals is brought about by the guest spices that occupy the channels and cavities of the aluminosilicates framework, and this species are referred to as templates [10]. The tetramethyl ammonium cation (TMA) was introduced as the first organic cation in the zeolites synthesis by Barrer and co-workers [11,12]. The large number of organic molecules used (Table 1.3) and their effects on zeolites synthesis and morphology have been discussed in several publications [13-17].

The exact role played by the template is rather complex and not yet fully understood, although it is believed that zeolites structures grow around the template thus stabilizing certain pore systems. In addition to this structure directing effect, template have roles such as a gel modifier, increasing the solubilities of different species in the gel, acting as a buffer to maintain the pH of the gel, and as a void filler to organize the water molecules [18].

1.4. PROPERTIES OF THE ZEOLITES

1.4.1. Ion exchange

Ion exchange is a function of the aluminium present in the zeolites framework. The negative charge created by each tetrahedral aluminium is balanced by cation to stabilize the zeolites framework. These charge compensating cations, usually alkali or alkaline earth metal cations, are loosely held to the framework aluminium, and they are easily exchangeable with different monovalent and multivalent cations [19,20]. The rate and the

degree of cation exchange in the zeolites depends upon several factors which includes size and charge of the cation, concentration of the exchanging solution,

TABLE 1.3. ORGANIC TEMPLATE ZEOLITE STRUCTURE RELATIONSHIPS [17]

Organic template	Structure
Tetraethylammonium (TEA)	Beta, ZSM-8, ZSM-12, ZSM-20, ZSM-25, Mordenite
Methyltriethylammonium (MTEA)	ZSM-12
Tetrapropylammonium (TPA)	ZSM-5
n-Propylamine	ZSM-5
Tetrabutylammonium (TBA)	ZSM-11
Choline	ZSM-38, ZSM-34, ZSM-43, CZH-5
TMA + TEA	ZSM-39
TMA + n-propylamine	ZSM-39, ZSM-48
Pyrrolidine	ZSM-35, ZSM-21, ZSM-23
1,2-Diaminoethane	ZSM-5, ZSM-21, ZSM-35
1,2-Diaminopropane	ZSM-5, ZSM-21
1,4-Diaminobutane	ZSM-5, ZSM-35
1,5-Diaminopentane	ZSM-5
1,6-Diaminohexane	ZSM-5
1,7-Diaminoheptane	ZSM-11
1,8-Diaminooctane	ZSM-11, ZSM-48
1,9-Diaminononane	ZSM-11
1,10-Diaminodecane	ZSM-11
DDO	ZSM-10
MDO	ZK-20
MQ	LZ-132
TQA	ZSM-18
Dihexamethylenetriamine	ZSM-30

Neopentylamine	Mordenite

temperature of the ion-exchange treatment, location of the cation in the zeolites and the structure of the zeolites.

1.4.2. Acid Properties of the Zeolites

1.4.2.1.Bronsted Acid Sites

Pure siliceous zeolites are electrically neutral. By replacing silicon (tetrahedrally co-ordinated with oxygen atoms) having a formal charge of 4^+ in the zeolites lattice with an aluminium (formal charge 3^+) a negatively charge tetrahedron is created. The negative charge is balanced by the cation either NH_4^+ or alkali cations like Na^+, K^+, H^+ ions. The protons are formally assigned as bonded to bridging oxygen of a Si-O-Al bond to form hydroxyl groups that act as a strong Bronsted acid at the solid/gas interface. The overwhelming evidence is that hydroxyls with in the zeolites channels provide the active Bronsted sites [21].

These are usually prepared via ammonium ion exchange:

$$NaZ + NH_4^+ (aq) \rightleftharpoons NH_4Z + Na^+ (aq)$$

$$NH_4Z \rightleftharpoons NH_3 (g) + HZ$$

They are also prepared via hydrolytic process involving water coordinated to polyvalent cations:

$$M(H2O)^{n+} \rightleftharpoons MOH^{(n-1)+} + H^+$$

This generates protonic sites within the zeolites. In silica rich zeolites, were acids do not destroy the structure, the hydrogen forms (HZ) can be prepared by direct exchange of Na^+ by H^+ using mineral acids. Bronsted acid sites will have acid strength, which depends on their environment, i.e. depending on chemical composition and the structure of the zeolites [22]. The local environment of the acid site in a molecular sieve is determined by the structure, i.e. the coordination of the TO_4 tetrahydra in the framework. This leads to different amount of topologically different T sites i.e. sites in the tetrahedral position. In this way, LTL zeolites would have two, MOR four MFI-twelve different T sites. [23], while FAU structures have no inequivalent T sites. These different tetrahedral positions differ in T-O-T bond angles and T-O bond length [24, 25].

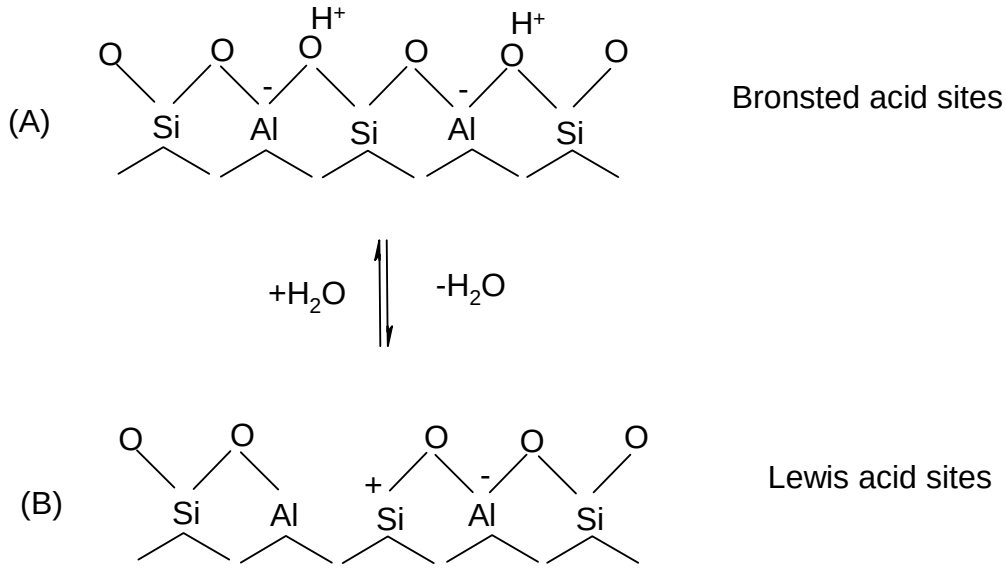

1.4.2.2. Lewis Acid Sites

Lewis acid sites (electron pair acceptor site) are related to the formation of positively charged oxide cluster or ions within the porous structure of the zeolites. These species are typically alumina or silica/alumina, formed by extraction of aluminium from

the lattice, or metal ions exchange for the protons of acid sites. The formal type of Lewis acidity i.e. aluminium oxide clusters containing alumina in octahedral or tetrahedral coordination and will usually be a stringer Lewis acid than the exchange metal cations (true Lewis acids) [26].

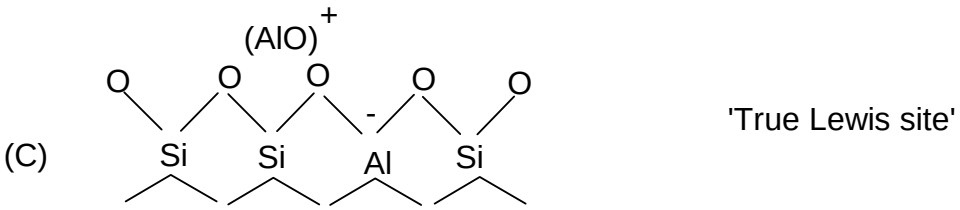

Lewis acid sites are acting also as hydride (or anion) receptors in variety of reactions.

1.4.2.3. Zeolite Beta

Zeolite beta, a high silica, large pore crystalline aluminosilicates material first synthesized by Wadlinger et al. in 1967 [29], possesses an intergrowth of two or three polymorphs having a three-dimensional system of inter connected 12-membered ring channels with pore diameter of 0.55 x 0.55 nm and 0.76 x 0.64 nm [30 a & b, 31]. Owing to its high acidity and peculiar pore system, zeolite beta receives much attention as a potential catalyst in fluid catalytic cracking [32], hydro treating [33], isobutene alkylation with 1-butene or 2-butene [34, 35], alkylation of C-8 aromatics [36 a & b], acylation of aromatics [37, 38] etc.

1.4.3. Adsorption and Diffusion

Zeolites posses uniform pores and internal channels with large void volume. Zeolites have also high surface area, which are accessible to molecules of comparable

size to diffuse through the pores. Due to the high surface area and void volume coupled with electrostatic field, zeolites act as selective adsorbents. Sorption studies of nitrogen, oxygen, water, n-hexane and other hydrocarbons give several types of information [18], which includes: void volume of the zeolites, pore size of the zeolites, degree of crystallinity, hydrophilicity/hydrophobicity and acidity. Sorption of various gases and vapors on natural and synthetic zeolites has been extensively studied by Barrer and co-workers [39-44]. Various thermodynamic parameters such as entropy, heat and free energy of sorption have also been studied by them. Sorption studies of zeolites also provide information about interactions between sorbate and sorbent [45].

Migration or diffusion of sorbed molecules through the pores and cages within the crystals plays an important role in the process of catalysis and selective adsorption/separation by the zeolites. The different aspects of diffusion in zeolites catalysis have been review by several authors [46-48]. There are three types of diffusion relevant to the zeolite system, namely molecular diffusion, Knudsen diffusion and configurational diffusion.

In molecular or bulk diffusion, the mean free path of a molecule is much smaller than the pore diameter of the zeolite and molecular collisions are more frequent than collisions with the walls of the catalyst pore. Here, the rate of molecular diffusion is independent of the pore radius. Knudsen diffusion occurs when the pore diameter of the solid is less than the mean free path of the molecule. In this case, molecules usually strike the pore wall before colliding with the second molecule. Configurational diffusion occurs when the sizes of the molecule and pores of the zeolites are comparable. A striking feature of this diffusion regime is that, very small change in the molecule to pore size

relationship induces very large changes in the diffusion coefficient, and this is the phenomenon that induces shape selectivity.

1.4.4. Shape Selectivity

The term 'shape-selective catalysis' was coined by Weisz and Frillette more than three decades ago [49]. A striking feature of the zeolites and related materials is that their pore sizes are in molecular dimensions (Fig. 1.1). The comparable sizes of the zeolite pores

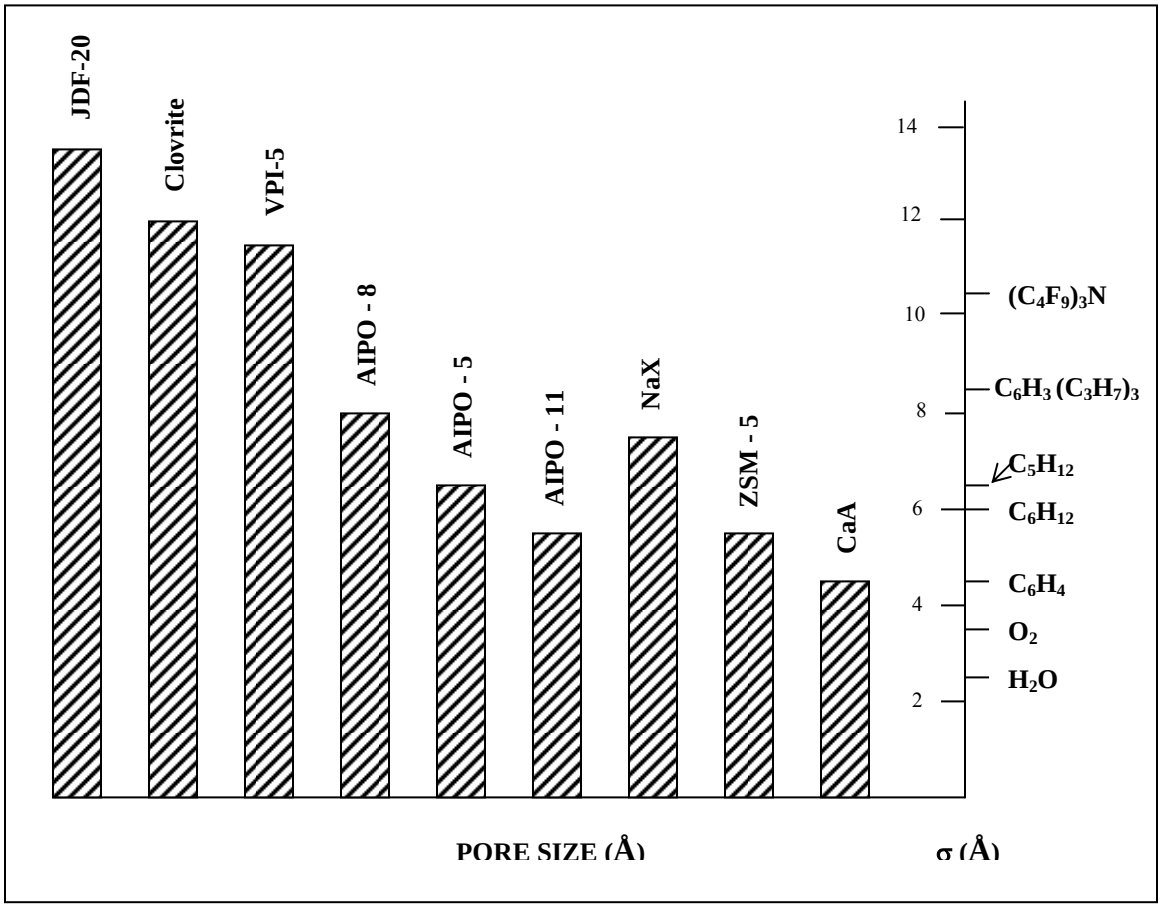

Figure 1.1. Correlation between the pore size of molecular sieves and the diameter (σ) of various molecules (Adapted from Ref. 122c)

and different organic molecules play a major role in the shape selectivity in the zeolite catalysis. The principles and applications of the shape selective catalysis have been comprehensively reviewed and critically discussed by several authors [50-57]. Shape selectivity consists of a combination of shape, size and configuration of reactants, transition states and products with dimension, geometry and tortuosity of the channels and cages of the zeolites. Csicsery [53] has categorized these shape selective effect as follows:

1.4.4.1. Reactant Selectivity

Reactant selectivity takes place when only part of the reactant molecules is small enough to diffuse through the catalyst pores. For example, due to their large size and bulky shape, highly branched C_{13} iso-parafins are prevented from entering and reacting inside the pore system of ZSM-5, whereas linear paraffins, due to the absence of steric constraints easily enters the pores and undergo reaction (Fig. 1.2 a) [54].

1.4.4.2. Product Selectivity

Product selectivity occurs when zeolite pores show 'molecular sieving effect', where some of the products formed within the pore are too bulky to diffuse out as observed products. This effect is demonstrated in fig.1.2 b [54]. Inside the small pore zeolite Linda A, isomerization of a n-C_6 paraffin to a branched isomer can occur with in the ~11.4- Å α cage, but egress of the iso product through the 4.1- Å 8-ring window is prevented due to its larger dimensions. Faster diffusion of para-xylene compared to its ortho- and meta- analogs from the pore of ZSM-5 is another example of the product selectivity.

1.4.4.3. Restricted Transition-State Selectivity

Restricted transition-state selectivity occurs when certain reactions are prevented because some transition state in the reaction pathway requires more space than is available inside the catalyst pore. An example of this type of selectivity is the reaction of 1-methyl-2-ethylbenzene over mordenite at 477-588 K [58]. Formation of unsymmetrical 1,3,5-isomer is significantly hindered because of spatial limitations on the formation of the diarylmethane intermediate (Fig.1.2 c). Other less common terminology for molecular shape selectivity includes the concentration effect [59], molecular traffic control [60], molecular circulation [61] and energy gradient selectivity [62].

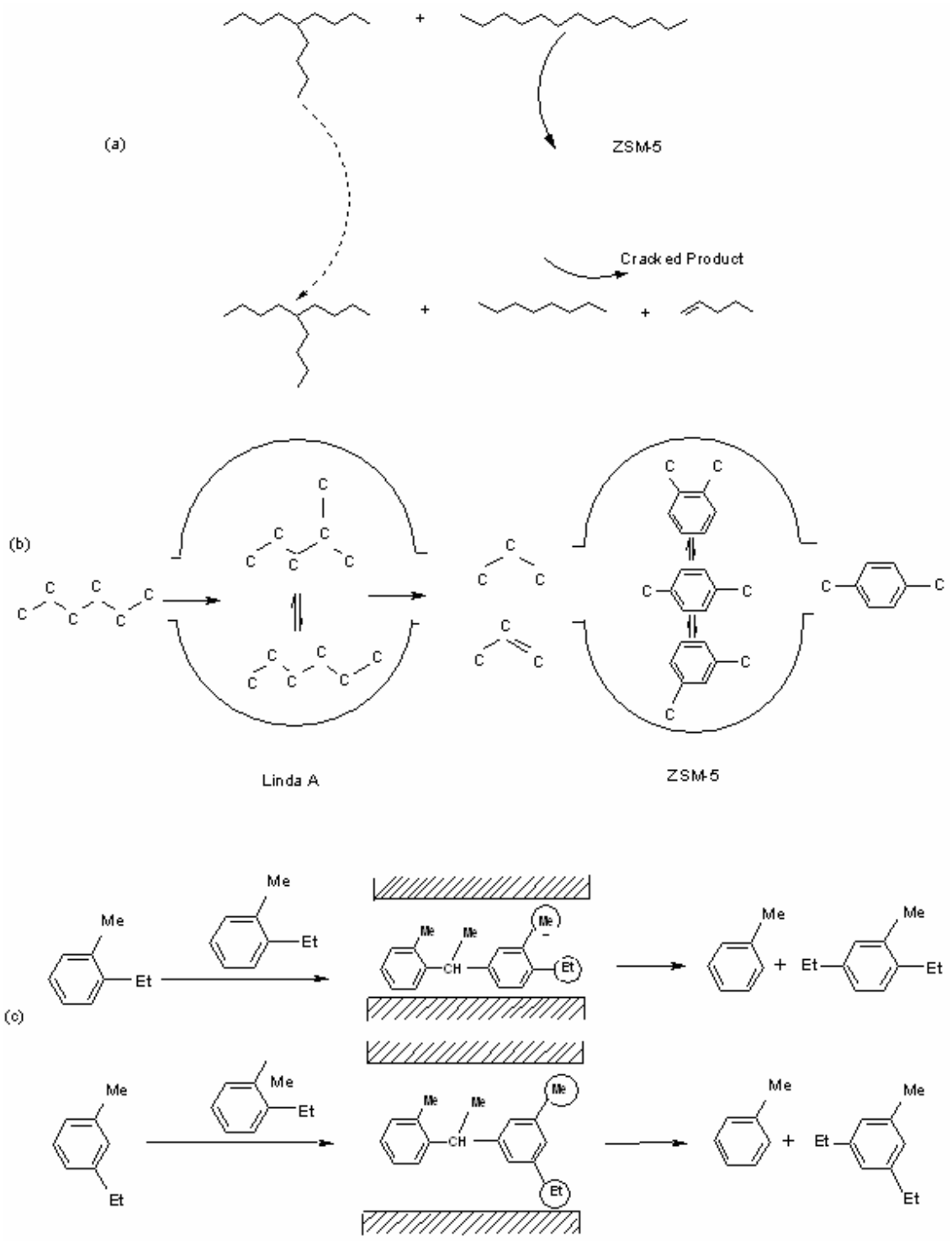

Figure 1.2. Shape Selectivity in Zeolites; (a) Reactant Selectivity, (b) Product Selectivity, and (c) Transition-State Selectivity

1.5. INTRODUCTION TO MESOPOROUS MATERIALS

An ever-growing interest in expanding the pore sizes of the zeolites type materials from micropore region to mesopores (pore size >20 Å) region in response to the increasing demand in both industrial and fundamental studies. Examples are treating heavy feeds, separating and selective synthesizing large molecules and intra zeolites fabricating technology [63-64]. Zeo types materials typically having a surface area of ca. >700 m^2 g^{-1}, which are not truly crystalline like microporous zeolites but because of rapid growth of the research on those materials make them to be classified as meso pore zeolites, with the majority of this surface inside the pores and accessible only through apertures of well defined dimensions [65]. In 1992, researchers at Mobil Corporation discovered the M41S family of silicate/aluminosilicates. Mesoporous molecular sieves with its exceptionally large uniform pore structures resulted in a worldwide resurgence in this area [65-67]. Three different mesophases in this family have been identified, i.e. lamellar [68], hexagonal [67], and cubic phases [69], in which the hexagonal mesophase, MCM-41, possesses highly regular arrays of uniform-sized channels whose diameters are in the range of 15-100 Å depending on the templates used, the addition of auxiliary organic compounds (co-template) and the reaction parameters. The pores of this novel material are nearly as regular, yet considerably larger than these present in crystalline materials such as zeolites, this offering new opportunity for applications in heterogeneous catalysis [70] and advanced composition materials [71]. Accordingly, MCM-41 has been investigated extensively because the other members in this family are either thermally unstable or difficult to obtain.

The purpose and advantages of synthesizing mesoporous materials are as follows:

1. To overcome the diffusional constraints as obtained with zeolites.
2. Very high surface area (>1000 m^2/g) and pore size distribution (20-100 Å).

3. Novel host materials for guest species (i.e. heterogenization of homogeneous species or metal complexes on the inner wall surfaces)
4. Easier to monitor the changes made with active species via surface area and pore size distribution (PSD) experiments.

1.6. SYNTHESIS AND MECHANISM OF FORMATION OF MESOPOROUS MATERIALS

The concept concerning M41S formation has been formulated based on the studies involving silica (or alumino-silicate) cationic surfactant systems. Rod-like micelles have been known to form in the presence of electrolytes. The M41S materials appear to be inorganic oxide congeners to lyotropic liquid crystals (LLC) formed by the surfactants in aqueous systems. The original proposed mechanistic pathways are illustrated in Fig.1.3 [67].

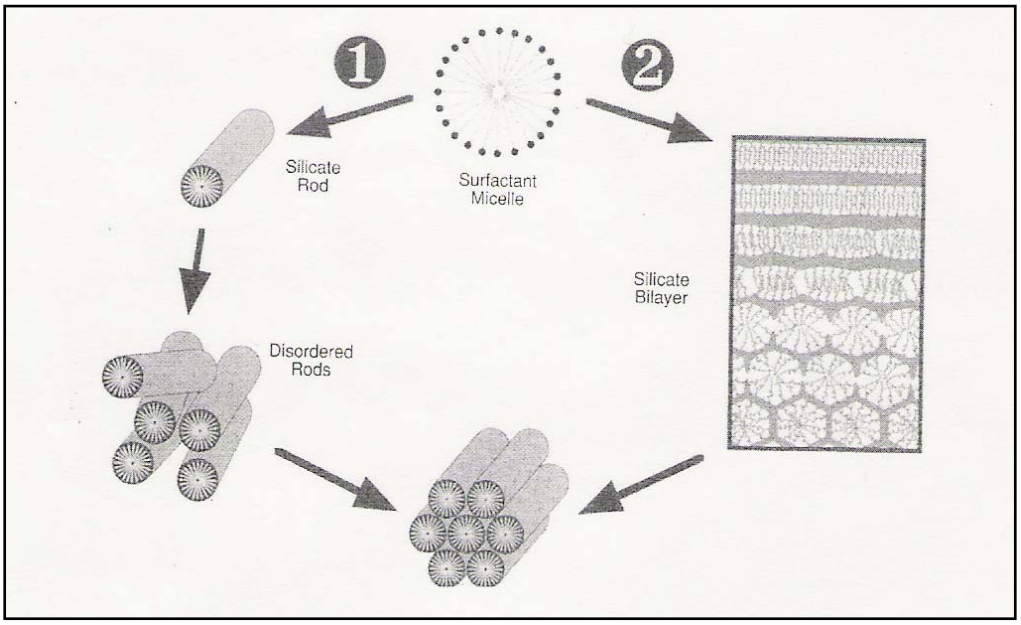

Figure 1.3 Mechanistic pathways by (1) stacking of silicated surfactant rods and (2) via formation of an initial lamellar intermediate

Under this general term, two possibilities were envisioned. The first one invoked pre-existence of surfactant aggregated or liquid crystal phase in the surfactant precursor solution. Subsequently, formation of M41S silica framework occurred due to migration and polymerization of silicate ions into the aqueous region. The second alternative pathway postulated self-assembly of liquid crystal like structure due to mutual interaction between dissolved silica and surfactant species.

The second mechanism has been proposed based on the observance of a layered silica/surfactant phase upon mixing of the reaction. In this mechanism Stucky et.al., carried out more detailed analysis of this phenomenon and described as cooperative mode of synthesis of mesostructure that involved the following three processes: multidentate binding of silicate oligomer to the cationic surfactant, preferred silicate polymerization in the interfacial region, and charge density matching between the surfactant and the silicate. This reasoning led to a two-step synthesis path way to M41S: precipitation of silica-surfactant and silica polymerization [72]. The mechanism pathway is also shown in Fig 1.3. Polymerization comprises three processes, which proceed simultaneously. First, silicate anion bound to the surface of micelles polymerizes to form polyanions (intermicellar polymerization). Second, micelles party covered with silicate poly anions are gradually arranged into a regular hexagonal array through intermicellar silicate condensation. Free silicate anions or polyanions provide further building material for the formation of the silica walls between the micelles. Davis et.al. identified silica-clad rod like aggregates in the synthesis mixture by ^{14}N NMR. The hexagonal MCM-41 could thus arise packing of

the silicate-surfactant rods [67]. The synthesis parameters (e.g. temperature, pH, compositions of reaction gel) are found to exert key influence on the surfactant behavior and the distribution of silicate species.

The formation of these materials can be viewed as the surface chemistry between the surfactant and inorganic specie (Fig1.4). The concept of synthesized mesoporous material by exploiting surface properties has been expanded from original positive surfactant and anionic silicate. These include positive inorganic oxide and negative surfactant, ionic inorganic species with similarly charged surfactant, which is medicated by counter ions of opposite charges, as well as neutral surfactant [73].

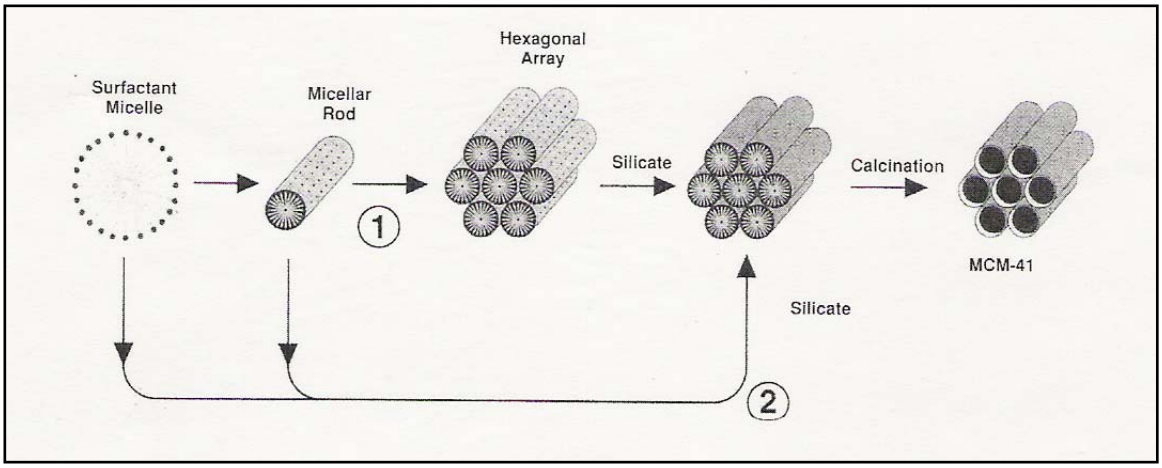

Figure 1.4 Liquid crystal template mechanism for the formation of (MCM-41).

1.7. ORGANO FUNCTIONALIZED MESOPOROUS MATERIALS

The mesoporous MCM-41 materials add a new dimension in the design of hybrid materials due to their abundant surface silanol sites and variable pore diameters. Grafting of functional organosilanes by using surface hydroxyl groups as anchor points has been widely used in the field of catalysis. Important application of these modified and functionalized systems is in heterogeneous catalysis and photocatalysis involving bulky

molecules. Other potential application includes ion exchange and separations, removal of heavy metals, chromatography, stabilization of quantum wires, stabilization of dyes, and polymer composites [74, 75]. The introduction of functional organic groups is usually performed through attachment of silane-coupling agents to mesoporous walls of previously synthesized and calcined materials. The functional group is either directly incorporated in the silane-coupling agent or it is grafted onto it in a second or further reaction step. Co-condensation of reactive species during the mesoporous synthesis is a method to incorporate functionality into the walls of the channel systems [76, 77]. Macquarrie et.al., and Brunel et.al., have detailed the covalent attachment of basic functional sites such as amino group on MCM-41 surface which can be either used as base catalysts or used as an anchor point for asymmetric ligands assembly [78 a & b, 79]. Surface modification techniques are enjoying a renewal interest, and it is clear that the pore walls of mesoporous materials are easily modified with either purely inorganic or with hybrid, semi-organic functional groups and can be successfully used as catalysts for green chemistry [80].

1.8. PHYSICO-CHEMICAL CHARACTERIZATION OF ZEOLITES

1.8.1. X-Ray Diffraction

Among the different analytical tools available for characterization of zeolites, X-ray diffraction is one of the most important and versatile technique [3,18,81 a & b]. Several important structural features of zeolites are obtained from XRD data; these include: phase purity, uniqueness of structure, and degree of crystallinity of the samples. When isomorphous substitution in zeolites occurs, the extent of incorporation of the isomorphous element can be correlated with unit cell expansion or contraction [82-85].

Elucidation of the structure of single crystals [86,87] and determination of new structures using Rietveld analysis and *abinitio* calculation are also possible with XRD [86-88].

1.8.2. Infrared Spectroscopy

IR-spectroscopy is a supplementary technique to X-ray diffraction since it is sensitive to zeolite framework vibration. In the IR spectrum of zeolites in the range of 300-1300 cm^{-1}, the lattice vibration can be divided into structure-insensitive and structure-sensitive vibrations. Flanigen et.al. [89] assigned the following bands position:

Structure Insensitive Vibrations

Asymmetric Stretch	950 – 1250 cm^{-1}
Symmetric Stretch	650 – 720 cm^{-1}
T-O Bending	420 – 500 cm^{-1}

Structure Sensitive Vibrations

Asymmetric Stretch	1050 – 1150 cm^{-1}
Symmetric Stretch	750 – 820 cm^{-1}
Double Ring Vibrations	500 – 650 cm^{-1}
Pore Opening Vibrations	300 – 420 cm^{-1}

Infrared data on the fundamental structures of may minerals and synthetic zeolites have been published by several authors [89-92]. Information about zeolite acidity can also be obtained from the IR spectroscopy of OH groups [93] and absorbed bases such as ammonia pyridine and benzene [94]. IR spectroscopy is also used to confirm

isomorphous substitution. Incorporation of B, Fe or Ga in place of Al shifts certain OH vibrations to lower or higher wave numbers [95].

1.8.3. Thermal Analysis

Thermal stability of zeolites is one of the important features that make zeolites applicable as selective sorbents and potential catalysts. Thermal behavior of zeolites as well as information regarding their syntheses and associated reaction mechanism can be obtained by thermal techniques. [96,97] The thermal stability of zeolites is often examined from the shape of the high-temperature differential thermal analysis (DYA) exotherm. Various physico-chemical changes such as the dehydration of absorbed water, the formation of Lewis acid sites during thermal treatment can be analyzed from the thermo-analytical curves. [98,99] Kinetics of the dehydration of zeolites as well as oxidative decomposition of occluded organic has also been extensively studied using this technique. [100,101]

1.8.4. Temperature Programmed Desorption of Ammonia

TPD of ammonia is a useful method for characterizing the acidity of zeolites on terms of acid strength and the number of acid sites. [102,103] Jacobs et. al. [104] have characterized acid sites as weak, medium and strong sites according to the temperature of release of ammonia from these sites over a large temperature range during acidity measurements USY and ZSM-5 zeolites. According to Lok et. al., [105] the first NH_3-TPD peak (< 473K) represents mainly physisorbed NH_3 molecules. The second peak (473 K-673 K) is associated with NH_3 molecules adsorbed on hydroxyl groups, and the

third peak (> 673 K) is associated with dehydroxylation, strong Bronsted acid sites and/or Lewis acid sites.

As catalysts, zeolites exhibit appreciable activity with shape selective features not available in compositionally equivalent amorphous catalysts. In addition, these materials can act as support for numerous catalytically active metals and metal oxides.

The industrial use of zeolites as catalysts started in the early 1960s with the replacement of cracking catalysts based on amorphous aluminosilicates. [106-109] As catalysts, zeolites have found greatest use in the hydrocarbon processing field in petroleum and petrochemical industries. Some major zeolite-based commercial process involving petroleum, petrochemicals and oil refining industries are listed in table 1.4. In more traditional oil refining, zeolite catalyst is involving in the processing of almost every fraction of the crude oil barrel. [110]

TABLE 1.4. MAJOR COMMERCIAL PROCESSES BASED ON SHAPE SELECTIVE ZEOLITES

Name of Process	Purpose	Reference
Selectoforming	Octane Boosting	76
M-Forming	Octane Boosting	77-80
Catalytic cracking	Octane Boosting	81,82
MDDW	Distillate dewaxing	83,84
Jet fuel dewaxing	Heavy distillate dewaxing	85
MLDW	Lube Dewaxing	86,87
MOGD	Light olefins to gasoline	88
M2-forming	Paraffins, olefins, naphthalene to aromatics and light gases.	89
MVPI, MHTI	Xylene isomerisation	90-92
MTDP	Toluene disproportionation	92

Mobil/Badger EB process	Ethylbenzene synthesis	93
ALBENE	Ethylbenzene synthesis	94
MTG	Methanol to gasoline	95
MTO	Methanol to light olefins	96

Composed to the successful use of zeolites in hydrocarbon processing, their use in the synthesis of organic intermediates and fine chemicals started at large stage, but the progress of research in this field is significant in recent years. The potential of zeolites in the field has been demonstrated for a Varity of organic reaction such as alkylation, [111-115], transalkylation, [116-118] isomerisation, [119-121] rearrangement, [122-124] oxidation, [125-128] reduction, [129] and condensation. [130-132].

1.9. ACYLATION REACTIONS OF AROMATICS

Friedel-Craft acylation reactions are widely used in the manufacturing of arylketones, which are of interest in the synthesis of a large number of the fine chemicals such as drugs, fragrances, dyes and pesticides. [133 a & b]. This process has been carried out in industry by working under batch conditions using acyl halides as acylation agents and homogeneous Lewis acids such as anhydrous metal halides ($FeCl_3$, $FeBr_3$, $SbCl_5$, $TiCl_4$, $ZrCL_4$) as catalysts [134]. Conventionally, in the Friedel-Craft ketone synthesis, homogeneous Lewis acid catalysts such as $AlCl_3$, BF_3 and HF have been used [135 a & b]. However, Lewis acids must be used in higher than stoichiometric amounts, and the catalyst must be destroyed at the end of the reaction with a significant production of undesirable wastes [136 a & b]. In order to overcome the difficulties of Lewis acid catalysts, several other acid catalysts such as iron sulfate [137], iron oxide [138], heteropoly acids [139], trifluromethane sulfonicacid [140] have been used as alternate catalysts. Various metal salts supported on zeolites and clays have also been reported for

Friedel-Craft reaction [141]. Besides, the use of solid acids such as zeolites enables one to beneficially use their shape selective properties (molecular sieving mechanism) to obtain the desired products. Zeolites catalysts and sulfated zirconia have been studied extensively for acylation of aromatics [142].

1.10. ALKYLATION REACTIONS OF AROMATICS

Electrophilic alkylation of aromatics can be carried out by variety of reactants such as olefins, alcohols and halogenated hydrocarbons [143]. Alkylation of aromatics is a good example of reaction where the diffusion and transition shape selectivity play a predominant role in controlling the selectivity of zeolites catalyst. Furthermore, it shows that depending on the size of reactant and product molecules, shape selectivity applies to either medium- or large pore size zeolites, and selective alkylation process have developed using both type of zeolites. Recently, isopropylation of xylenes and ethyl benzene have been studied thoroughly with medium and large pore zeolites in our lab [27]. Many solid bases have recently been found useful in the production of alkylation products. Several alkali doped silica, zeolites, mesoporous silica have been recently reported for base catalyzed reactions [28,144-147]. Macquarrie et al. reported that KF supported on natural phosphate could act as a green base catalyst [148]. Base catalyzes selective side chain monoalkylation of methylene, which is an active compound important in industrial process for the formation of intermediates [149-151]. Alkali metal carbonates and organic bases have been studied in the selective monomethylation of arylacetonitriles and methyl aryl acetates in detail under batch wise condition [152, 153].

1.11. OXIDATION REACTION

In the area of catalytic oxidation, the role of hydrogen peroxide has progressively, driven by two converging incentives i.e. the growing interest for clean technologies and the discovery of new and effective catalysts, particularly redox molecular sieve. These are wholly inorganic materials, inherently stable to oxidative degradation, in contrast to organometallic ones. Their number has sharply increased throughout the 1990s, generating a multiplicity of (potential) catalysts characterized by a variety of compositions, structures and porosities. Transition metals, incorporated into or grafted on the molecular sieve matrix, constitute redox sites. Mixed organic/inorganic catalysts also have been prepared, through the encapsulation of metal complexes in zeolites cavities or through their immobilization via chemical bonding with surface silanols.

Catalytic properties are greatly dependent on the individual nature of the metal site, the structure and the sorption properties of the molecular sieve. In Ti- and V-zeolites, having the similar composition and structural features, different catalytic properties correspond to the different redox sites, under analogous reaction conditions. Besides dimension, the hydrophilic/hydrophobic properties of pores have also a major effect on the course of the reaction. Selective adsorption phenomenon concentrate specific components of the reaction mixture in the close proximity of the active sites while excluding others [154]. Thus, the catalytic behavior of the transition metals inserted into molecular sieves can differ to the highest degree from that of corresponding soluble species. Illuminating is the case of TS-1, that is able to carry out oxidation reaction with hydrogen peroxide in polar and protic solvents, in contrast to the soluble Ti-alkoxides, which are active only in the absence of water and protic solvents.

To this stage, redox molecular sieves have been applied to the epoxidation of double bonds, the hydroxylation of aliphatic and aromatic C-H bonds and the oxidation of O, N and S functionalities, in relatively simple molecules. Studies on fine chemicals synthesis are still rare, possibly for the relative youth of this branch of catalysis and the priority given so far to material preparation and characterization aspects. It is also pertinent to mention that catalytic oxidation have been generally carried out in excess substrate reflecting a petrochemical-type of attitude, that privileges. Most relevant is the production of cyclohexanone oxime from cyclohexanone and H_2O_2/NH_3. TS-1, Ti-ZSM-48, Ti, Al-β and Ti-MOR have been studied as catalysts. In a few cases, the interest extended to comprise other carbonyl compounds. The ammoximation of *p*-hydroxyacetophenone was the subject of a detailed investigation by Le Bars et.al. the corresponding oxime is used in the synthesis of analgesic *p*-acetaminophenol (Paracetamol) produced by the Beckmann rearrangement. Best results, i.e. 100 % selectivity to oxime at 50 % ketone conversion, were afforded by TS-1. The yield was lower on Ti, Al-β and Ti-ZSM-48. The reverse reaction, i.e. the regeneration of carbonyl groups from oximes and tosylhydrazones in alternative to usual methods, was also studied for its synthetic value. Yields were in the range 60 – 85 %. Owing to molecular dimension of most substrate, it is likely that the reaction occurred on the external surface of TS-1 crystallites.

Relatively few studies concern the oxidation of sulfur compounds. Thiophenol and ethane thiol produced corresponding methyl and phenyl disulfides quantitative on TS-2/H_2O_2. Alkyl and aryl thioethers were oxidized by hydrogen peroxide to sulfoxides on TS-1 and Ti-β, at near room temperature. Sulfones were minor by products.

1.12. SCOPE OF THE WORK

The present work aims at the design and development of solid catalysts for selective acylation/alkylation/oxidation of aromatics. In the first phase, microporous molecular sieves have been synthesized and modified according to the requirement and studied for acylation/alkylation reactions. Fridel-carfts acylation and alkylation reactions of aromatics to the corresponding ketone is of considerable interest for making aromatic intermediates which are used for the production of pharmaceuticals, pesticides, photographic agents, UV absorbents, plastics, paints, dyes and other commercial products [155]. The problems created by the homogeneous Lewis acid catalyst and non-selective solid catalyst could be easily overcome using zeolite catalysts. Zeolite catalyst due to their shape selectivity, thermal stability, ease of separation from the products and regeneration of deactivated catalysts, has been widely used in the field of petrochemistry [156, 157]. However the use of zeolite catalysts in fine organic synthesis and particularly in these acylation reactions is limited and most of the zeolite catalysts in these reactions are patented [158, 159]. Furthermore, various zeolite catalysts have been extensively studied in the alkylation reactions and proved to be more promising solid acids for achieving highly shape selective catalysis. The development of new catalytic process using solid catalysts is becoming increasingly interest. With ever growing environmental and economic concerns, the present study comparises of the following: selective acylation of phenol and substituted phenols to their corresponding ketone, alkylation of benzene, and design and development of heterogeneous Mn and Co (salen) immobilized mesoporous alumina catalyst for oxidation of styrene and cyclohexene.

1.13. REFERENCES

1. D. A. Breck, *Zeolite Molecular Sieves*, John Wiley and Sons, NEW York, (1974)
2. R. M. Barrer, *Hydrothermal Chemistry of Zeolites*, Academic Press, New York, (1982).
3. W. M. Meier and D. H. Olson, *Atlas of Zeolite Structure Types*, 2nd Edn. Butterworths, London, (1987).
4. W. L. Bragg, *The Atomic Structure of Minerals*, Cornell University Press, Ithaca, New York, (1937).
5. W. M. Meier, *Molecular Sieves*, Soc. Chem. Ind., London (1968) 10.
6. E. M. Flanigen, *Proc. 5th Int. Zeol. Conf.*, L. V. C. Rees (Ed.), Heyden and Sons, London, (1980) 760.
7. L. B. Sand, *Econ. Geol.* (1967) 191.
8. R. M. Barrer, *Pure Appl. Chem.* (1979) 1091.
9. L. B. Sand, *Pure Appl. Chem.* (1980) 2105.
10. E. M. Flanigen, *ACS Symp. Ser.* 121 (1973) 119.
11. R. M. Barrer and P. J. Denny, *J. Chem. Soc.* (1961) 971.
12. R. M. Barrer, P. J. Denny and E. M. Flanigen, *US Pat*, 3,306,922 (1967).
13. E. Moretti, S. Contessa and P. Padovan, *Chim. Ind.* 76 (1985) 21.
14. E. W. Valyocsik and L. D. Rollmann, *Zeolites* 5 (1985) 123.
15. F. J. van der Gaag, J. C. Jansan and H. van Bekkum, *Appl. Catal.* 17 (1985)

261.

16. J. L. Casci, *Stud. Surf. Sci. Catal.* 28 (1986) 215.

17. B. M. Lok, T. R. Cannan and C. A. Messina, *Zeolites*, 3 (1983) 282

18. R. Szostak, *Molecular Sieves, Principles of Synthesis and Modification*, Van Nostrand Reinhold, New York, (1989)

19. H. S. Sherry, *Molecular Sieve Zeolites, Adv. Chem. Ser.* 101 (1971) 350

20. L. V. C. Rees and A. Rao, *Trans. Faraday Soc*. 62 (1970) 2103.

21. R. S. Hansford, *Ind. Eng. Chem*. 39 (1947) 849; J. B. Peri, *J. Catal*. 41 (1976) 227.

22. D. Barthomeuf, *Mat. Chem. Phys*. 17 (1987) 49.

23. W. M. Meir, D. H. Olson, C. Baerlocher, (1996) *atlas of Zeolite Structure types*, 4th Edn**.** Elsevier, London.

24. A. Redondo, P. J. Hay**,** *J. Phys. Chem*. 97 (1993) 11754.

25. R. A. van Santen, G. J. Kramer, W. P.J. H. Jacobs, *Theory of Bronsted Acidity in Zeolites*. In: R. W. Joyner, R. A. van Santen (Eds.) *Elementary Reaction steps in heterogeneous Catalysis*. Kluwer Academic Publishers, (1993) 113.

26. H. G. Karge, Stud. *Surf. Sci. Catal.* 65 (1991) 133.

27. C. R. Patra, R. Kumar, *J. Catal*. 212 (2002) 216.

28. H. Hattori, *Chem. Rev*. 95 (1995) 537; R. J. Davis, *J. Catal.* 216 (2003) 396.

29. R. L. Wadlinger, G. T. Kerr, E. J. Rosinski, *US. Patent* 3 308 069, 1967.

30. (a) M. M. J. Treacy, J. M. Newsam, *Nature* 332 (1988) 249; (b) J. B. Higgins, R. B. LaPierre, J. L. Schlenker, A. C. Rorman, J. D. Wood, G. T. Kerr, W.J.Rohrbaugh, *Zeolites* 8 (1988) 446.

31. P. Ratnasamy, R. N. Bhat, S. K. Pokhriyal, S.G. Hegde, R. Kumar, *J. Catal*. 119 (1989) 65.

32. L. Boretto, M. A. Camblor, A. Corma, J. Perez-Pariente, *Appl. Catal. A: Gen*. 82 (1992) 37.

33. I. Kirisci, C. Flego, G. Pazzuconi, W. O. Parker, R. Millini, C. Perego, G. Bellussi, *J. Phys. Chem*. 98 (1994) 4627.

34. M. Sun, J. Sun, Q. Li, *Chem. Lett.* (1998) 519.

35. A. Corma, A. Martinez, P. A. Arroyo, J. L. F. Monteiro, E. F. Sousa-Aguiar, *Appl. Catal.A: Gen.* 142 (1996) 139.

36. A. K. Pandey, A.P. Singh, *Catal. Lett*. 44 (1997) 129; T. Jaimol, P. Moreau, A. Finial, A.V. Ramaswamy, A. P. Singh, *Appl. Catal. A; Gen*. 214 (2001) 1.

37. V.D. Chaube, P.Moreau, A. Finial, A.V. Ramaswamy, A.P.Singh, *J.Mol. Catal*. 174 (2001) 255; *Catal. Lett*. 79 (2002) 89

38. H. Hattori**,** *Chem. Rev*. 95 (1995) 537; R.J. Davis, *J.Catal*. 216 (2003) 396

39. R. M. Barrer, *Proc. Royal Soc*. A 167 (1938) 392.

40. R. M. Barrer and D. W. Riley, *Trans Faraday Soc*. 46 (1950) 853.

41. R. M. Barrer and A. B. Robins, *Trans Faraday Soc*. 49 (1953) 1049.

42. R. M. Barrer and W. I. Stuart, *Proc. Royal Soc. A* 249 (1959) 464 484.

43. R. M. Barrer and R. M. Gibbons, *Trans Faraday Soc*. 59 (1963) 2569 2875.

44. R. M. Barrer, *Pure Appl. Chem.* 52 (1980) 2143.

45. R. J. Neddenriep, *J. Colloid Interface Sci.* 28 (1968) 293.

46. P. B. Weisz, *Chemtech,* 3 (1973) 498.

47. M. F. M. Post, *Stud Surf. Sci. Catal*, 58 (1991) 391.

48. J. Karger and D. M. Ruthven, in *Diffusion in Zeolites and other Mesoporous Solids*, John Wiley and Sons, New York, (1992).

49. P. B. Weisz and V. J. Frilette, *J. Phys. Chem.,* 64 (1960) 382.

50. S. M. Csicsery, *Zeolites Chemistry and Catalysis*, ACS monograph 171, J. A. Rabo (Ed.), American Chemical Society, Washington DC (1976) 680.

51. N. Y. Chen, W. E. Garwood and F. G. Dwyer, *Shape Selective Catalysis in Industrial Applications*, Marcel Dekker, New York (1989).

52. S. M. Csicsery, *Zeolites* 4 (1984) 202.

53. S. M. Csicsery, *Pure Appl. Chem.* 58 (1986) 841.

54. P. B. Venuto, *Microporous Mater.* 2 (1994) 297.

55. E. G. Derouane, in *Zeolites: Science and Technology*, F. Ramôa Ribeiro et. al., (Eds.) NATO ASI Series E 80, Martinus Nijhoff Pub, The Hague (1984) 347.

56. P. B. Weisz, *Pure Appl. Chem.* 52 (1980) 2019

57. F. Ramôa Ribeiro, F. Alvarez, C. Henriques, F. Lemos, J. M. Lopes and M. F. Rebeiro, *J. Mol. Catal,* 96 (1995) 245.

58. S. M. Csicsery, *J. Catal.* 23 (1971) 124.

59. J. A. Rabo, R. Bezman and M. L. Postma, *Acta Phys. Chem.* 24 (1987) 39.

60. E. G. Derouane and Z. Gabelica, *J. Catal.* 65 (1980) 486.

61. C. Mirodatos and D. Barthomeuf, *J. Catal.* 57 (1979) 136.

62. C. Mirodatos and D. Barthomeuf, *J. Catal*. 93 (1985) 246.

63. G. A. Ozin, C. Gil, *Chem. Rev.* (1989) 1749.

64. M. E. Davis, R. F. Loba, *Chem. Mater.* 4 (1992) 756.

65. X. S. Zhao, G. Q. Lu, G. J. Millar, *Ind. Eng. Chem. Res*. 35 (1996) 2075.

66. C. T. Kresge, M. .E Leonowicz, W. J. Roth, J. C. Vartulli, J. S. Beck, *Nature* 359 (1992) 710.

67. J. S. Beck, J. C. Vartulli, W. J. Roth, M. E. Leonowicz, C. T. Kresge, K. D. Schmitt, C. T. W. Chu, D. H. Olson, E. W. Sheppard, S. B. McCullen, J. B. Higgins, J. L. Schlenker, *J. Am. Chem. Soc.* 114 (1992) 10834.

68. M. Dubois, Th. Gulik-krzywicki, B. Cabane, *Langmuir* (1993) 673.

69. J. C. Vartulli, K. D. Schmitt, C. T. Kresge, W. J. Roth, M. E. Leonowicz, S.B. McCullen, S. D. Hellring, J. S. Beck, J. L. Schlenker, D. H. Olson, E. W. Sheppard, *Chem. Mater*. 6 (1994) 2317.

70. A. Corma, A. Martinez, *Adv. Mater*. (1995) 137.

71 C. Huber, K. Moller, T. Bein, *J. Chem. Soc. Chem. Commun*. (1994) 2619.

72. A. Monnier, F. Schuth, Q. Huo, D. Kumar, D. Margalose, R. S. Maxwell, G. D. Stucky, M. Krishnamurthy, P. Petroff, A. Firouzi, M. Janicke, B. F. Chmelka, *Science* 261 (1993) 1299.

73. Q. Huo, D. I. Margalose, U. Ciesla, P. Feng, T. E. Gier, P. Sieger, R. Leon, P. Petroff, F. Schuth, G. D. Stucky, Nature 368 (1994) 317; P. T. Tanev, T. J. Pinnavaia, *Science* 267 (1995) 865.

74. K. Moller, T. Bein, *Chem. Mater*. 10 (1998) 2950

75. W. M. Van Rhijn, D. E. De Vos, F. Sels, W. D. Bossaert, P. A. Jacobs, *J Chem. Soc., Chem. Commum*. (1998) 317.

76. C. E. Fowler, S. L. Burkett, S. Mann**,** *J. Chem. Soc. Chem. Commun*. (1997) 1769.

77. A. P. Wight, M. E. Davis, *Chem. Rev*. 102 (2002) 3589.

78. (a) D. J. Macquarrie, D. B. Jackson, *J. Chem. Soc. Chem. Commun*. (1997) 1781; (b) J. H. Clark, D. J. Macquarrie, *J. Chem. Soc. Chem. Commun*. (1998) 853.

79. D. Brunel, *Microporous Mesoporous Mater.* 27 (1999) 329.

80. D. Brunel, *Microporous Mesoporous Mater.* 27 (1999) 329.

81. (a) X. S. Zhao, G. Q. Lu, A. K. Whittakar, G. J. Millar, *J. Phys. Chem*. B 101 (1997) 6525; (b) K. A. Koyano, T. Tatsumi, Y. Tanaka, S. Nakata, *J. Phys. Chem. B* 101 (1997) 9436.

82. G. Perego, G. Bellussi, C. Corno, M. Taramaso, F. Buonomo and A. Esposite *New Developments in Zeolites Science and Technology*, Y. Murakami et. al. (Eds.), Elsevier, Amsterdam (1986) 129.

83. P. Ratnasamy, A. A. Kotasthane, V. P. Shiralkar, A. Thangraj and S. Ganapathy, *Zeolites Synthesis*, ACS Symp. Ser. 398 (1989) 405.

84. R. Szostak and T. L. Thomas, *J. Catal.* 100 (1986) 555.

85. D. K. Simmons, R. Szostak and P. K. Agarwal, *J. Catal.* 106 (1987) 287.

86. J. J. Pluth, J. V. Smith and J. M. Bennett, *Acta Crystallog*. C42 (1986) 283

87. J. F. Charnell, *J. Cryst*. Growth 8 (1971) 291.

88. H. M. Rietveld, *J. Appl. Crystallog*. 2 (1969) 65.

89. E. M. Flanigen, H. Khatami and H. A. Szymanski, *Adv. Chem. Ser*. 101 (1971) 201.

90. A. C. Wright, J. P. Rupert and W. T. Granquist, *Am. Miner*. 53 (1968) 1293.

91. S. P. Zhdnov, A. V. Keseler, V. I. Lygin and T. I. Titova, Russ. *J. Phys. Chem.*

38 (1964) 1299.

92. E. M. Flanigen and R. W. Grose, *Adv. Chem. Ser*. 101 (1971) 76.

93. W. J. Ward, ACS *Monograph 171*, J. A. Rabo (Ed.), (1976).

94. P. A. Jacobs, J. A. Martens, J. Weitkamp and H. K. Beyer, *Selectivity in Heterogeneous Catalysis*, Far. Disc. Chem. Soc. 72 (1981) 351.

95. C. T. W. Chu and C. D. Chang, *J. Phys. Chem.* 89 (1985) 1569

96. E. G. Derouane, S. Detremmerie, Z. Gabelica and N. Blom, *Appl. Catal.* 1 (1981) 20.

97. R. M. Barrer and D. A. Langley, *J. Chem. Soc.* (1958) 3804, 3811, 3817.

98. I. G. Gal, O. Tankovie, S. Malcis, R. Raoovanor and M. Tadorivic, *Trans Faraday, Soc.* 67 (1971) 999.

99. H. Bremer, W. Morke, P. Schodel and F. Vogt, *Adv. Chem. Ser*. 121 (1973) 249.

100. P. A. Jacobs, *Carboniogenic Activities of Zeolites*, Elsevier, Amsterdam, (1977) 33.

101. L. S. de Saldarriga, C. Saldarriga and M. E. Davis, *J. Am. Chem. Soc*. 109 (1987) 2686.

102. J. R. Anderson, F. K. Mole, R. A. Rajadhyaksha and J. V. Sanders, *J. Catal.* 58 (1979) 114.

103. J. G. Post and J. H. C. van Hooff, *Zeolites* 4 (1984) 9.

104. P. A. Jacobs, J. B. Utterhoeven, M Steyns, G. Froment and J. Weitkamp*, Proc. 5th Int. Zeol. Conf.*, L. V. C. Rees (ED.) Heyden and Sons, London, (1980) 607.

105. B. M. Lok, B. K. Marcus and C. L. Angel, *Zeolite*s 6 (1986) 185.

106. P. B. Weisz, V. J. Frilette, R. W. Mattman and E. B. Mower, *J. Catal,* 1 (1962) 307.

107 C. J. Plank, E. J. Rosinski and M. P. Hawthorne, *Ind. Eng. Chem. Proc. Des. Dev*. 3 (1964) 165.

108. P. B. Venuto and E. T. Habib, Jr., *Chemical Industries*, Marcel Dekker, New York 1 (1979).

109. W. Hölderich and E. Gallei, *Chem. Eng. Tech*. 56 (1984) 908.

110. I. E. Maxwell and W. J. H. Stork, *Stud. Surf. Sci. Catal*. 58 (1991) 571.

111. P. B. Venuto, L. A. Hamilton, P. S. Landis and J. J. Wise, *J. Catal.* 5 (1966) 81.

112. W. W. Kaeding, M. M. Wu, L. B. Young and G. T. Burress, *US Pat.* 4,197,413 (1980).

113. P. Y. Chen, M. C. Chen, H. Y. Chu, N. S. Chang and T. K. Chuang, *Stud. Surf. Sci. Catal.* 28 (1986) 739.

114. K. S. N. Reddy, B. S. Rao and V. P. Shiralkar, *Appl. Catal.* 95 (1993) 53.

115. A. R. Pradhan, A. N. Kotasthane and B. S. Rao, *Appl. Catal.* 72 (1991) 311.

116. A. R. Pradhan, and B. S. Rao, *Appl. Catal*. 106 (1993) 143.

117. R. Bandyopadhyay, P. S. Singh and R. A. Sheikh, *Appl. Catal.* 135 (1996) 249.

118. L. Forni, G. Cremona, F. Missineo, G. Bellusi, C. Perego and G. Pazzuconi, *Appl. Catal.* 121 (1995) 261.

119. P. Cartraud, A. Cointot, M. Dufour, N. S. Gnep, M. Guisnet, H. Joly and J.

Tejada, *Appl. Catal*. 21 (1986) 85.

120. R. J. Pellet, P. K. Coughlin, E. S. Shamshoum, and J. A. Rabo, *ACS Symp. Ser.* 368 (1988) Ch. 33.

121. A. Molner, I. Bucsi and M. Bartok, *Acta Phys. Chem*. 31 (1985) 571.

123. C. Neri and F. Buonomo, *Eur. Pat. Appl.* 110, 117 (1983).

124. P. S. Singh, R. Bandyopadhyay and B. S. Rao, *Appl. Catal*. 136 (1996) 249.

125. R. A. Sheldon, *J Mol. Catal.* 7 (1980) 107.

126. P. R. H. P. Rao, A. V. Ramaswamy and P. Ratnasamy, *J. Catal.* 141 (1993) 604.

127. J. S. Reddy, S. Shivasankar and P. Ratnasamy, *J. Mol. Catal.* 71 (1992) 373.

128. A. Thangraj, S. Shivasankar and P. Ratnasamy, Zeolites. 12 (1992) 135.

129. M. Iwamoto, H. Yahiro, K. Tanda, N. Mizumo, *J. Phys. Chem.* 95 (1991) 3727.

130. M. A. Tobias, *US Pat*. 3,739,408 (1973)

131. C. J. Plank, E. J. Rosinski and G. T. Kerr *US Pat* 4,011,278 (1977)

132. Y. Servotte, J. Jacobs and P. A. Jacobs, *Acta. Phys. Chem*. 31 (1985) 609.

133. (a) H. W. Kouwenhoven, H. van Bekkum, Handbook of *Heterogeneous Catalysis.* (G. Ertl, h. Knozinger, J. Weitkamp, Eds.) Vol. 5, P 2358. VCH, Weinheim, 1997; (b) J. March, *Advanced Organic Chemistry,* 4th Ed. Wiley, New York 1992.

134. G. A. Olah, *Friedel-Crafts and Related Reactions,* Vol. I – IV, Wiley-Interscience, New York 1963- 1964.

135. (a) J. I. Kroschwitz, M. Howe-Gremt, Eds. *Encyclopedia of Chemical*

Technology, 4th Ed. Vol. II. Wiley-Interscience, New York, p 1055; (b) M. Aslam, K. G. Davenport, W. F. Stansbury, *J. Org. Chem*. 56 (1991) 5955.A.

136. (a) Kaward, S. Mitamurd, S. Kobayashi, *J. Chem. Soc. Chem. Commun*. (1993) 1157; (b) Chemistry of Waste Minimization, J. H. Clark, Ed. 1995, 522; *Org. Process Res. Dev.* 2 (1998) 221.

137. M. Hino, M. Arata, *Chem. Lett*. (1978) 325.

138. K. Arata, M. Hino, *Chem. Lett.* (1980) 1479.

139. K. Nomiya, Y. Sugaya, S. Sasa, M. Miwa, *Bull. Chem. Soc. Jpn.* 53 (1980) 2089.

140. F. Effenberger, G. Epple, *Angew, Chem. Int. Ed. Eng*. 11 (1972) 300.

141. D. B. Baudry, A. Dormond, F. D. Montagne, *J. Mol. Cat. A: Chem*. 149 (1999) 215.

142. N. Mizuno, M. Misono, *Chem. Rev*. 98 (1998) 199.

143. P. B. Venuto, *Micropor. Mater*. 2 (1994) 297.

144. D. Barthomeuf, *Catal. Rev. Sci. Eng.* 38 (1996) 521.

145. Z. –H. Fu, Y Ono, *J. Catal*. 145 (1994) 166.

146. D. Brunel, *Micropor, Mesopor. Mater*. 27 (1999) 329.

147. R. Bal, K. Chaudhary, S. Sivashankar, *Catal. Lett.* 70 (2000) 75.

148. D. J. Macquarrie, R. Nazih, S. Sebti, *Green Chemistry* 4 (2002) 56.

149. Y. Ono, *Appl. Catal. A: Gen* 155 (1997) 133.

150. P.Tundo, M. Selva, *Chem. Tech*. 25 (1995) 31.

151. J. P. Rieu, A. Boucherle, H. Cousse, G. Mouzin, *Tetrahedron,* 42 (1986) 4095.

152. P. Tundo, G. Malagho, F. Trotta, *Ind. Eng. Chem. Res*. 28 (1989) 881.

153. M. Selva, C. A. Marques, P. Tundo**,** *J. Chem. Soc. Perkins Trans*. I (1994) 1323.

154. G. Langhendries, D. E. De Vos, G. V. Baron, and P. A. Jacobs, *J. Catal*. 187 (1999) 453.

155. J. H. Clark, Ed., *Chemistry of Waste Minimization*, Chapman and Hall, London. (1995).

156. G. A. Olah, *Friedel Craft Chemistry*, Wiley, New York (1973) p. 509.

157. D. W. Breck, *Zeolite Molecular Sieves*, Wiley, New York (1974).

158. S. Matsu and S. Kawahara, *Jpn. Kokai Tokyo Koho* 92, 368, 340 (1992).

159. M. Neber, E. I. Leupold, *Eur. Pat. Appl.* 459, 495 (1991).

CHAPTER 2

SYNTHESIS, MODIFICATION AND CHARACTERIZATION OF CATALYSTS

2.1. INTRODUCTION

Zeolite Beta was first synthesized by Wadlinger, Kerr and Rosinski [1]. The silica to alumina ratio of the as the synthesized sample was between 10-200 and tetraethylammonium hydroxide (TEAOH) was used as the organic templating agent. Perez-Pariente et.al. [2] found that zeolite Beta nuclei were formed via liquid phase synthesis mechanism and aluminium is an essential element of the precursor species. It possesses a three dimensional, 12 membered ring (MR) pore system. Other researchers have since found [3,4] that the zeolite beta is a disordered intergrowth of two isomers, which are permeated by a tridimensional network of 12-MR ring channels. Both isomers result from the same centrosymmerical, tertiary building units arrange in layers. Fig 2.1 (a) and (b) depict representation of the framework structures of these zeolite beta polymorphs. The density of the stacking faults in the zeolite beta structure is highly relative to other zeolites because successive layers must interconnect in either a left - or right – handed fashion. The dimension of the pores is 7.5 x 5.7 Å along the linear channels and 6.5 x 5.6 Å along the tortuous channels [5].

Zeolite ZSM-5 (Zeolite Sycony Mobil-5) is a highly siliceous zeolite, widely employed as a catalyst in organic synthesis, petroleum refining and petrochemical industries. It was first developed in 1972 by Argauer and Landolt [6, 7]. ZSM-5 is categorised as a medium pore class zeolite, having channels system with pore sizes between 4.5 Å to 6.5 Å, formed by two types of 10-membered oxygen rings. The first type is a straight and elliptical channel, with a free cross-section of 5.5 x 5.1 Å. The second type, perpendicular to the first channel is a sinusoidal channel with a cross-section of 5.6 x 5.4 Å [8]**.** Its catalytic properties are due to its acidity while the unique pore systems gives the catalyst its shape selective character [9]**.**

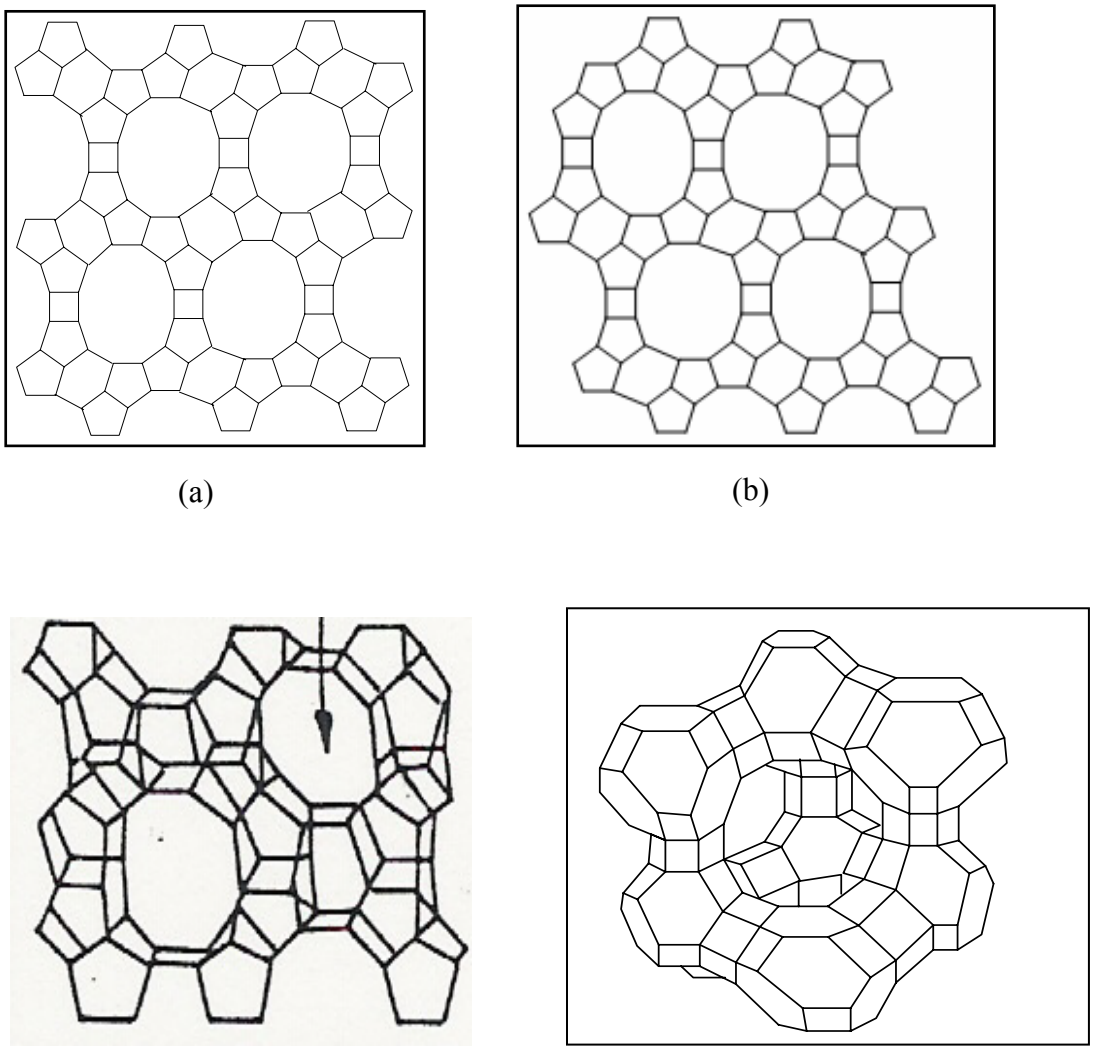

Figure 2.1. Frame Work Structures of Zeolites (a) Beta: Polymorph A, (b) Beta: Polymorph B, (c) ZSM-5, and (d) Y

Zeolite Y consists of linked truncated octahedra called sodalite units, which have a cage of diameter 6.5Å (β cage) and accessible through six membered rings of oxygen atoms [10]. These units are connected along to six membered ring, giving rise to hexagonal prism. The polyhedra form in this way encloses a super case (α cage) with an

internal diameter of 12.5 Å and accessible through four 12-membered rings of oxygen atoms with a free aperture of 7.4 Å. The framework structure of zeolite Y is depicted in Fig 2.1d.

In this chapter, synthesis of zeolite Beta and ZSM-5 are described. Beta has also been modified by ion exchange with cations such as sodium and by changing the Si/Al ratio. All samples are characterized by various physico-chemical techniques. Commercially obtained NH_4-Y zeolite has been converted to its protonic form and also modified by ion exchange with rare earth cations.

2.2. SYNTHESIS AND MODIFICATION

2.2.1. Synthesis of Zeolite Beta

Zeolite Beta was synthesized hydrothermally from a $(TEA)_2O$-Na_2O-SiO_2-Al_2O_3-H_2O system. The reaction gel was prepared by mixing appropriate amount of silica sol (31.3 wt. % SiO_2), sodium aluminate (39 wt. % Al_2O_3, 27 wt. % Na_2O), sodium hydroxide (99 wt. %, AR Grade), Tetraethylammonium hydroxide (TEAOH, 40 wt. % solution in water, Aldrich) and distilled water. Atypical synthesis procedure of the sample with silica to alumina ratio 30 is as follow: 1.42 g sodium aluminate, 1.28 g sodium hydroxide, 30 g TEAOH and 18.18 g distilled water were mixed together and stirred vigorously to obtain a homogeneous mixture. The mixture was then added slowly to 31.21 g silica sol in a polyethylene beaker and the mixture was stirred vigorously for 1 h. The pH of the final gel was 13.8 and the calculated molar composition of the gel was

$$4.5\ Na_2O : 7.5\ (TEA)_2O : 30\ SiO_2 : Al_2O_3 : 593\ H_2$$

The final gel was transferred into a Teflon line stainless steel autoclave (capacity 200ml, see Fig 2.2) and hydrothermally treated at 423 K and autogeneous pressure for 7

days. After that the autoclave was quenched to room temperature in clod water. The solid material obtained was filtered, washed with distilled water and dried at 393 K. The crystalline sample thus obtained was calcined at 773 K for 24 h to decompose the organic template. The protonic form of the zeolite was obtained by repeated exchange with ammonium acetate solution (10 wt %), followed by calcinations at 773 K for 24 h in a flow of dry air. The yield based on total alumina input was more than 90 %.

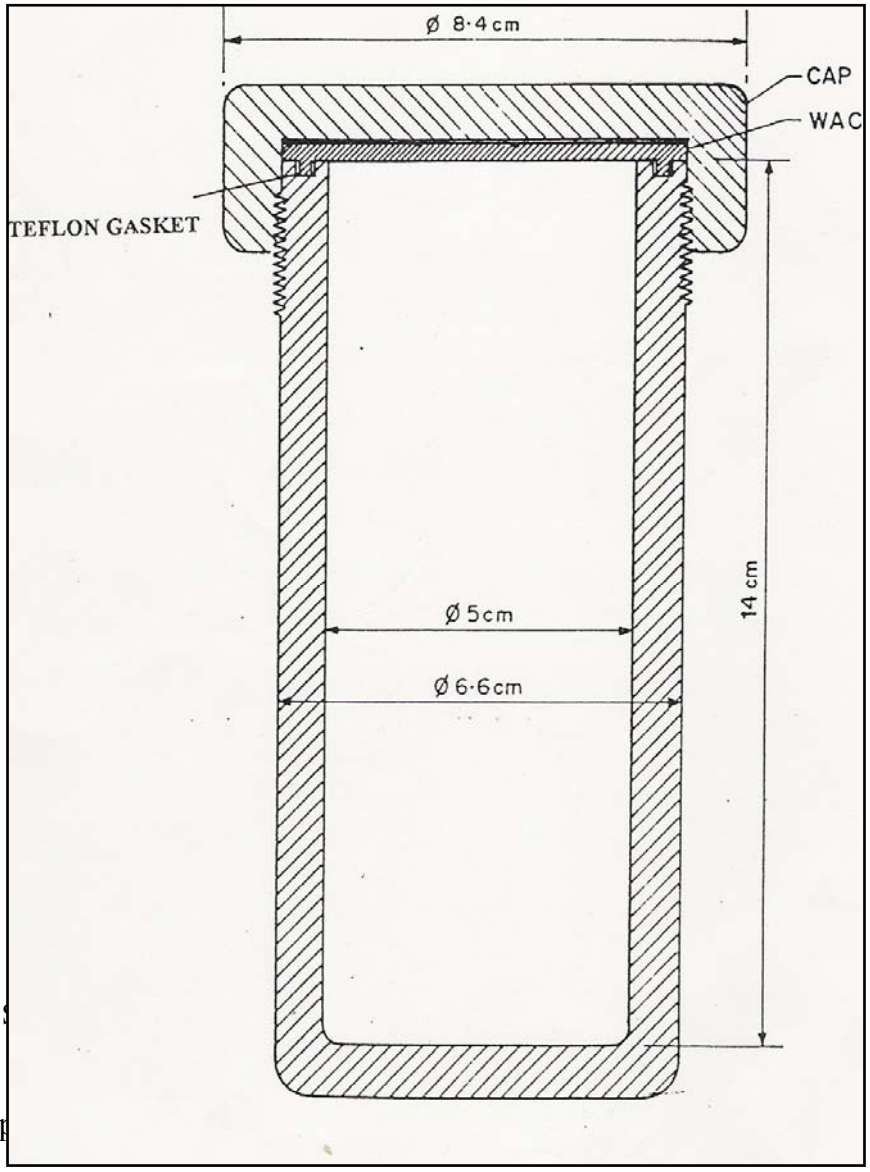

Figure 2.2.

2.2.2. Prep

Na-H-Beta of different molar ratio was prepared by ion exchange with 0.5 M solution of sodium Nitrate. 5 g of H-Beta were treated with 100 mL of a 0.5 M nitrate solution at 353 K for 8 h. The material was then washed with distilled water until the filtrate was free from nitrate ions followed by drying and calcining in the same manner followed by drying at 393 K and calcined at 773 K for 12 h.

2.2.3. Synthesis of Zeolite ZSM–5

Zeolite ZSM–5 was synthesized as per the procedure described in the literature. Appropriate amounts of aluminium sulfate and sulfuric acid were dissolved in the distilled water to yield solution (A). A calculated quantity of Tetrapropyl Ammonium Bromide (TPABr) was added to the solution of sodium silicate of required strength to get the solution (B). The solution A and B were then mixed in a stainless steel autoclave with continuous stirring to get a gel, which had a molar composition as follows:

4.38 $(TPA)_2O$: 27.6 Na_2O : Al_2O_3 : 44.2 SiO_2 : 32.62 H_2O

The autoclave was then tightly closed and kept at the desired temperature (453 K) under autogenously developed pressure for about 24 h. The reactor was cooled and then the contents were filtered, washed with de-ionized water, and then dried at 393 K overnight. It was then calcined at 823 K for 8 h to decompose the organic template. Thus, Na-ZSM-5 was obtained. The H-form of the sample was obtained by exchanging it thrice with 1 M NH_4NO_3 solutions at 353 K to get NH_4-ZSM-5, which was then calcined at 823 K for 8 h to get H-ZSM-5.

2.2.4. Preparation of Zeolite H-Y and RE-Y

H-Y was prepared from Na-Y by three ion exchanges with 1 M aqueous solution of NH_4NO_3 (1 M: Solid /solution (g/mL)= 1: 10, 8 h) and the resulting sample was then calcined at 773 K for 12 h to get H form. RE-Y was prepared from Na-Y by exchange with 1 M NH_4NO_3 (3 exchanges, 353 K for 8 h) and thus the resulting NH_4-Y was treated with 5 % rare earth nitrate solution followed by the analogous procedure employed for NH_4-Y exchange.

2.2.5. Preparation of Zeolite H-mordenite

Zeolite mordenite was synthesized hydrothermally using a molar composition of 6 Na_2O: Al_2O_3: 3 SiO_2: 780 H_2O system. The reaction gel was prepared by mixing appropriate amount of NaOH (19 g), sodium aluminate (14.3 g), silica (98.2 g) and distilled water mix them together and stirred vigorously to obtain a homogeneous mixture. The final gel was transferred into a Teflon lined stainless steel autoclave and hydrothermally treated at 343 K at autogeneous pressure for 24 h. the solid material obtained was filtered and washed with distilled water and dried at 373 K. The crystalline sample thus obtained was calcined at 773 K for 24 h to decompose the organic template. The protonic form of the zeolite was obtained by repeated exchange with ammonium acetate solution (10 wt %), followed by calcinations at 773 K for 24 h in a flow of dry air.

2.2.6. Preparation of mesoporous alumina (MA)

Non-siliceous mesoporous alumina was synthesized according to the following procedure at a temperature of 110 °C using carboxylic acid (Lauric acid) as surfactant [11]. The composition of gel mixture is Al-isopropoxide: Lauric acid: 1-propanol as 1: 0.03: 26. Typically, an aluminum hydroxide suspension was prepared by the hydrolysis

of 43.8 g of Al-isopropoxide with 10.3 g of deionised water in 275 g of 1-propanol (99 %). After stirring for 1 h, 10.8 g of lauric acid (99.5 %) was added slowly to the gel mixture. The mixture was aged for 24 h at room temperature and then heated under static conditions at 110 °C in 1-L glass jar for two days. The solid material obtained was then filtered, washed with ethanol and dried at 100 °C for 4-5 h. Finally, the material was calcined at a temperature of 450 °C with a temperature ramp of 1 °C/min from room temperature to the final temperature. The calcination atmosphere was nitrogen during the earlier stages (<200 °C) and air at final temperatures.

2.2.7. Preparation of 3-APTES functionalized mesoporous alumina (NH_2-MA)

To a suspension of 10 g of calcined mesoporous alumina in 50 mL dry toluene, 2.68 g of 3-aminopropyl triethoxy silane (3-APTES) was added slowly and heated to reflux with continuous stirring for 8 h under nitrogen atmospheres (Scheme 1). The powdery sample containing amino groups was filtered, washed with acetone and then soxhlet extracted using a solution mixture of diethyl ether and dichloromethane (1:1) for 24 h and dried under vacuum. Elemental analysis shows that 0.89 % of nitrogen gets introduced into the mesoporous support, which indicates that ~52 % of 3-APTES was immobilized per gram of mesoporous alumina.

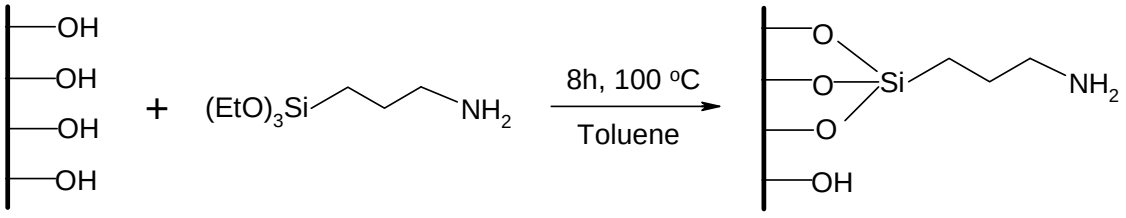

Scheme.5.1

2.2.8. Preparation of neat Co (II) and Mn (III) complexes

Cobalt and manganese (salen) precursors were prepared according to the following procedure. The appropriate metal (cobaltous and manganese) acetate hydrate (6.0 mmol) in ethanol (10 ml) was added slowly to a solution of salicylaldehyde (2.94 g, 24.0 mmol) in ethanol (40 ml). The solutions were stirred at room temperature for 24 h and their subsequent concentration leads to precipitation of the corresponding metal (salen) precursor (Scheme 2). The solid product obtained was washed with copious amounts of chloroform and dried in vacuum at 100 °C for 24 h. Elemental analysis datas obtained after purification are as follows; theoretical value (actual value) of C (%) 56.56 (58.18), H (%) 3.36 (4.11) for Mn-complex, while Co-complex shows C (%) 58.18 (56.49) and H (%) 3.32 (3.01).

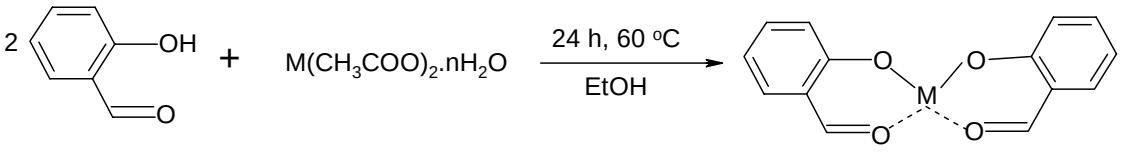

where, M= Mn, Co

Scheme.5.2

2.2.9. Preparation of salen Co (II) and salen Mn (III) complexes immobilized on modified mesoporous alumina (Co/Mn-S-NH_2-MA).

The synthesized neat complex, *viz.,* (bis-salicyl aldehyde) M, has been chemically anchored to the aminopropyl modified alumina support, using a procedure as shown in

the Scheme 3 [12]. The material was then soxhlet extracted, using a mixture of $CHCl_3$-EtOH mixture for 12 h to remove the unreacted organic residue from the mixture.

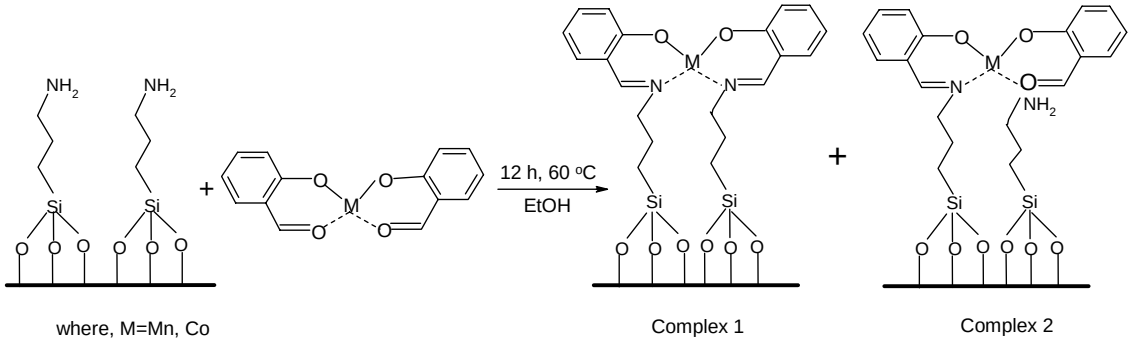

Scheme.5.3

2.3. PHYSICO- CHEMICAL CHARACTERIZATION

2.3.1. X-Ray Diffraction (XRD)

The structure of a crystal can be determined using the technique of X-ray diffraction (XRD). X-rays have wavelength in the Å range, are sufficiently energetic to penetrate solids and are well suited to probe their internal structure. It is used to identify the bulk phases, degree of crystallinity, unit cell parameters and to estimate particle size [13].

In XRD, X-rays are generated by bombarding a metal target (often copper) with high-energy electron inside a vacuum tube. Then X-rays are directed at the crystal surface/ the crystal mount is rotated so that incident X-rays can be oriented with respect to these crystallographic axes. While most of the X-rays pass straight a small amount of radiation are diffracted by atoms in a periodic lattice. The scattered monochromatic X-rays that are in phase give constructive interference. The detector records the pattern of

diffracted light to give diffraction pattern. To observe a diffraction signal, the diffracted light must interfere constructively. For this, the crystal plane must be oriented with respect to the incident rays, so that the path difference is equal to integrated multiple of the wavelength of X-ray radiation.

One can derive lattice spacing, d, by measuring the angles, 2θ, under which constructively interfacing X-rays with wavelength, λ, leave the crystal, by using Bragg relation:

$n\lambda = 2d \sin\theta$; n= 1,2….

The XRD pattern of a powdered sample is measured with a stationary X-ray source (usually Cu Kα) and a movable detector, which scans the intensity of the diffracted radiation as a function of the angle 2 θ between the incoming and the diffracted beams. When working with powdered sample, an image of diffraction lines occurs because a small fraction of the powder particles will be oriented such that by chance a certain plane (*hkl*) is at the right angle with the incident beam of constructive interference. Synthesized catalysts were characterized by X-ray diffraction using a Rigaku Miniflex powder diffractometer on finely powdered samples using Cu-Kα radiation and 45 kV and 40 mA. The scans were done at 1° per minute for low angle scanning and 4° per minute for microporous zeolites and suphated zirconia. The XRD patterns were recorded for 2 θ's between 1.5 and 50° for mesoporous materials; 5 and 50° for microporous materials.

2.3.2. Chemical composition by EDAX, ICP-OES and CHN analysis.

The compositions of zeolite were analyzed by EDAX. Inductively Coupled Plasma-Optical Emission Spectra (ICP-OES) determined the palladium content in the

materials on a Perkin-Elmer P1000 instrument. An average of two analyses was done to calculate average concentration of Pd in the samples. Samples for ICP analyses were prepared by dissolving 0.05 g of sample in approximately 5 mL of HF and subsequently with 5 mL of aqua regia and then diluting to 50 mL with double de-ionized water (DDW). Analysis of the organic content presents in the catalysts was carried out using a Carlo-Erba CHN analyzer.

2.3.3. Surface area (BET) and Pore size distribution (BJH)

The most common method of measuring surface area, pore volume and pore size distribution of a catalyst (solid material) is developed by Brunauer, Emmett and Teller using nitrogen as an adsorbent. Measurement of the amount of nitrogen gas adsorbed or desorbed is the most commonly used procedure for determining the pore size distribution of mesopores. Adsorption of nitrogen was carried out at 77 K using a NOVA 1200 (Quantachrome) instrument. The sample was evacuated at 673 K for 2 h under high vacuum (10^{-6}mm). The anhydrous weight of the sample is measured. The sample was then cooled to 94 K using liquid nitrogen and then allowed to adsorb nitrogen gas. Surface area of the sample was calculated by using BET method.

For a multiplayer adsorption the heat of adsorption for all layers except the first layer is assumed to be equal to the heat of liquefication of the adsorbed gas. So the BET equation comes for summation over an infinite number of adsorbed layers. The general form of the BET equation may be written as follows:

$1/V_{ads} (P_0-P) = 1/V_mC + [C-1/V_mC] P/P_0$ ----------{eq. 1}

Where, V_{ads} = volume of gas adsorbed at pressure P, P_0 = saturated vapour pressure,

V_m = volume of gas adsorbed for monolayer coverage, C = BET constant

By plotting left side of equation 1 against P/P_0, a straight line is obtained with a slope of $C-1/V_mC$ and an intercept $1/V_mC$. The BET surface area is calculated using the formula

$S_{BET} = X_M . N . A_M . 10^{-20}$

Where, N is the Avagadro number, A_M is the cross-sectional area of the adsorbate molecule (N_2, 16.2 $Å^2$) and X_M is the moles of N^2 adsorbed.

Pore size distribution was obtained by using BJH pore analysis applied to the adsorption branch of the nitrogen adsorption -desorption isotherm.

2.3.4. Fourier transform infrared spectra (FTIR)

FTIR is used to determine a variety of materials property including structure details and functional groups confirmations, strength and distribution of the acid sites in porous materials. Infrared spectroscopy is the measurement of the wavelength and intercity of absorption of middle IR by a sample. Middle IR light (400-4000 cm^{-1}) is energetic enough to excite molecular vibration to higher energy levels. The wavelength of IR absorption bands are characterized of specific types of chemical bonds and IR spectroscopy finds its greatest utility for the identification of organic and organo metallic molecules.

Infrared spectra of the solid samples diluted in KBr were recorded at room temperature in the transmission mode, in the range 4000 to 450 cm^{-1} resolution, using Spectra one Spectrometer.

2.3.5. Thermal Studies

Thermal methods of analysis may be defined as those techniques in which changes in physical and/or chemical properties of substances are measured as a function of temperature. Two important thermal analytical techniques are thermogravimetry (TGA) and differential assessment analysis (DTA). Thermogravimetric analysis is a valuable technique for the assessment of the purity of the materials. Organic matter which is burn out can be clearly seen from TG plot in terms of weight loss at corresponding temperature ranges. These data can be useful for knowing the chemical stability of the organic matter anchored into the inorganic materials. Differential thermal analysis gives information about thermal stability against decomposition, fusion and phase changes.

Thermal analyses were performed using a Rheometric scientific (STA 1500) analyzer, from 303 to 1173 K at a heating rate of 20 K min^{-1} under airflow.

2.3.6. Electron Microscopy (SEM/TEM)

Electron Microscopes are an instrument, which uses beams of highly energetic electrons to create magnified images of tiny crystals or particles. An electron gum emits a beam of high-energy electron that travels through a series of magnetic lenses, which focus the electron to a very fine spot or sample. Interactions occur inside the irradiated sample. The electrons emitted from each point of the sample form the final image. The striking electron may remain unscattered and transmitted through the specimen (TEM) or may be elastically scattered (without loss of energy) or may be inelastically scattered (SEM) producing low energy secondary electrons. The main difference between SEM and TEM is that SEM sees contrast due to the topology of surface, whereas TEM projects all information in a two dimensional image, which however, is of sub nanometer resolution.

Scanning Electron microscope (SEM) has been used particularly to examine the topology and morphology of the sample. It is used for thick specimen. The incoming beam of electrons interacts with sample inelastically and causes ionization of the electron in the sample atom. These ionized electrons are termed as 'secondary electron'. The detector detects either secondary electron or back-scattered electrons as a function of the position of the primary beams. The secondary electrons have low energies (10-50 eV) and originate from the surface region of the sample whereas back-scattered electrons come from deeper and carry information on the composition of the sample, because heavy elements are more efficient scattered and appear brighter in the image. The SEM micrographs of the samples were obtained in a Leica Steroscan 440 instrument.

Transmission electron microscope uses thin specimens in which the unscattered transmitting electrons provide the image. TEM provide information about the size, shape and arrangement of particles in specimen. In TEM, a high intensity primary electron beam passes through a condenser to produce parallel rays, which impinge on the sample. As the attenuation of the beam depends on the density and the thickness, the transmitted electron form a two-dimensional projection of the sample mass, which is subsequently magnified by the electron optics to produce a so-called bright field image. The pore structures are also seen through TEM images. Transmission electron micrographs were recorded using a JEOL JEM-1200EX transmission electron microscope operating at 100 kV.

2.3.7. X-ray photoelectron spectra (XPS) studies

XPS is based on the photoelectric effect. Routinely used X-ray sources are Mg, Kα, ($h\nu$= 1253.6 eV) and Al Kα ($h\nu$= 1486.3 eV). In XPS one measures the intensity of photoelectronic N (E) as a function of their kinetic energy, E. Because a set of binding

energies is characterized for an element, XPS can be used to analyze the composition samples. Binding energies are not only element specific but contain chemical information as well: the energy levels of core electrons depend on the chemical state of the atom. Photoelectron peaks are labeled according to the quantum numbers of the level from which the electron originates. An electron coming from an orbital with main quantum number n, orbital quantum number 1 (0, 1, 2, 3… indicated as s, p, d, f) and spin quantum numbers (+1/2 or –1/2) is indicated as n^{l+s}. X-ray photoelectron spectra (XPS) were obtained using VG Microtech Multilab-ESCA-3000 spectrometer equipment with a twin anode of Al and Mg. All the measurements are made on as received powder samples using Mg *Kα* X-ray at room temperature. Base pressure in the analysis chamber was 4 x 10^{-10} Torr. Multichannel detection system with nine channels is employed to collect the data. The overall energy resolution of the instrument is better than 0.7 eV, determined from the full width at half maximum of $4f^{7/2}$ core level of gold surface. The errors in all B.E (binding energy) values were with in ± 0.1 eV.

2.3.8. UV-Visible spectroscopy

Absorption bands in the visible and ultra violet regions have proved interesting for study. The location of electronic band depends on the energy involved in electronic transition responsible for absorption. When the energy involved in the electronic transition is large, the adsorption will take place primarily in ultra violet. With smaller energies, however, the absorption will occur in the ultra or in the visible light region.

The diffuse reflectance UV-Vis spectra in the 200-800 nm ranges were recorded with a Shimadzu UV-2101 PC spectrometer equipped with a diffuse reflectance attachment, using $BaSO_4$ as a reference.

2.3.9. Acidity Measurement

The acidity and the acid strength distributed of the zeolite were measured by the temperature programmed desorption (TPD) of ammonia [14-16]. The sample 20-30 mesh size (~1.0 g) was activated in a flow of N_2 at 773 K for 8 h and cooled to room temperature. NH_3 gas (25 mL/min) was then passed continuously for a period of 30 min, and then the physically adsorbed NH_3 was desorbed by passing N_2 for 15 h (15 mL/min). Acid strength distribution was obtained by raising the temperature with a ramping rate of 10 °C/min, from 303 to 773 K in a number of steps in a flow of N_2 (10mL/min). The NH_3 evolved was trapped in HCl solution and titrated with standard NaOH solution. The higher the temperature required for desorption the stronger is the acidity of that portion of acid sites. Hence it provides a quantitative (total number of acid sites either Bronsted or Lewis) information about the acid sites.

2.3.10. Catalysis and analysis of products

Anhydrous AR grade chemicals were used without further purification. The liquid phase reaction was carried out in a 50 mL two necked flask attached to a condenser and a septum. The temperature of the reaction vessel was maintained using an oil bath. The reaction mixture was magnetically stirred and heated to the required temperature at atmospheric pressure. The product samples were withdrawn at regular intervals of time and analyzed periodically on a gas chromatography (HP 6890) equipped with a flame ionization detector and a capillary column (5 μm thick cross-linked methyl silicone gum, 0.2 mm x 50 m long). The products were also identified by injecting authentic samples and GCMS (Shimadzu 2000 A) and ^{1}H-NMR analysis.

Autogenously pressure-developing alkylation reaction was carried out in a 250 mL stainless Parr autoclave equipped with a stirrer and a temperature controller. The reaction mixture was flushed with nitrogen before heating to required temperature.

The percentage conversion of reactant is defined as the total percentage of reactant transformed. The rate of reactant conversion (TOF) was calculated as the moles of reactant converted per second per ml of active site. The selectivity to a product is expressed as the amount of a particular product divided by the amount of total products and multiplied by 100.

2.4. RESULTS AND DISCUSSIONS

The X-ray diffraction pattern of all the synthesized as well as modified zeolites matched with those in the literature (Fig 2.3 a, b, c, d). In addition, the crystallinity and phase purity of the zeolite samples as well as the absence of any amorphous matter within the pore structure were confirmed by XRD. Also, the XRD examination gave no evidence of structure damage or change of the zeolite as a result of various treatments. The surface area and scanning electron micrographs showed the absence of amorphous matter inside the channels and on the external **surface of the zeolites, respectively.**

Figure

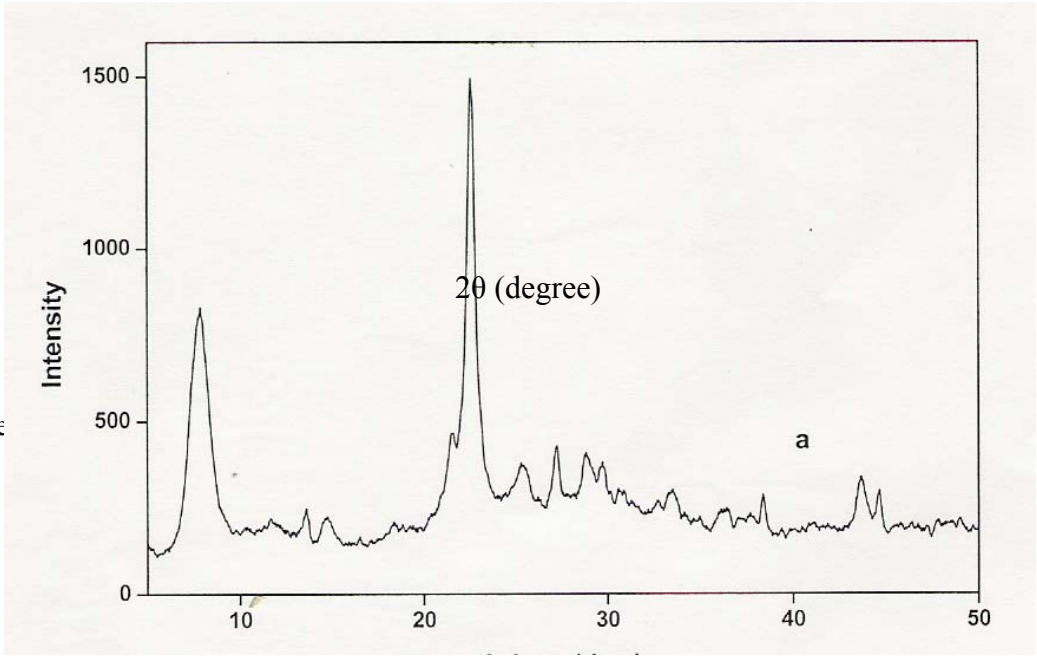

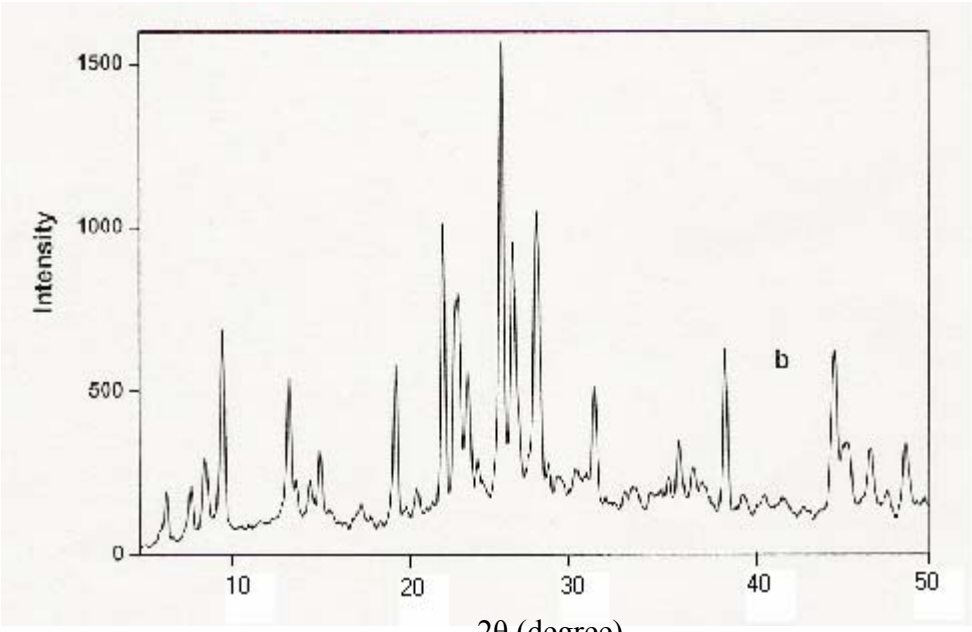

Figure 2.3b. X-Ray diffractogram of Zeolite H-mordenite

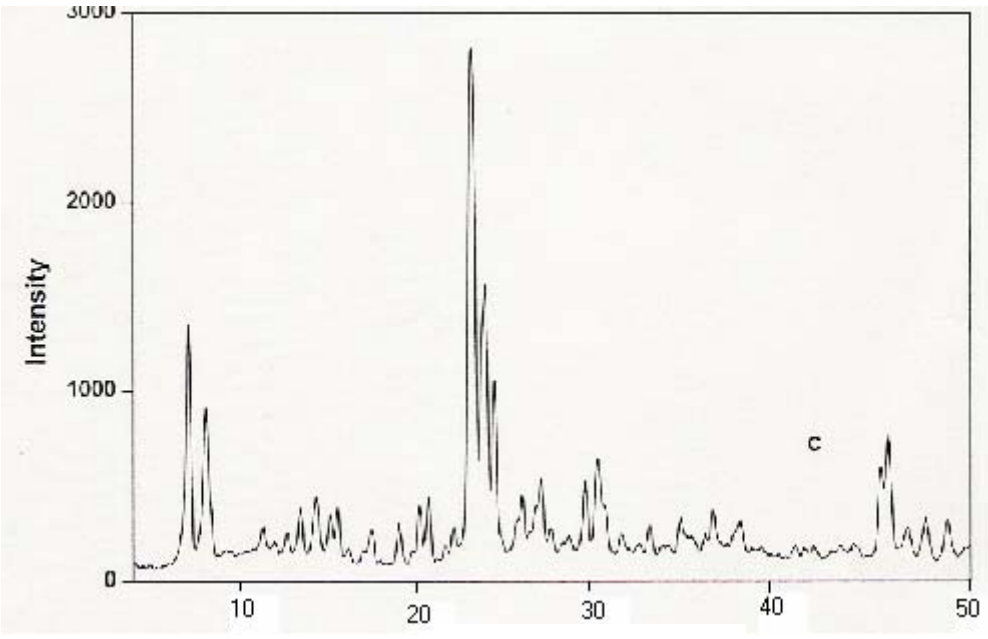

Figure 2.3c X-Ray diffractogram of Zeolite H-ZSM-5

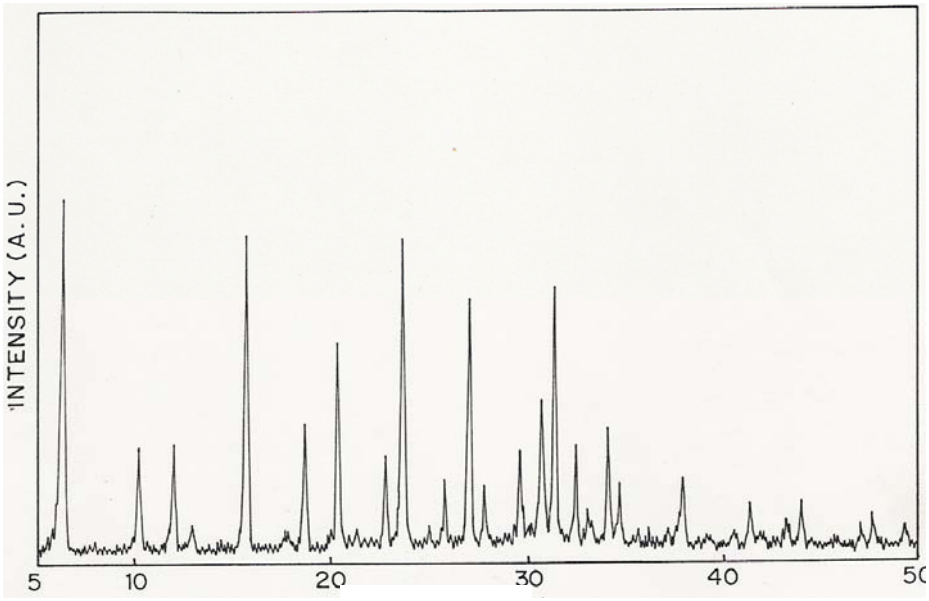

Figure 2.3d X-Ray diffractogram of Zeolite NH_4-Y

All the zeolite samples consisted of particles of about 0.2 – 1.0 μm size. The properties as well as chemical composition of all the zeolites used in the present study that are obtained by a combination of wet chemical analysis, are reported in Table 2.1a. The results of the stepwise thermal desorption of ammonia from the zeolite catalysts are presented in Table 2.1b. Though, TPD of ammonia, do not reveal the qualitative information about the acid sites, (whether Lewis or Bronsted), this method can suggest the weaker/stronger nature of acid sites depending upon the desorption range. Zeolite ZSM-5 and H-Y having SiO_2/Al_2O_3 ratio of 40 and 4.1, respectively, show acid sites concentration nearly similar (> 1.2 mmol/g). H-Mordenite, H-beta and RE-Y show acid sites concentration nearly similar (0.7 mmol/g). H-beta catalysts exhibit higher acid strength, which was evident from higher conversion of the reactant than other zeolite catalysts, which was having higher acid sites concentration. In general, higher the

desorption temperature of ammonia, stronger the strength of the sites present in the catalyst.

Table 2.1a. Properties of acidic zeolites

Catalyst	SiO_2/Al_2O_3 Molar ratio	Crystal Size (μm)	Surface Area[a] (m^2/g)	NH_3 Chemisorbed at 303 K (mmol/g)
H-ZSM-5	41.0	0.4	413	1.23
H-Mordenite	22.0	1.0	552	0.71
H-beta	26.0	0.5	645	0.75
H-Y	4.1	1.0	615	1.45
H-RE (70.6)Y[b]	4.1	1.0	659	0.75

[a] N_2 adsorption

[b] The percentage of RE^{3+} exchange in H-Y is given in the parenthesis.

Table 2.1b Acid sites distribution

Zeolites	NH_3 desorbed (mmol/g) at different temp. (K)					NH_3 Chemisorbed at 303 K (mmol/g)
	303-353	353-433	433-513	513-653	653-773	
H-ZSM-5	0.55	0.16	0.05	0.26	0.21	1.23
H-mordenite	0.20	0.17	0.15	0.12	0.07	0.71
H-beta	0.14	0.24	0.05	0.16	0.16	0.75
H-Y	0.29	0.55	0.49	0.11	0.01	1.45
H-RE (70.6)Y	0.17	0.10	0.26	0.11	0.10	0.74

Results of Structural characterization of mesoporous alumina and modified mesoporous alumina show that the metal complex is firmly held inside the pore channels of mesoporous alumina and hence the present materials are applied in the liquid phase epoxidation reaction of styrene and cyclohexene to see the catalytic activity of the catalyst. The results obtained from the epoxidation reaction of neat as well as immobilized complexes clear that mesoporous alumina functionalized metal complexes show an enhanced activity (calculated in terms of turn over number, TON) and selectivity towards the desired epoxide product than the neat metal complexes. Since the support alumina had a high surface area and moderate pore size, we believe that the confined environment of the metal complex avoids undesirable side reactions like the over oxidation process, as observed with the neat complexes, leading to better activity as well as selectivity to epoxides [17,18]. However, as mentioned earlier, it is inappropriate to compare the catalytic results under neat as well the heterogenized conditions, since the coordination sphere of both complexes is different. Among olefins, styrene conversion is higher than cyclohexene, which may be due the comparatively easier side chain oxidation than the reactions in the aromatic ring. Interestingly, even though benzaldehyde was the major product obtained during styrene epoxidation, kinetic studies revealed that the formation of phenyl acetaldehyde, an isomerized product of styrene epoxide, is not formed over immobilized catalysts while under neat catalysts a significant amount of its formation is noted. Hence, it is reasonable to assume that the reaction proceeds under different mechanisms over the homogenous complexes and heterogeneous catalysts. Further, in order to ascertain whether the activity of the immobilized catalysts arise from true heterogeneous catalysts, the stability of metal complexes were probed by performing typical leaching studies. For that, the catalyst was separated from the reaction mixture

after a definite period of time (viz. 2 h) and the hot filtrate was probed for further reactions. Interestingly, it was found that the conversion rate essentially gets terminated after the removal of the catalyst sample, which confirms that the present anchored metal complexes are stable in the reaction medium and are not prone for leaching.

2.5. CONCLUSION

Zeolites such as Na-beta, and Na-ZSM-5 have been synthesized by hydrothermal method. The commercially obtained Na-Y and Mordenite along with the synthesized Na-beta, Na-ZSM-5 were ion exchanged with NH_4NO_3 solution and activated at 793 K for 6 h to get respective H-forms. Synthesized zeolites were characterized by wet chemical analysis, XRD, N2 adsorption, EDX, and SEM analysis. Mesoporous materials were prepared by reflux method. Mesoporous aluminas were used as the basic supports for organo functional such as APTES. The attachment of organo functional molecules to the mesoporous alumina walls has been achieved by the direct reaction of surface hydroxyl groups with reactive alkoxy groups of organosilanes. Fraction of organo functionalized alumina atom has been varied from 0.03 to 0.3 in the synthesis gel to get maximum concentration of the organo-functionalized group inside the mesopores. It was observed that above the optimum level of concentration of organo functionalized alumina atom, there is a gradual decrease in the structural integrity. XRD, FT-IR, UV-vis, XPS, N_2 adsorption-desorption and thermal analysis techniques were used for the characterization of mesoporous materials.

\2.6. REFERENCES

1. R. L. Wadlinger, G. T. Kerr, E. J. Rosinski, *US Pat*. 3,308,069 (1969)
2. J. Perez-Pariente, J. A. Martens, P. A. Jacobs, *Appl. Catal*. 31 (1978) 35.
3. M. M. J. Treacy, J. M. Newsam, *Nature*, 332 (1988) 249.
4. J. M. Newsam, M. M. J. Treacy, W. T. Koetsier, C. B. de Gruyter, *Proc. Royal. Soc. Lond.* A. 420 (1988) 375.
5. R. Szostak, *Handbook of Molecular Sieves*, Van Nostrand Reinhold, New York (1992) 92.
6. R. J. Argauer, G. R. Landolt, (1972) "Crystalline Zeolite ZSM-5 and Methods of Preparing." *U.S. Patent* 3, 702 886
7. R. Szostak (1989) "*Molecular Sieves: Principal of Synthesis and Identification*", New York: Van Nostrand, *Reinholg Catalysis Series.*
8. Bekkum H. V., Flanigen E. M., Jansen J. C., (Eds) (1991), "Introduction to Zeolite Science and Practice." *Stud. Sur. Sci. Catal*." Netherlands: Elsevier, 58.
9. N. Y. Chen, R.G. William, G. D. Frank (1989) *Shape selective Catalysis in Industrial Applications, Chemical Industries.* New York: Marcel Dekker Inc. 36.
10. D. W. Breck, *US Pat.* 3,130,007 (1964).
11. L. Frunza, H. Kosslick, H. Landmesser, K. Hoft, R. Fricke, *J. Mol. Catal. A Chem.*123 (1997) 179.
12. E. F. Murphy, A. Baiker, *J. Mol. Catal. A. Chem*. 179 (2002) 233-241.
13. J. B. Cohen, L. H. Schwartz, *Diffraction from Materials*, Academic Press, New York 1977.

14. M. Chamumi, D. Brunel, F. Fajula, P. Geneste, P. Moreau, J. Solof, *Zeolites* 14 (1994) 283.

15. A. P. Singh, D. Bhattacharya, *Catal. Lett*. 32 (1995) 327

16. A. P. Singh, D. Bhattacharya, S. Sharma*, Appl. Catal. A: General* 150 (1997) 767.

17. S. Shylesh, A. P. Singh, *J. Catal*. 228 (2004) 333.

18. T. Joseph, D. P. Sawant, C. S. Gopinath, S. B. Halligudi, *J. Mol. Catal. A. Chem.* 184 (2002) 289.

CHAPTER 3

ACYLATION REACTIONS OF AROMATICS

3.1. PROPIONYLATION OF PHENOL TO 4-HYDROXYPROPIOPHENONE OVER ZEOLITE H-BETA

3.1.1. INTRODUCTION

4-Hydroxypropiophenone and 2-Hydroxypropiophenone are used as intermediate for the manufacture of perfumes, pharmaceuticals and as UV adsorbent [1]. *O*- and *p*-acylated products of phenol have been made from the direct reaction of phenol with acylating agent or by the Fries rearrangement of aryl esters using Lewis acid catalyst, $AlCl_3$ [2-4]. The use of conventional catalyst, $AlCl_3$, causes important environmental problems and involves a tedious work up procedure. Zeolites have been used in the acylation of aromatics [5-17] due to their activity, shape selectivity, reusability, and easy separation from the reaction products. Recently few studies have been reported on the direct acetylation of phenol over zeolite H-ZSM-5 [18-20] and Fries rearrangement of phenyl acetate over zeolite H-beta [21-22]. However, there is no report yet on the direct propionylation of phenol using zeolite catalysts and particularly H-beta. It is reported that Fries rearrangement of phenylacetate on HZSM-5 produces lower yield of smaller p-isomer than the o-isomer [18,23,24-26] and hence the second route (direct acylation of phenol) is preferable to achieve the higher yield for *p*-isomer. A reaction scheme is proposed for the propionylation of phenol with propionyl chloride using zeolite H-beta as catalyst which explain the formation of the main reaction products *e.g.* PP, 4-HPP, 2-HPP and 4-PXPP including the difference in the formation of 4-HPP and 2-HPP. In order to confirm the reaction pathways, additional experiments such as Fries rearrangement of PP and propionylation of phenol with equimolar quantity of PP were carried out at 413 K using zeolite H-beta. The objective of the present work is to replace the conventional Lewis acid catalyst $AlCl_3$, with the solid zeolite catalyst and to achieve the 4-HPP in one

step by the propionylation of phenol over solid zeolite H-beta catalyst. In addition, we report the results of the effect of various zeolite catalysts, duration of the run using zeolite H-beta, acidity of the zeolite catalysts, SiO_2/Al_2O_3 ratio, catalyst concentration, reaction temperature, and molar ratio of the reactants and reuse of the zeolite H-beta on the formation of 4-HPP. The results obtained over various zeolites are compared with the conventional catalyst, $AlCl_3$.

3.1.2. EXPERIMENTAL

3.1.2.1. Materials

Zeolites Na-Y and H-mordenite were obtained from Laporte Inorganics, Cheshire, U.K. Zeolites ZSM-5 and beta were prepared using the methods described in the literature [27-28]. The synthesized zeolites were washed with deionized water, dried and calcined at 813 K for 16 h in the presence of air to eliminate the organic templates from the zeolite channels. The resultant samples were thrice NH_4^+-exchanged for 8 h at 353 K. The NH_4^+-exchanged samples were again calcined at 823 K for 8 h to get their protonic forms. RE-Y was prepared from Na-Y by exchange with 1 M NH_4NO_3 (three exchanges, 353 K, 8 h) and thus the resulting NH_4-Y was treated with 5 % rare earth chloride solution by following the analogous method employed for other zeolites to get their protonic forms.

3.1.2.2. Characterization

The SiO_2/Al_2O_3 ratio of various zeolites and degree of ion- exchange were carried out by a combination of wet and atomic absorption methods (Hitachi 800). X-ray powder diffraction (XRD) was carried out on a Rigaku, D-Max/III-VC model using the CuK_α

radiation and was used to evaluate the peak positions of various zeolite samples. The surface area of the catalysts was measured by nitrogen BET method using an area meter. The size and morphology of the zeolite catalysts were estimated by scanning electron microscope (Cambridge Stereoscan 400).

3.1.2.3. Acidity measurements

Temperature programmed desorption measurements were carried out to measure the acid strength of the zeolite catalysts using ammonia as an adsorbate (Table.2.1 a, b) [29,30]. In a typical run, 1.0 g of a calcined sample was placed in a quartz tubular reactor and heated at 773 K under a nitrogen flow of 50mL/ min. for 4 h. The reactor was then cooled to 303 K and adsorption conducted at that temperature by exposing the sample to ammonia for 30 min. Physically adsorbed ammonia was removed by purging the sample with a nitrogen stream flowing at 50 mL/min. for 15 h at 303 K. Acid strength distribution was obtained by raising the catalyst temperature (10 °C/min) from 303 K to 773 K in a number of steps in a flow of nitrogen (10 mL/min.). The NH_3 evolved was trapped in an HCl solution and titrated with a standard NaOH solution (Table.2.1 a, b).

3.1.2.4. Catalytic reactions

The propionylation reactions were carried out batch wise in a glass reactor. Typically, 0.5 g of catalyst, 0.106 moles of phenol and 0.035 moles of PC were introduced. The reaction was continued for 4 h at 413 K. Product samples were analysed by a gas-chromatograph (HP 6890) equipped with a flame ionisation detector and capillary column (50 m * 0.2 mm) of methyl silicone gum. The products were characterized by GC-MS and compared with authentic samples.

3.1.3. RESULTS AND DISCUSSION

The properties of zeolite catalysts are given in Table.2.1a, b. The X-ray diffraction pattern of the zeolites match well with the literature values and are found to be highly crystalline. The scanning electron microscopy and surface area show that there is no pore blocking or amorphous material inside the channels and on the external surface of the zeolites.

3.1.3.1. Activity of various catalysts

The propionylation of phenol with PC over H-beta, RE-Y, H-Y, H-Mordenite, H-ZSM-5 and conventional catalyst $AlCl_3$ is investigated under atmospheric pressure at 413 K. The results of 4 h reaction time are summarised in Figure.3.1. As is evident from the Figure.3.1, the conversion of phenol remains nearly constant due the rapid formation of primary product phenylpropionate (PP) (eq.3.1).

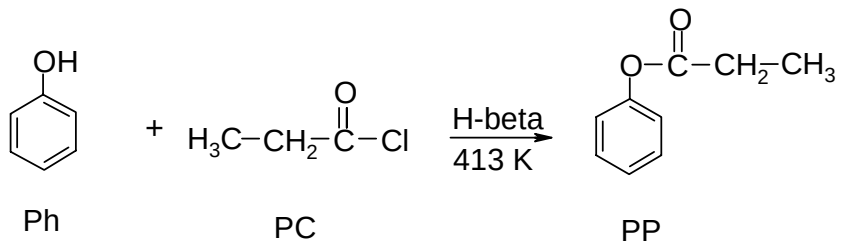

····· eq. 3.1

The formation of various products (2-HPP, 4-HPP and 4-PXPP) is established by different reaction pathways (eq.3.1-3.7) [18-20]. Zeolite H-beta is found to be the most active in the formation of ring products and selective for 4-HPP among 4-HPP and 2-HPP (4-HPP/2-HPP = 1.9) catalyst to achieve higher yields of 2-HPP (2.8 wt. %) and 4-HPP

(5.3 wt. %) compared to the other zeolite catalysts. The conventional catalyst, $AlCl_3$, is less active and selective (4-HPP/2-HPP = 0.9) than H-beta and a higher yield of others

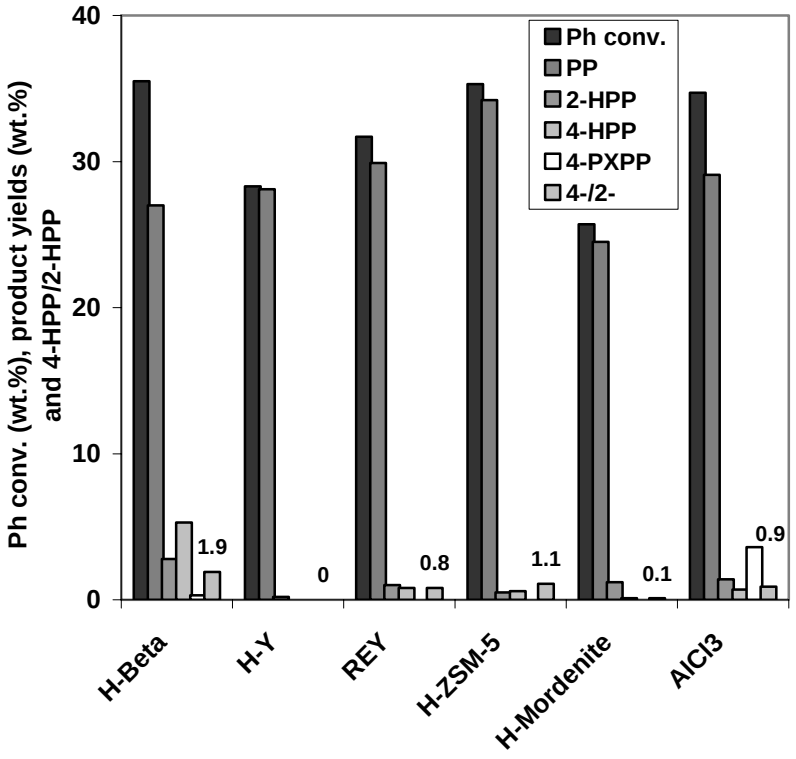

Figure.3.1. Propionylation of phenol over various catalysts; Reaction conditions: Catalyst (g) = 0.5; phenol (mol) = 0.106; PC (mol) = 0.035; phenol/PC (molar ratio) = 3; reaction temp. (K) = 413; reaction time (h) = 4. PP = phenylpropionate; Ph = Phenol; 2-HPP = 2-hydroxypropiophenone; 4-HPP = 4-hydroxypropiophenone; 4-PXPP = 4-propionyloxypropiophenone; 4-/2- = isomer ratio of 4-HPP/2-HPP.

(3.6 wt. %) is obtained over $AlCl_3$ due to its non shape-selective character. RE-Y sample produced lower yields of 2-HPP (1.0 wt. %) and 4-HPP (0.8 wt. %) than H-beta. However, RE-Y was found to be more active than H-Y, H-Mordenite and H-ZSM-5. The higher activity of RE-Y in the formation of 2-HPP and 4-HPP compared to H-Y may be attributed to its higher strength of acid sites, which are generated by the exchange of Re^{+3}-cations in H-Y (Table.2.1 a, b) [12]. The lower activity of H-ZSM-5 (pore size = 6.0

X 5.7 Å and 5.6 X 5.4 Å) in the formation of 2-HPP and 4-HPP may be due to its small pore openings than the size of the various reactants (intermediates), which are formed by different reaction pathways in the propionylation of phenol (eq.3.1-3.7). The catalysts used in the study show the following decreasing order of activity in the formation of hydroxypropiophenones (2-HPP and 4-HPP):

H-Beta > $AlCl_3$ > RE-Y > H-Mordenite > H-ZSM-5 > H-Y

3.1.3.2. Acidity vs 2-HPP and 4-HPP formation

The effect of the number of acid sites and acid strength distribution of various catalysts on the formation of 2-HPP and 4-HPP in the propionylation of phenol are shown in Table.2.1 a, b and Figure.3.1. The formation of 2-HPP and 4-HPP over various catalysts not only seems to be dependent on the number of acid sites but also on their strength. On the very strong sites of the H-beta the propionylation of phenol and intermediates produced during the propionylation such as PP and 4-PXPP transformed into the expected 2-HPP and 4-HPP (eq.3.1-3.7), which was not the case on the weak acid sites of the H-Y and H-mordenite (Table.2.1 a, b) and Figure.3.1). The higher yields of 2-HPP and 4-HPP obtained over zeolite H-beta could be related to the presence of very strong acid sites compared to the other zeolite catalysts (Table.2.1 a, b and Figure 3.1).

The results indicate that the H-beta has high activity in the formation of 2-HPP and 4-HPP and selectivity for 4-HPP (4-HPP/2-HPP = 1.9) compared with other catalysts used in this reaction and hence further studies were carried out using zeolite H-beta to see the influence of various parameters on the yields of 2-HPP and 4-HPP and selectivity for 4-HPP in the propionylation of phenol.

3.1.3.3. Duration of the run

Figure 3.2 shows the conversion of phenol, product yields and ratio of 4-HPP/2-HPP at 413 K using zeolite H-beta as a function of reaction time. It can be seen from

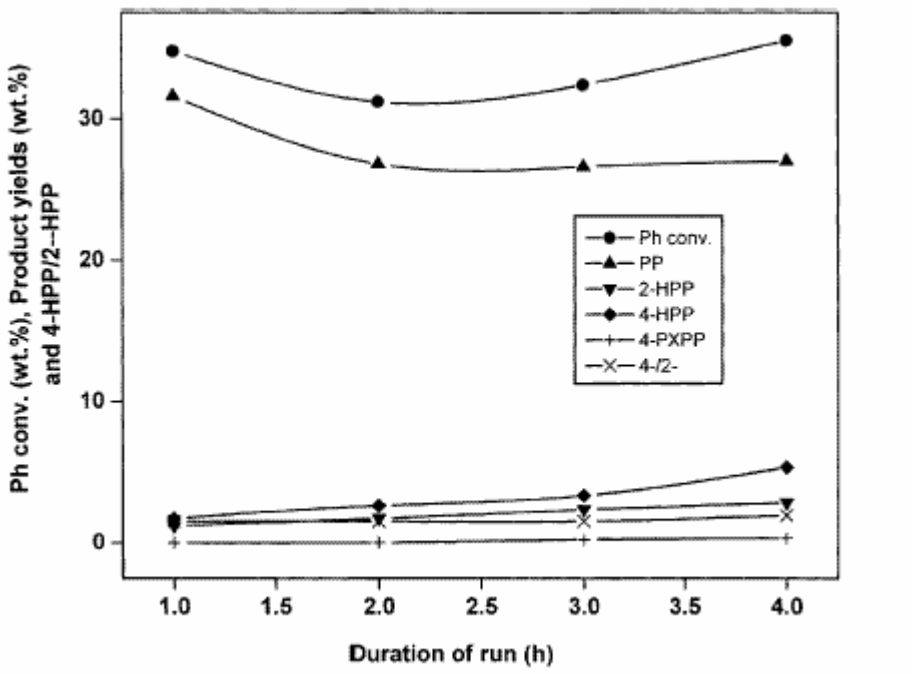

Figure.3.2. Conversion of Phenol and product yields as a function of reaction time; Reaction conditions: duration of run (h) = 4; PP = phenylpropionate; Ph = Phenol; 2-HPP = 2-hydroxypropiophenone; 4-HPP = 4-hydroxypropiophenone; 4-PXPP = 4-propionyloxypropiophenone; 4-/2- = isomer ratio of 4-HPP/2-HPP

the Figure.3.2 that the conversion of phenol remains practically constant due to rapid formation PP. However, the yield of 2-HPP, 4-HPP and 4-PXPP increases gradually but slowly with the progress of the reaction. The ratio of 4-HPP/2-HPP also increases from 1.5 to 1.9 when the reaction time was increased from 1 h to 4 h, respectively. From the Figure.3.2 it can be concluded that the O-acylation of phenol is much more rapid than the C-acylation [18-20]. Under the reaction conditions PP was the predominant product along

with 2-HPP, 4-HPP and 4-PXPP and the conversion of phenol was roughly proportional (32.4 wt %) to the reactant molar ratio (Ph/PC = 3).

3.1.3.4. Influence of SiO_2/Al_2O_3 ratio of H-beta

H-beta used for the propionylation of phenol differs only in the SiO_2/Al_2O_3 that is in its acid strength. Increasing the SiO_2/Al_2O_3 ratio and thus decreasing the number of acid centres leads to a decrease in the yield of the ring products i.e. the decrease in direct propionylation of phenol to ring products or transformation of O-acylated products to C-acylated products. The 4-HPP/2-HPP ratios also change by varying the SiO_2/Al_2O_3 of H-beta (Figure.3.3). The present study demonstrates that the conversion of phenol to the C-acylated products decreases as the SiO_2/Al_2O_3 ratio increases from 26 to 60 (Figure.3.3).

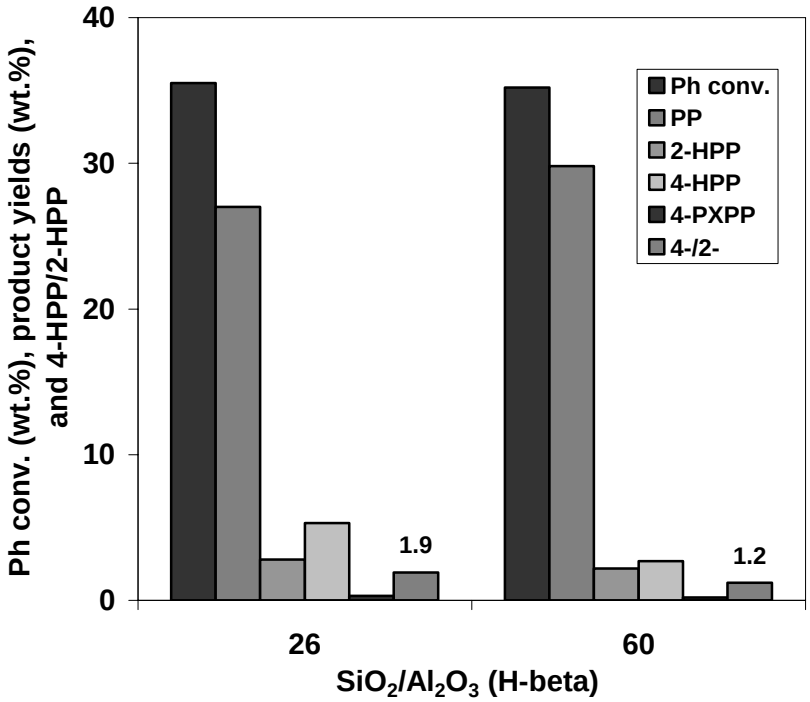

Figure.3.3. Influence of SiO_2/Al_2O_3 ratio of H-beta on the conversion of Ph, product yields and 4-/2- isomer ratio; Reaction conditions: reaction time (h) = 4; PP = phenylpropionate; Ph =

Phenol; 2-HPP = 2-hydroxypropiophenone; 4-HPP = 4-hydroxypropiophenone; 4-PXPP = 4-propionyloxypropiophenone; 4-/2- = isomer ratio of 4-HPP/2-HPP

3.1.3.5. Influence of catalyst concentration

Figure 3.4 shows the conversion of phenol, yields of PP, 2-HPP, 4-HPP and 4-PXPP and 4-HPP/2-HPP ratio as a function of H-beta to phenol ratio (wt./wt.) in the propionylation of phenol. The H-beta to phenol ratios are obtained by varying the amount of H-beta and keeping the constant concentration of phenol. The total surface area available for the reaction depends upon the loading of the catalyst. The conversion of phenol remains practically constant at all H-beta to phenol ratios. However, the yield of O-acylated product (PP) decreases from 35.3 wt. % to 26.0 wt. % with the increase in H-beta to phenol ratio (wt. / wt.) from 0.01 to 0.10. The decrease in the O-acylated product and simultaneously increase in the ring products with the increase in H-beta to phenol ratio may be due to the increase in medium and strong Bronsted acid sites which are available for the reaction. In the absence of catalyst mainly the O-acylated product is noticed. In addition, the 4-HPP/2-HPP ratio increases from 0.5 to 2.1 with the enhancement of H-beta to phenol ratio from 0.01 to 0.10, respectively. These results indicate that H-beta catalyzes directly the propionylation of phenol to some extent and mainly the transformation of O-acylated product to ring acylated products by various reactions (eq. 3.1-3.7).

3.1.3.6. Influence of reaction temperature

Figure 3.5 indicates the influence of reaction temperature on the product yields and ratio of 4-HPP/2-HPP in the propionylation of phenol using zeolite H-beta (SiO_2/Al_2O_3 = 26). As the temperature was increased from 403 K to 443 K, the transformation of PP into 2-HPP, 4-HPP and 4-PXPP increased significantly by various reaction pathways (eq.3.1-3.7). However, the possibility of conversion of small amount of phenol into products cannot be ruled out. The PP yield (converted to products) decreased from 35.3 to 26.8 wt. % when temperature was raised from 403 to 443 K. The corresponding yields of 2-HPP, 4-HPP and 4-PXPP increased simultaneously from 0.6 to 2.4 wt. %, 1.3 to 3.8 wt. % and 0.1 to 0.5 wt. %, repectively, which confirms the transformation of PP into products. The ratio of 4-HPP/2-HPP decreased from 2.0 to 1.5 with the increase in reaction temperature.

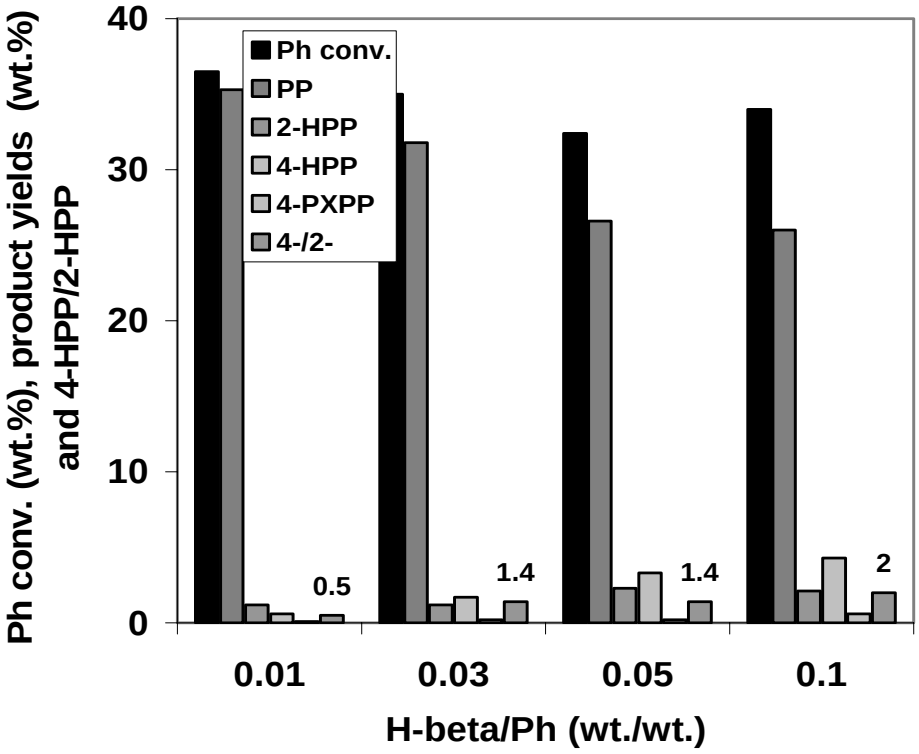

Figure.3.4. Influence of H-beta/Ph (wt./wt.) ratio on the Ph conversion, product yields and 4-/2-isomer ratio; Reaction conditions: reaction time (h) = 3; PP = phenylpropionate; Ph = Phenol; 2-HPP = 2-hydroxypropiophenone; 4-HPP = 4-hydroxypropiophenone; 4-PXPP = 4-propionyloxypropiophenone; 4-/2- = isomer ratio of 4-HPP/2-HPP

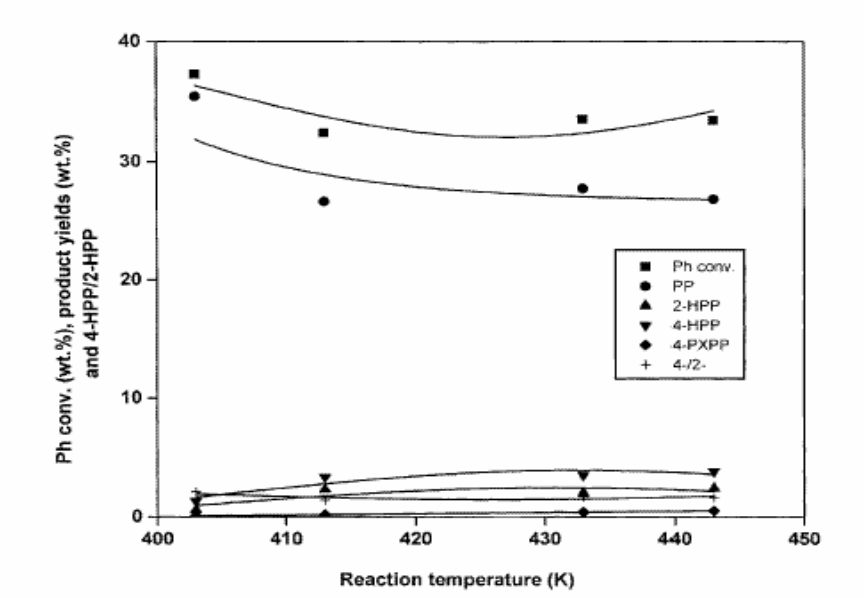

Figure.3.5. Influence of reaction temperature on the conversion of Ph, product yields and 4-/2-isomer ratio; Reaction conditions; reaction time (h) = 3; H-beta (SiO_2/Al_2O_3 = 26) g = 0.5; PP = phenylpropionate; Ph = Phenol; 2-HPP = 2-hydroxypropiophenone; 4-HPP = 4-hydroxypropiophenone; 4-PXPP = 4-propionyloxypropiophenone; 4-/2- = isomer ratio of 4-HPP/2-HPP

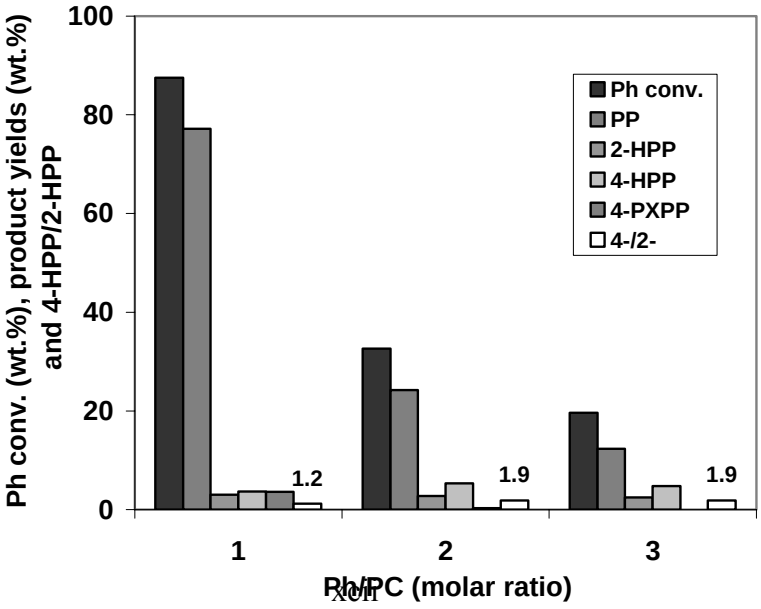

Figure.3.6. Influence of Ph/PC molar ratio on the conversion of Ph, product yields and 4-/2-isomer ratio; Reaction conditions: reaction time (h) = 4; PP= phenylpropionate; Ph = Phenol; 2-HPP = 2-hydroxypropiophenone; 4-HPP = 4-hydroxypropiophenone; 4-PXPP = 4-propionyloxypropiophenone; 4-/2- = isomer ratio of 4-HPP/2-HPP

3.1.3.7. Influence of phenol to PC molar ratio

A series of catalytic experiments were performed to investigate the effect of the phenol to PC molar ratio on the yields of O-acylated (PP), C-acylated ring products (2-HPP, 4-HPP and 4-PXPP) and 4-HPP/2-HPP ratio (Figure.3.6). The phenol to PC molar ratio was varied in the range of 1 to 3 by keeping the constant concentration of phenol. It is evident that the proportion of PC in the reaction mixture greatly affects the conversion of

phenol, product yields and ratio of 4-HPP/2-HPP. As the phenol/PC ratio increases from 1 to 5, the conversion of phenol decreases from 87.5 to 19.6 wt. %. Simultaneously, the transformation of PP into 4-PXPP is also affected greatly by the change in the phenol to PC ratio. The formation of 4-PXPP (by the autoacylation of PP) decreases from 3.6 wt. % to 0 wt. % and the 4-HPP/2-HPP ratio increases from 1.2 to 1.9 with the increase in phenol/PC molar ratio from 1 to 5, respectively. The formation of higher yield of 4-PXPP at lower ratio of phenol/PC may be attributed to the presence of higher concentration of PP in the reaction mixture.

3.1.3.8. Recycling

To conclude this study, the H-beta was examined for recycling in the propionylation of phenol. After a first experiment, the zeolite was separated from the reaction mixture, washed with acetone, dried at 383 K for 4 h and regenerated by calcination in air at 773 K for 16 h. As can be seen in Table 3.1, the recycled material was less active in the

formation of C-acylated products than the fresh sample. X-ray powder diffractometry shows that during the catalytic tests the structure of H-beta remains undamaged.

Table.3.1. Effect of recycling[a]

Catalyst (g)	Ph conv. (wt. %)[b]	Product yields (wt. %)[c]				4-/2-HPP[d]	Crystallinity of catalyst
		PP	2-HPP	4-HPP	4-PXPP		
Fresh	35.5	27.1	2.8	5.4	0.3	1.9	100
1st recycle	34.2	27.2	2.5	4.3	0.3	1.7	100
2nd recycle	35.7	28.2	2.5	4.2	0.2	1.6	100

[a] Reaction conditions: Catalyst H-beta (g) = 0.5; Phenol (mol) = 0.106; PropionylChloride (mol) = 0.032; reaction time (h) = 4

[b] Phenol conversion (wt.%), [c] PP = Phenylpropionate; 2-HPP = 2-hydroxypropiophenone; 4 - hydroxypropiophenone; 4-PXPP =4-propionyloxypropiophenone, [d] Ratio of 4-hydroxypropiophenone/2-hydroxypropiophenone

3.1.3.9. Reaction pathways

In order to clarify the reaction pathways for the formation of phenol, PP, 2-HPP, 4-HPP and 4-PXPP in the propionylation of phenol, additional experiments such as Fries rearrangements of PP (Figure.3.7) and propionylation of phenol with PP (Figure.3.8) were carried out at 413 K using zeolite H-beta as catalyst. Based on additional experimental results, various reaction schemes could be postulated as depicted in eq.3.1-3.7.

The Fries rearrangements of PP (Figure3.7) and propionylation of phenol with PP (Figure.3.8) show that 2-HPP and 4-HPP are formed through different reaction pathways

which are also in agreement with the previous studies on the acylation of phenol [18-20]. The formation of 2-HPP may be attributed through direct C-propionylation of phenol with PC (eq.3.2), propionylation of phenol with with equimolar quantity of PP (eq.3.3) and Fries rearrangement of PP (eq.3.4).

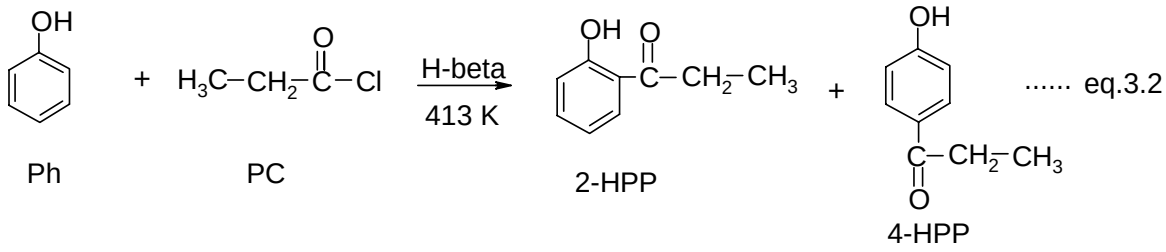

..... eq.3.2

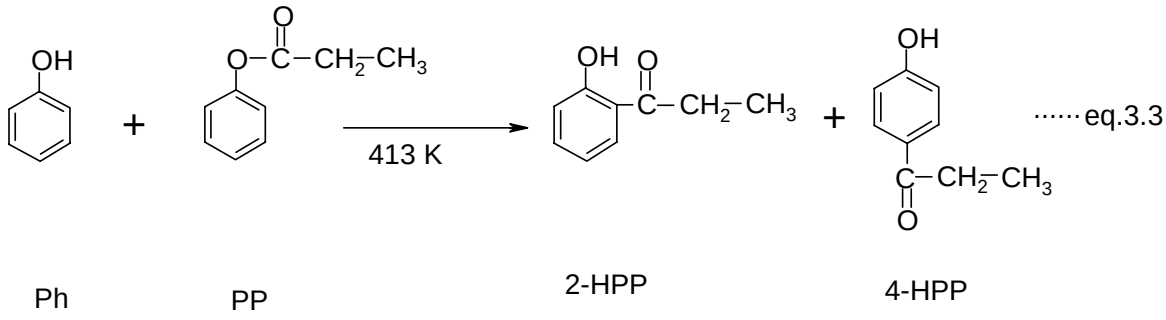

..... eq.3.3

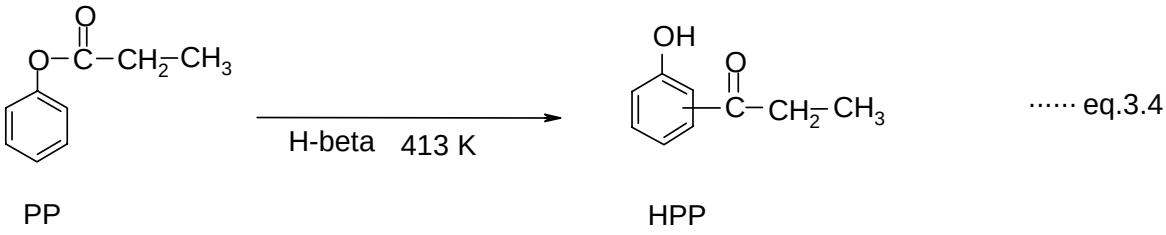

..... eq.3.4

The Fries rearrangement of PP affords a mixture of 2-HPP and 4-HPP, together with phenol and 4-PXPP. The formation of phenol results from the decomposition of PP

(eq.3.5) or bimolecular reaction of two PP molecules (eq.3.6) [19,22] or from the autoacylation of phenol with PP (eq.3.3) [19]. 4-PXPP results from the bimolecular reaction of two PP molecules (eq.3.6) [18,19].

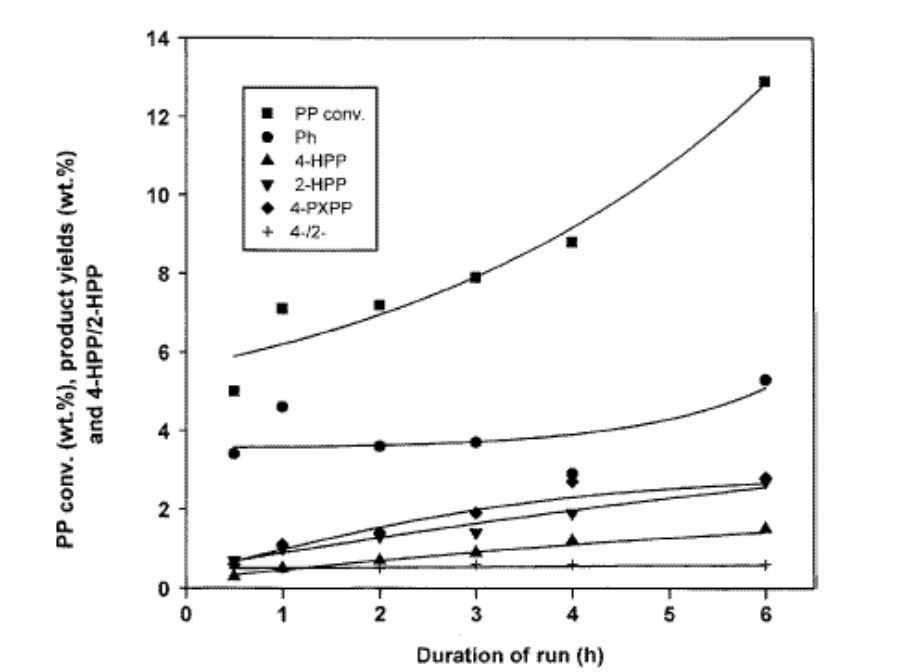

Figure.3.7. Fries rearrangement of phenylpropionate over H-beta; Reaction conditions: H-beta (g) = 0.5; PP (mol) = 0.075; reaction temp.(K) = 413; duration of Run (h) = 6. PP = phenylpropionate; Ph = Phenol; 2-HPP = 2-hydroxypropiophenone; 4-HPP = 4-hydroxypropiophenone; 4-PXPP = 4-propionyloxypropiophenone; 4-/2- = isomer ratio of 4-HPP/2-HPP

.

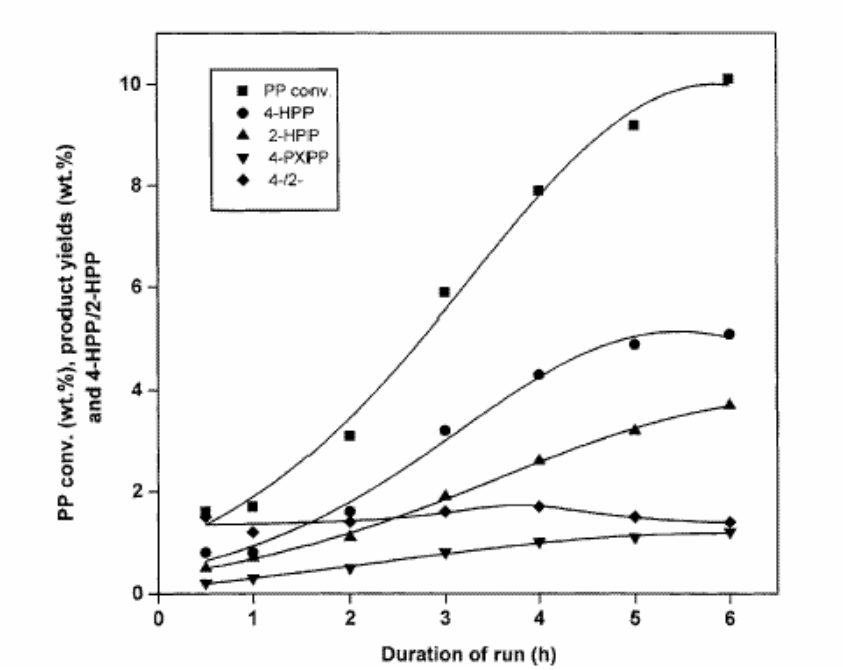

Figure.3.8. Transformation of PP + Ph mixture on H-beta; Reaction conditions: H-beta (g) = 0.5; PP (mol) = 0.059; Ph (mol) = 0.059; PP/Ph (molar ratio) = 1; reaction temp.(K) = 413; duration of run(h) = 6; PP = phenylpropionate; Ph = Phenol; 2-HPP = 2-hydroxypropiophenone; 4-HPP = 4-hydroxypropiophenone; 4-PXPP = 4-propionyloxypropiophenone; 4-/2- = isomer ratio of 4-HPP/2-HPP

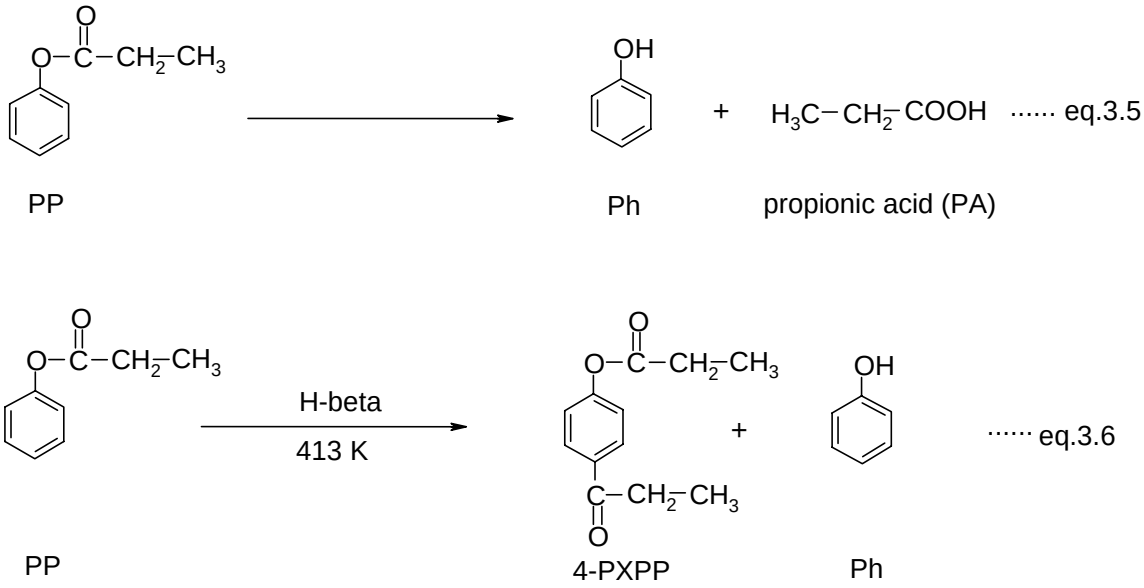

The results of the Fries rearrangement of PP are presented in Figure.3.7. The conversion of PP and product yields enhance gradually and significantly for the entire 6 h on stream but did not effect the isomer ratio (4-/2-HPP = 0.5) (Figure.3.7). The formation of 2-HPP was much more than 4-HPP at all reaction time. The higher ortho-selectivity may be attributed to the easy migration of propionyl cation to the ortho-position than para. The formation of 2-HPP from the phenol and PP (produced during Fries rearrangement) could not be ruled out and hence these results confirm that formation of higher yield of 2-HPP takes place either by the Fries rearrangement of PP or by the propionylation of phenol with PP or by both the routes (eq.3.3, 3. 4).

In order to re-establish the reaction path for the formation of 2-HPP, the propionylation of phenol was carried out for 6 h as a function of reaction time with the equimolar quantity of PP (eq.3.3) at similar reaction conditions those details in Figure.7 (Fries rearrangement). The reaction leads to a mixture of products such as 2-HPP, 4-HPP and 4-PXPP. The conversion of PP and simultaneously the yields of all the products increase linearly with the progress of the reaction where as the ratio of 4-/2-HPP were not affected significantly. In contrast to the Fries rearrangement results (discussed above)(Figure.3.7), the formation of 2-HPP was lower and consequently the isomer ratio was found to be higher (4-HPP/2-HPP = 1.5) in the propionylation of phenol with PP. These results further confirm that the formation of 2-HPP results from both the routes (eq.3.3, 3.4).

A possible route for 4-HPP formation is through the reaction of 4-PXPP (produced from the bimolecular reaction of PP, (eq.3.6) with the zeolite hydroxyl groups or trace amount of water present in the reaction mixture (eq.3.7) [22]. However, the formation of

small amount of 4-HPP through the direct propionylation phenol with PC (eq.2.2) and propionylation of phenol with PP (eq.3.3) could not be ruled out [18].

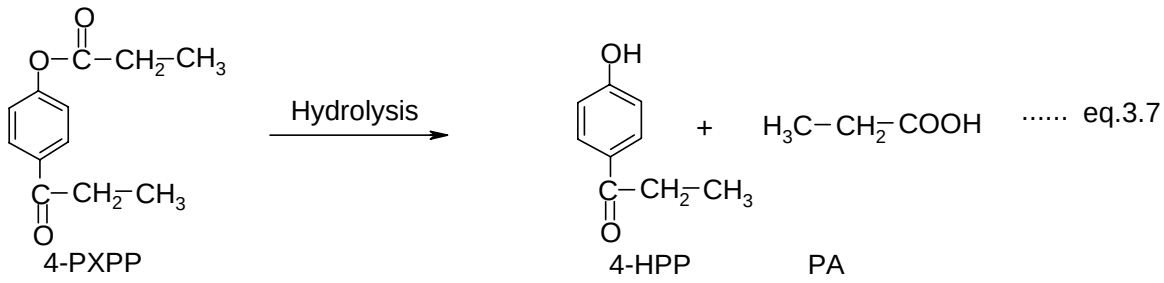

..... eq.3.7

The increase in the yields of 4-HPP and 4-PXPP with the reaction time in the Fries rearrangement of PP (Figure.3.7) and propionylation of phenol with PP (Figure.3.8) confirm this hypothesis.

3.1.4. CONCLUSIONS

In summary, zeolite H-beta catalyses the propionylation of phenol with PC efficiently compared to other catalysts, which leads to the formation of 4-HPP selectively among 2-HPP and 4-HPP. The conventional catalyst, $AlCl_3$, is less active and selective (4-HPP/2-HPP = 0.9) than H-beta (4-HPP/2-HPP = 1.9). The higher activity of H-beta in the formation of 2-HPP and 4-HPP could be related to the presence of very strong acid sites than other zeolite catalysts. The higher yields of hydroxypropiophenone (2-HPP and 4-HPP) could be achieved by increasing the values of reaction time, H-beta to PC ratio (wt./wt.) and reaction temperature. The H-beta was recycled two times and a decrease in the yields of 2-HPP and 4-HPP was observed after each recycle in the propionylation of phenol. The plausible pathways for the formation of phenol, PP, 2-HPP, 4-HPP and 4-PXPP are confirmed by the additional experiments such as Fries rearrangement of PP and

propionylation of phenol with PP using zeolite H-beta as catalyst. The PP results from the rapid o-propionylation of phenol with PC. 2-HPP is produced through the intramolecular rearrangement of PP, propionylation of phenol with PP and direct C-propionylation of phenol with PC, 4-HPP is produced by the reaction of 4-PXPP with zeolite hydroxyl groups.

3.2 SYNTHESIS OF 4-HYDROXY3-CHLOROPROPIOPHENONE USING ZEOLITE H-BETA

3.2.1. INTRODUCTION

The preparation of 4-H3-ClPP, which is an intermediate for dyes, polymers, drugs and perfumeries [31,36], is accomplished industrially using Friedel-Crafts homogeneous Lewis acid catalyst such as $AlCl_3$ and $FeCl_3$. Another important process for the manufacture of hydroxypropiophenones begins with the treatment of phenols and substituted phenols with aromatic carboxylic acids in the presence of strongly acidic ion exchangers (Amberlyst-15) [36]. Hydroxypropiophenones are also prepared through reaction of propionic acids with phenols and substituted phenols in the presence of nitrobenzene using BF_3 as catalyst. Hydroxyketones such as hydroxyacetophenones and hydroxypropiophenones can be obtained through catalytic rearrangement of phenylesters or direct acetylation or propionylation of phenol and substituted phenols with acylating agents on acid zeolites [18-23,34], however, due to the difference in the rates of catalyst deactivation and lower yield of para-product in the Fries rearrangement of phenylesters, direct acetylation or propionylation of phenols and substituted phenols (in single step) is preferred [18,34]. The mechanism of formation of 4-hydroxy3-chloroprpiophenones in higher yield (in the direct propionylation of 2-ClPh) and 2-hydroxy3-

chloropropiophenone (2-H3-ClPP) is also discussed in the paper. The traditional procedures using acyl halides as acylating agent and soluble Lewis acids as catalyst exist drawback to these reaction systems. In general, they are pollutant, non shape-selective, difficult to work with and more than the stoichiometric amount of catalyst is required which ends up as waste. This may pose increasing problems due to environmental considerations. In addition, unwanted heavier (consecutive) products in the Friedel-Crafts reaction with Lewis acids complicate the separation process. In order to diminish the waste problem and to increase the yield of para-product, there is a need to develop a solid recyclable catalyst for the synthesis of 4-hydroxy3-chloropropiophenone in a single step. The use of zeolites in the field of fine chemical synthesis has grown continuously in recent years. In addition, zeolites meet the essential requirements for industrial processing of organic chemicals taking into account their environmental advantages. Zeolites have been used in the acylation of aromatics [5-17] and Fries rearrangement of phenylesters [18,23,24-26]. However, there is no report on the direct propionylation of 2-ClPh using zeolites as catalyst and hence in the continuation of our studies on the catalytic activities of zeolites in acylation reactions, the present paper is concerned to get higher yield of 4-H3-ClPP in the direct propionylation of 2-ClPh using zeolite H-beta as catalyst and propionic anhydride as propionylating agent. The influence of various catalysts, duration of the run, SiO_2/Al_2O_3 of H-beta and molar ratio of 2-Chlorophenol / propionic anhydride (ClPh/PA) is investigated on the conversion of 2-ClPh to the ring products and mainly to the 4-H3-ClPP. The results obtained in the propionylation of 2-ClPh over H-beta are compared with the conventional catalyst, $AlCl_3$.

3.2.2. EXPERIMENTAL

Zeolite H-ZSM-5 and H-beta were prepared according to published procedures [27-28]. Zeolite H-Y and H-mordenite were obtained from Laporte Inorganics, Cheshire, U.K. The synthesized zeolites were washed with deionised water, dried and calcined at 813 K for 16 h in the presence of air to eliminate the organic templates from the zeolites channels. Thus zeolites obtained were pre-treated with 1M NH_4NO_3 solutions to get their protonic forms. Zeolite NH_4-Y was exchanged with 5% rare earth chloride solution at 353 K to gets its RE-Y form.

The chemical compositions of the zeolites were estimated by the combination of wet and atomic absorption (Hitachi 800) methods. The X-ray powder diffraction patterns of various zeolites samples were recorded on X-ray diffractometer. The surface area of the catalyst was measured by nitrogen BET method using an area meter. The size and morphology of the zeolite catalysts were estimated by scanning electron microscope (SEM). The acidity of the zeolites was evaluated using procedure described in the literature [29]. Typical characteristic data is reported in Table 2.1a, b.

Anhydrous AR grade chemicals were used without further purification and the reaction was carried out in a batch reactor. A mixture of 0.04 moles of 2-ClPH, 0.01 moles PA and 0.5g of catalyst were taken in a two necked flask and heated to 443 K for 20 h under autogeneous pressure. The product was analysed with gas chromatograph (HP 6890) equipped with flame ionisation detector and capillary column (50 m * 0.2mm) of methyl silicone gum. GC/MS, IR and H'NMR also identified the samples.

The spectroscopic H-NMR and IR data of 4-hydroxy 3-chloropropiophenone:

For 4-H3-ClPP:

H-NMR (200MHz) ($CDCl_3$): 1.27 (3H, t, J8) $–CH_2-\underline{CH_3}$, 3.06 (2H, q, J8) $–\underline{CH_2}-CH_3$, 6.88 (1H, d, J8) aromatic, 7.60 (2H, m) aromatic.

IR (cm^{-1}): 3580s (–O-H), 3086s (-C-H), 1481s (-C=O), 745s 840w 679w (aromatic H).

For 2-H3-ClPP:

H-NMR (200MHz) ($CDCl_3$): 1.25 (3H,t, J8) $–CH_2-\underline{CH_3,}$ 3.05 (2H,q, J8) $–\underline{CH_2}-CH_3$, 7.78 (3H,m) aromatic.

IR (cm^{-1}): 2991m (-O-H bonded), 1658s (-C=O), 770m (adjacent H-atoms of aromatic ring).

3.2.3. RESULTS AND DISCUSSION

Zeolites used in this study and their physico-chemical properties are presented in Table 2.1b. Table 2.1a lists the SiO_2 / Al_2O_3 ratios, acid strength distributions (mmol/g), H^+ or Na^+ exchange (%), crystal size and surface area of zeolites used in this work. These data reveal that zeolite samples are highly crystalline and in protonic forms. No reflections of a dense phase or any other zeolite phase are found. Table 2.1a, b also illustrates the amount of NH_3 desorbed from zeolites in different temperature steps equivalent to the concentration of Brönsted acid sites.

3.2.3.1 Activity of various catalysts

The catalytic activities of different catalysts such as H-beta, H-Y, RE-Y, H-ZSM-5, and conventional catalyst,$AlCl_3$, in the propionylation of 2-ClPh at 443 K are shown in Figure 3.9. It is seen that all catalysts readily forms the 2-chlorophenyl propionate (2-ClPP) as a major product by the O-acylation of 2-ClPh. Further, reaction mechanisms have been discussed for the formation of nuclear products such as 2-hydroxy3-chloropropiophenone (2-H3-ClPP) and 4-hydroxy3-Chloropropiophenone (4-H3-ClPP). Zeolite H-beta, H-Y and RE-Y were found to be the most active catalysts for the formation of nuclear products whereas the selectivity of H-beta was much higher (4-/2- = 2.0) than those of H-Y (4-/2-= 1.4) and RE-Y (4-/2- = 1.0). The most attractive shape-selectivity of H-beta among the zeolites and conventional catalyst, $AlCl_3$, is attributed to the three dimensional pore system with straight channels of *ca.* 7.3 * 6.5 Å and tortuous channel of 5.5 * 5.5 Å of H-beta [30, 35]. In addition, the inactivity of H-ZSM-5 might be explained on the basis of its smaller pore size (5.4 * 5.6 and 5.1 * 5.5 Å) compared to the bulkier size of the products. For comparison, the results over conventional Lewis acid catalyst, $AlCl_3$, are also obtained in the propionylation of 2-ClPh. Obviously the $AlCl_3$ catalyst demonstrates the reasonable activity for nuclear products (lower than H-Y, RE-Y and H-beta) but lower selectivity for 4-H3-ClPP (4-/2- = 0.8) than H-beta (4-/2-= 2.0). The Activity of various catalysts in the formation of 2-H3-ClPP and 4-H3-ClPP and others (consecutive products in the case of $AlCl_3$) decreases in the sequence: H-Y >RE-Y > H-beta > $AlCl_3$ > H-ZSM-5 the selectivity for 4-H3-ClPP (4-/2- ratio) decreases in the following order: H-beta > RE-Y > H-Y > $AlCl_3$ > H-ZSM-5.

The effect of the number and strength of acid sites [represented for instance by NH_3 desorption at different temperature (mmol g^{-1})] on the various reaction steps similar to (scheme 3.1) in the propionylation of 2-ClPh is shown in Table 2.1a, b. The formation of

2-H3-ClPP and 4-H3-ClPP is considered to be dependent on the number and strength of acid sites. The formation of 2-H3-ClPP and 4-H3-ClPP by the Fries rearrangement of 2-ClPP and the reaction of 2-ClPh with 2-ClPP not only seems to be dependent on the number of acid sites but also on their strength [34]. The H-beta offers acidic centres with higher acid strength that is very well suited for the transformation of 2-ClPP into 2-H3-ClPP and 4-H3-ClPP by the Fries rearrangement and propionylation of 2-ClPh with 2-ClPP into 2-H3-ClPP and 4-H3-ClPP [18-20]. The higher values of 4-H3-ClPP /2-H3-ClPP found with the H-beta in the propionylation of 2-ClPh could be related to the presence of very strong acidic sites and its pore structure (Table 2.1a, b).

The 2-ClPh propionylation may occur through different reaction pathways. The formation of 2-ClPP occurs rapidly via O-acylation of 2-ClPh with propionic anhydride

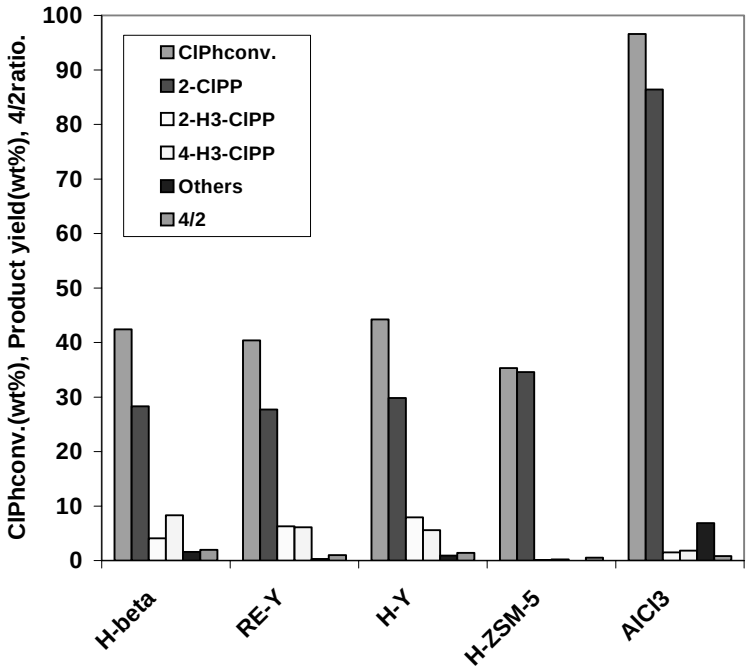

(PA)[34]. Further, the depropionylation of 2-ClPP leads to the formation of ClPh, and propionic acid (PAC). ClPh, which again reacts by an intermolecular reaction with 2-ClPP resulting in the formation of 2-H3-ClPP and 4-H3-ClPP [18-20]. In addition, 2-H3-ClPP and 4-H3-ClPP ould be produced through different reaction pathways: via C-acylation of 2-ClPh with PA and also by the intramolecular rearrangement (Fries rearrangement) of 2-Chlorophenyl propionate over zeolite H-beta [18,34].

Figure.3.9. Propionylation of 2-ClPh over various catalysts [a] Reaction conditions: Catalyst (g) = 0.5; 2-ClPh (mol) = 0.04; PA (mol) = 0.01; 2- ClPh/PA (molar ratio) = 3; Reaction temperature (K) = 443; Reaction time (h) = 20, [b] 2-ClPh = 2-chlorophenol, [c]2-ClPP = 2-chlorophenylpropionate; 2-H3-ClPP = 2-Hydroxy 3-chloropropiophenone; 4-H3-ClPP = 4-Hydroxy 3-chloropropiophenone; Others = 3-chloro 4-propionyloxypropiophenone; 4/2- = 4-H3-ClPP/2-H3-ClPP.

3.2.3.2 Duration of the run

In order to investigate the effect of duration of run on the 4-H3-ClPP/2-H3-PP ratios and the yield of 2-H3-ClPP and 4-H3-ClPP obtained by different reaction pathways, the reaction was performed for 20 h over zeolite H-beta at 443 K. The results are presented in Figure 3.10. The yield of 4-H3-ClPP slowly but steadily increases from 1.9 wt% to 8.3 wt% and simultaneously the yield of 2-ClPP decreases from 39.2 wt% to 28.3 wt% when reaction time was increased from 4 h to 20 h, respectively. The results suggest that mostly increase in the yield of 4-H3-ClPP with reaction time takes place by the transformation

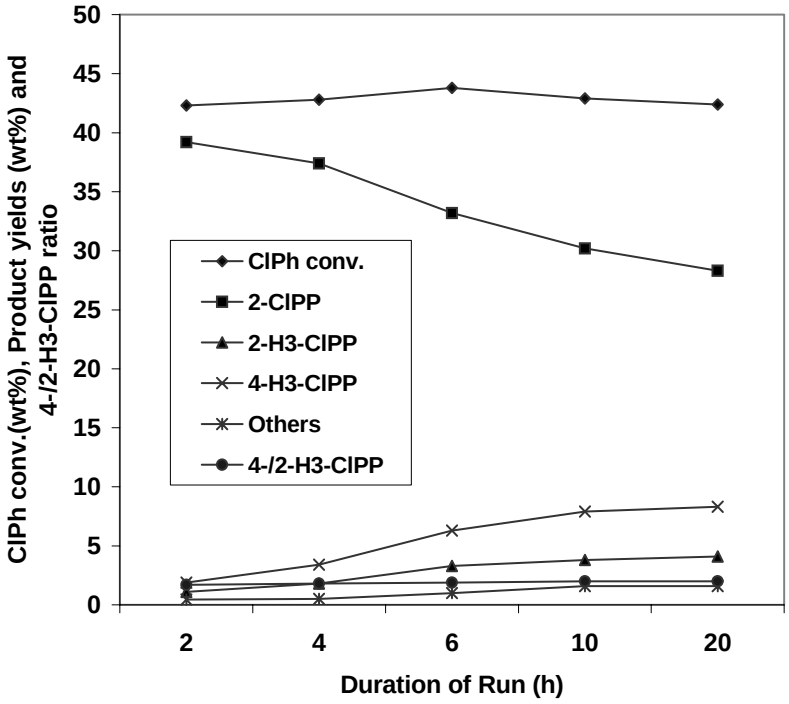

Fig

ure.3.10.Conversion of 2-ClPh and product yields as a function of reaction time [a] Reaction conditions: Catalyst (g) = 0.5; 2-ClPh (mol) = 0.04; PA (mol) = 0.01; 2- ClPh/PA (molar ratio) = 3; Reaction temperature (K) = 443; Reaction time (h) = 20. [b]2-ClPh = 2-chlorophenol. [c]2-ClPP = 2-chlorophenylpropionate ; 2-H3-ClPP = 2-Hydroxy 3-chloropropiophenone ; 4-H3-ClPP = 4-

Hydroxy 3-chloropropiophenone ; Others = 3-chloro 4-propionyloxypropiophenone ; 4/2- = 4-H3-ClPP/2-H3-ClPP.

(Intramolecular reaction) of 2-ClPP into 4-H3-ClPP and the reaction of 2-Chlorophenol with 2-ClPP (intermolecular reaction). However, a small increase in the yield of 2-H3-ClPP (from 1.5 wt% to 4.1 wt%) could not be avoided when the reaction time was increased from 4 h to 20 h, respectively. In addition an increase in the ratio of 4-H3-CLPP/2-H3-CLPP with the increase in the reaction time may be attributed to the transformation of higher amount of 2-ClPP into 4-H3-ClPP.

3.2.3.3. Influence of the SiO_2/Al_2O_3 ratio

Figure 3.11 shows the influence of SiO_2/Al_2O_3 ratio of H-beta on the yield of 2-H3-ClPP, 4-H3-ClPP and 4-/2- ratio in the propionylation of 2-ClPh as a function of aluminum content of H-beta. Increasing the SiO_2/Al_2O_3 ratio from 26 to 80 decreases the yield of 2-H3-ClPP and 4-H3-ClPP formations. In addition, the yield of 4-H3-ClPP decreases with a faster rate compared to the yield of 2-H3-ClPP and as a result, the 4-H3-ClPP/2-H3-ClPP ratio in the product mixture is significantly decreased from 2 to 1.3 when SiO_2/Al_2O_3 ratio of H-beta is increased from 26 to 80, respectively It appears that the transformation of 2-ClPh is catalyzed by both weak and stronger acid sites, so the higher is the acid site density (lower SiO_2/Al_2O_3 ratio), the higher is the catalytic activity of beta.

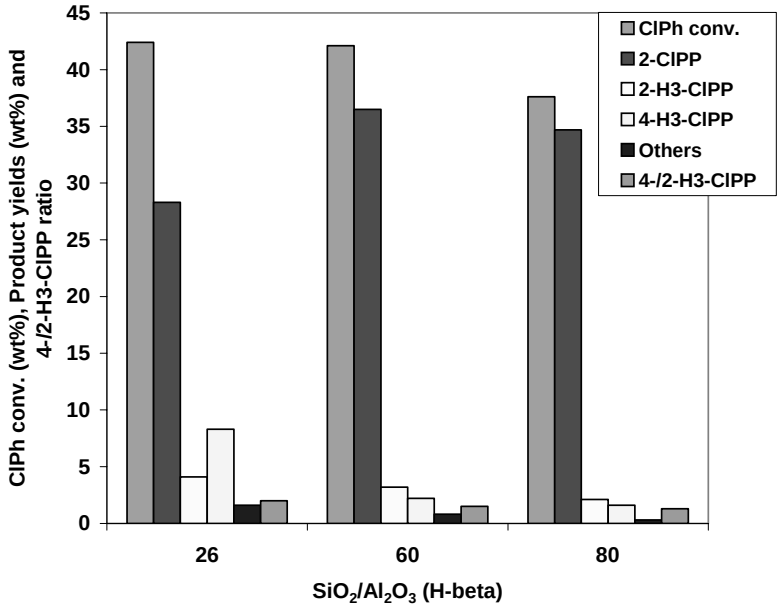

Figure.3.11. Influence of SiO_2/Al_2O_3 ratio of H-beta on the conversion of PA, product Yields and 4-/2- isomer ratio [a] Reaction conditions: Catalyst (g) = 0.5; 2-ClPh (mol) = 0.04; PA (mol) = 0.01; 2- ClPh/PA (molar ratio) = 3; Reaction temperature (K) = 443; Reaction time (h) = 20. [b] 2-ClPh = 2-chlorophenol. [c]2-ClPP = 2-chlorophenylpropionate ; 2-H3-ClPP = 2-Hydroxy 3-chloropropiophenone; 4-H3-ClPP = 4-Hydroxy 3-chloropropiophenone; Others = 3-chloro 4-propionyloxypropiophenone ; 4/2- = 4-H3-ClPP/2-H3-ClPP.

3.2.3.4 Influence of 2-ClPh/PA molar ratio

A series of catalytic activity test were performed to investigate the effect of ClPh/PA ratio on the 2-H3-ClPP and 4-H3-ClPP formations. The ClPh/PA ratio was varied in the

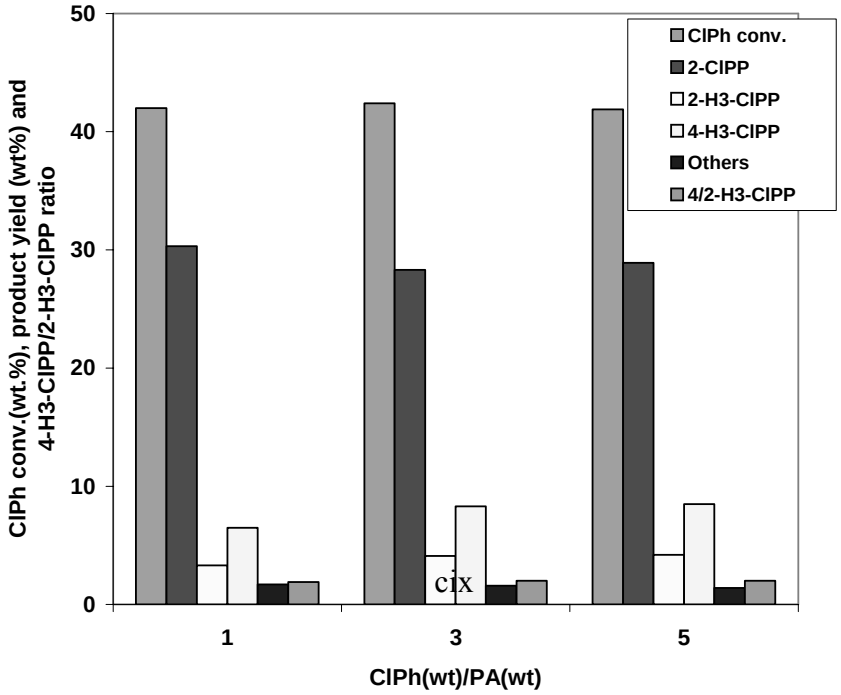

(by keeping the amount of 2-ClPh constant) range of 1 to 5. Figure 3.12 clearly shows that the gradual increase in the Ph/PA molar ratio causes a progressive but small increase in the 2-H3-ClPP and 4-H3-ClPP formation and the 2-ClPP transformations. The 4-H3-ClPP/2-H3-ClPP ratios are not significantly affected by the increase in the ClPh/PA molar ratio from 1 to 5.

Figure.3.12. Influence of 2-ClPh/PA molar ratios on the conversion of 2-ClPh, product Yields and 4-/2- isomer ratio [a] Reaction conditions : Catalyst (g) = 0.5 ; 2-ClPh (mol) = 0.04 ; PA (mol) = 0.01 ; 2- ClPh/PA (molar ratio) = 3 ; Reaction temperature (K) = 443 ; Reaction time (h) = 20. [b] 2-ClPh = 2-chlorophenol. [c]2-ClPP = 2-chlorophenylpropionate ; 2-H3-ClPP = 2-Hydroxy 3-chloropropiophenone ; 4-H3-ClPP = 4-Hydroxy 3-chloropropiophenone ; Others = 3-chloro 4-propionyloxypropiophenone ; 4/2- = 4-H3-ClPP/2-H3-ClPP.

3.2.3.5. Recycle

In order to check the stability and reusability of the catalyst, two reaction cycles were carried out using the same catalyst. After completion of the reaction on fresh catalyst, it was separated from the reaction mixture via sedimentation, filtration and subsequent washing with the acetone, further the catalyst was dried at 383 K for 2 h and calcined in air at 773 K for 16 h then the next run was carried out. The reaction was performed for 20 h at 443 K. The results are given in the Table 3.2. It was found that the activity of the catalyst in the formation of 2-H3-ClPP and 4-H3-ClPP does not distinctly decreases when catalyst was used from fresh to first recycle and the product selectivity (4-H3-ClPP/2-H3-ClPP) seemed to remain unchanged. In order to study the structure change of the catalyst after third run, X-ray powder diffraction patterns were recorded. XRD measurement

indicated that the catalyst retained its structure, which suggests that the catalyst was found to be stable.

Table 3.2. Recycling of H-beta[a]

Run	Conversion of 2-ClPh (wt%)[b]	Product Yield (wt%)[c]					Crystallinity of H-beta
		2-ClPP	2-H3-ClPP	4-H3-ClPP	Others	4/2-	
1(fresh catalyst)	45.1	31.7	3.6	7.9	1.6	2.1	100
2	42.7	30.2	3.6	7.4	1.5	2.0	100
3	43.2	30.7	3.5	7.2	1.5	2.0	100

[a] Reaction conditions : Catalyst (g) = 0.5 ; 2-ClPh (mol) = 0.04 ; PA (mol) = 0.01 ; 2- ClPh/PA (molar ratio) = 3 ; Reaction temperature (K) = 443 ; Reaction time (h) = 20. [b] 2-ClPh = 2-chlorophenol. [c]2-ClPP = 2-chlorophenylpropionate ; 2-H3-ClPP = 2-Hydroxy 3-chloropropiophenone ; 4-H3-ClPP = 4-Hydroxy 3-chloropropiophenone ; Others = 3-chloro 4-propionyloxypropiophenone ; 4/2- = 4-H3-ClPP/2-H3-ClPP.

3.2.4. CONCLUSIONS

Catalytic behaviour of the zeolite catalysts in the propionylation of 2-ClPh was studied. Results showed that only H-beta has higher selectivity (4-H3ClPP/2-H3-ClPP = 2.0) and reasonable stable catalytic performance for the formation of 2-H3-ClPP and 4-H3-ClPP in the reaction. The activity of the catalyst increases with the increase in the number of acid site whereas the selectivity for 4-H3-ClPP (4-H3ClPP/2-H3-ClPP was found to increase with the increase in acid strength of acid sites. The yield of 2-H3-ClPP and 4-H3-ClPP are mainly dependent on the duration of the run, SiO_2/Al_2O_3 ratio of H-beta and 2-ClPh to PA molar ratio. Recycle of H-beta does not appreciably decreases its

activity and selectivity in the propionylation of 2-ClPh. 2-ClPh propionylation to 2-H3-ClPP and 4-H3-ClPP can occurs through several pathways: The reaction of 2-ClPh with PA rapidly forms the 2-ClPP through O-acylation. The propionylation of 2-ClPP leads to the formation of 2-ClPh, which further reacts with 2-ClPP by an intermolecular reaction and produces 2-H3-ClPP and 4-H3-ClPP. Direct C-acylation of 2-ClPh with PA and Fries Rearrangement of 2-ClPP also results in the formation 2-H3-ClPP and 4-H3-ClPP.

3.3 A NOVEL SINGLE STEP SELECTIVE SYNTHESIS OF 4-HYDROXYBENZOPHENONE (4-HBP) USING ZEOLITE H-BETA

3.3.1 INTRODUCTION

The preparation of 4-HBP, which is an intermediate for dyes, polymers, drugs and perfumeries [31], is accomplished industrially using Friedel-Crafts homogeneous Lewis acid catalyst such as $AlCl_3$ and $FeCl_3$. In one industrial process, the 4-HBP is prepared in high yield by the treatment of phenol with anhydrous $AlCl_3$, then treatment of the resulting Al dichloride phenoxide with CCl_4, further treatment of the resulting benzotrichlorides with benzene in the presence of $AlCl_3$ and then hydrolysis of the resulting product gives 50 % 4-hydroxybenzophenone [32]. Another important process for the manufacture of hydroxybenzophenones begins with the treatment of phenols with aromatic carboxylic acids in the presence of strongly acidic ion exchangers (Amberlyst-15) [31]. Hydroxybenzophenones are also prepared through reaction of benzoic acids with phenols in the presence of nitrobenzene using BF_3 as catalyst [33]. Hydroxyketones such as hydroxyacetophenones and hydroxypropiophenones can be obtained through catalytic rearrangement of phenylesters or direct acetylation or propionylation of phenol with acylating agents on acid zeolites [18-23,34], however, due to the difference in the rates of catalyst deactivation and lower yield of para-product in the Fries rearrangement of phenylesters, direct acetylation or propionylation of phenol (in single step) is preferred [18, 34]. The mechanism of formation of 4-hydroxybenzophenones in higher yield (in the direct benzoylation of phenol) and 2-hydroxybenzophenone (2-HBP) is also discussed in the paper. The traditional procedures using acyl halides as acylating agent and soluble Lewis acids as catalyst exist drawback to these reaction systems. In general, they are

pollutant, non shape-selective, difficult to work with and more than the stoichiometric amount of catalyst is required which ends up as waste. This may pose increasing problems due to environmental considerations. In addition, unwanted heavier (consecutive) products in the Friedel-Crafts reaction with Lewis acids complicate the separation process. In order to diminish the waste problem and to increase the yield of para-product, there is a need to develop a solid recyclable catalyst for the synthesis of 4-hydroxybenzophenone in a single step. The use of zeolites in the field of fine chemical synthesis has grown continuously in recent years. In addition, zeolites meet the essential requirements for industrial processing of organic chemicals taking into account their environmental advantages. Zeolites have been used in the acylation of aromatics [5-17] and Fries rearrangement of phenylesters [18,23,24-26]. However, there is no report on the direct benzoylation of phenol using zeolites as catalyst and hence in the continuation of our studies on the catalytic activities of zeolites in acylation reactions, the present paper is concerned to get higher yield of 4-HBP in the direct benzoylation of phenol using zeolite H-beta as catalyst and benzoic anhydride as benzoylating agent. The influence of various catalysts, duration of the run, SiO_2/Al_2O_3 of H-beta and molar ratio of phenol / benzoic anhydride (Ph/BA) is investigated on the conversion of phenol to the ring products and mainly to the 4-HBP. The results obtained in the benzoylation of phenol over H-beta are compared with the conventional catalyst, $AlCl_3$

3.3.2 EXPERIMENTAL

Phenol and benzoic anhydride (99 % purity) were purchased from S.D. Fine chemicals and Aldrich, respectively, and used without further purification. The reactants were dried over 4 Å molecular sieves.

Zeolite H-ZSM-5 and beta were prepared according to published procedures [27-28]. Zeolite H-Y and H-mordenite were obtained from Laporte Inorganics, Cheshire, U.K. The synthesised zeolites were washed with deionised water, dried and calcined at 813 K for 16 h in the presence of air to eliminate the organic templates from the zeolites channels. Thus zeolites obtained were pre-treated with 1M NH_4NO_3 solution to get their protonic forms. Zeolite NH_4-Y was exchanged with 5 % rare earth chloride solution at 353 K to gets its RE-Y form.

The chemical compositions of the zeolites were estimated by the combination of wet and atomic absorption (Hitachi 800) methods. The X-ray powder diffraction patterns of various zeolites samples were recorded on X-ray diffractometer. The surface area of the catalyst was measured by nitrogen BET method using an area meter. The size and morphology of the zeolite catalysts were estimated by scanning electron microscope (SEM). The acidity of the zeolites was evaluated using procedure described in the literature [29]. Typical characteristic data is reported in Table 2.1a, b.

Anhydrous AR grade chemicals were used without further purification and the reaction was carried out in Parr reactor. Mixture of 0.21 moles of phenol, 0.01 moles BA and 0.5 g of catalyst were taken in a parr reactor and heated to 493 K for 20 h under autogeneous pressure. The product was analysed with gas chromatograph (HP 6890) equipped with flame ionisation detector and HP-5 capillary column (50 m × 0.2mm × 32μm) of methylsilicone gum. The samples were also identified by injecting the authentic samples and GC-MS.

Table. 3.3. Benzoylation of Phenol.[a]

Catalyst	Conv.[b] BA (wt%)	Product yields (wt%)[c]				4-/2-[d]
		PB	2-HBP	4-HBP	Others	
H-beta	95.3	61.2	11.4	23.3	-	2.1
H-Y	96.2	55.0	25.7	16.9	-	0.6
RE-Y	87.3	56.5	16.5	16.5	-	1.1
H-mordenite	87.8	87.0	0.7	-	-	-
H-ZSM-5	86.1	86.1	-	-	-	-
AlCl3	93.2	70.8	5.4	3.3	11.9	0.1

[a] Reaction conditions : Catalyst (g) = 0.5 ; Phenol (mol) =μ 0.21 ; BA (mol) = 0.01 ; phenol/BA(molar ratio) = 20 ; reaction temperature (K) = 493 ; reaction time (h) = 20 . [b] BA = Benzoic anhydride. [c] PB = phenylbenzoate ; 4-HBP = 4-hydroxybenzophenone ; 2-HBP = 2-hydroxybenzophenone ; Others = consecutive products [d] 4-/2- = 4-HBP/2-HBP ratio

3.3.3. RESULTS AND DISCUSSION

Table 2.1a, b lists the SiO_2 / Al_2O_3 ratios, acid strength distributions (mmol/g), H^+ or Na^+ exchange (%), crystal size and surface area of zeolites used in this work. These data reveal that zeolite samples are highly crystalline and in protonic forms. No reflections of a dense phase or any other zeolite phase are found.

3.3.3.1 Activity of various catalysts

The catalytic activities of different catalysts such as H-beta, H-Y, RE-Y, H-ZSM-5, H-mordinite and conventional catalyst, $AlCl_3$, in the benzoylation of phenol at 493 K are summarised in Table 3.3. It is seen that all catalysts readily forms the phenyl benzoate (PB) as a major product by the O-acylation of phenol (Scheme 3.1). Further, reaction mechanisms have been proposed for the formation of nuclear products such as 2-

hydroxybenzophenone (2-HBP) and 4-hydroxybenzophenone (4-HBP) (Scheme3.1). Zeolite H-beta, H-Y and RE-Y were found to be the most active catalysts for the formation of nuclear products whereas the selectivity of H-beta was much higher (4-/2- = 2.1) than those of H-Y (4-/2-= 0.6) and RE-Y (4-/2- = 1.1). The most attractive shape-selectivity of H-beta among the zeolites and conventional catalyst, $AlCl_3$, is attributed to the three dimensional pore systems with straight channels of *ca.* 7.3 * 6.5 Å and tortuous channel of 5.5 * 5.5 Å of H-beta [30, 35]. Very small amount of 2-HBP was formed over H-mordenite. In addition, the inactivity of H-ZSM-5 might be explained on the basis of its smaller pore size (5.4 * 5.6 and 5.1 * 5.5 Å) compared to the bulkier size of the products. For comparison, the results over conventional Lewis acid catalyst, $AlCl_3$, are also obtained in the benzoylation of phenol. Obviously the $AlCl_3$ catalyst demonstrates the reasonable activity for nuclear products (lower than H-Y, RE-Y and H-beta) but lower selectivity for 4-HBP (4-/2- = 0.6) than H-beta (4-/2-= 2.1). The Activity of various catalysts in the formation of 2-HBP and 4-HBP and others (consecutive products in the case of $AlCl_3$) decreases in the sequence: H-Y >RE-Y > H-beta > $AlCl_3$ > H-mordenite whereas the selectivity for 4-HBP (4-/2- ratio) decreases in the following order: H-beta > RE-Y > H-Y ≈ $AlCl_3$.

The effect of the number and strength of acid sites [represented for instance by NH_3 desorption at different temperature (mmol g^{-1})] on the various reaction steps (scheme 3.1) in the benzoylation of phenol is shown in Table 2.1a, b. The formation of 2-HBP and 4-HBP is considered to be dependent on the number and strength of acid sites. The formation of 2-HBP and 4-HBP by the Fries rearrangement of PB and the reaction of phenol with PB not only seems to be dependent on the number of acid sites but also on their strength [34]. The H-beta offers acidic centres with higher acid strength that is very

well suited for the transformation of PB into 2-HBP and 4-HBP by the Fries rearrangement and benzoylation of phenol with PB into 2-HBP and 4-HBP [18-20]. The higher values of 4-HBP/2-HBP found with the H-beta in the benzoylation of phenol could be related to the presence of very strong acidic sites and its pore structure (Table 2.1a, b).

The phenol benzoylation may occur through different reaction pathways. The formation of PB occurs rapidly via O-acylation of phenol with benzoic anhydride (BA)[34]. Further, the debenzoylation of PB leads to the formation of phenol, and benzoic acid (BAC). Phenol which again reacts by an intermolecular reaction with PB resulting in the formation of 2-HBP and 4-HBP [18-20]. In addition, 2-HBP and 4-HBP would be produced through different reaction pathways: via C-acylation of phenol with BA and also by the intramolecular rearrangement (Fries rearrangement) of phenyl benzoate over zeolite H-beta (scheme 3.1)[18,34].

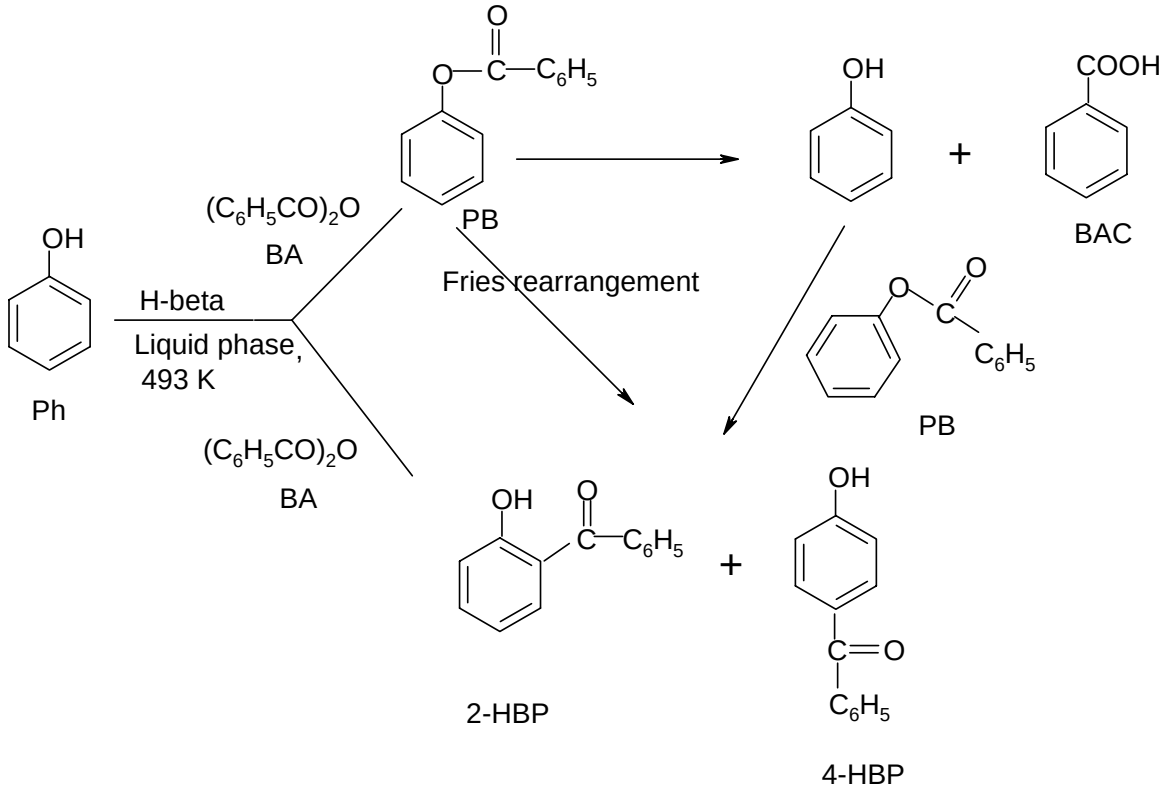

Scheme 3.1.

3.3.3.2 Duration of the run

In order to investigate the effect of duration of run on the 4-HBP/2-HBP ratios and

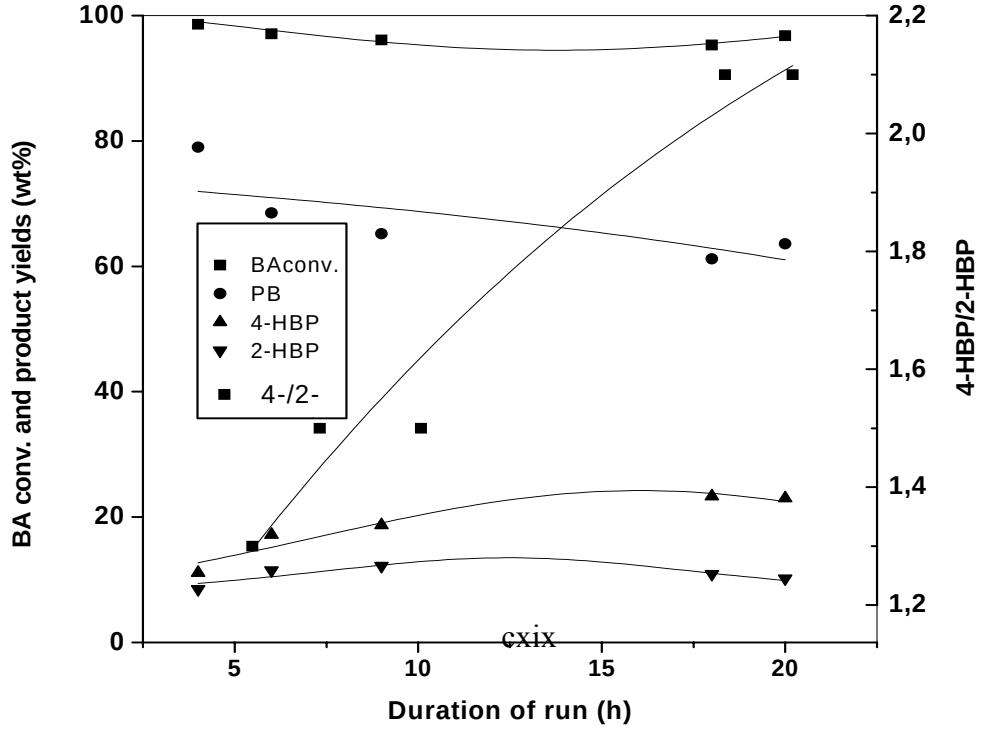

the yield of 2-HBP and 4-HBP obtained by different reaction pathways (Scheme 3.1), the reaction was performed for 20 h over zeolite H-beta at 493 K. The results are presented in Figure 3.13.

Figure.3.13.Conversion of BA and product yields as a function of reaction time; Reaction conditions: Catalyst (g) = 0.5; phenol (mol) = 0.21; BA (mol) =0.01; phenol/BA (molar ratio) = 20; reaction temperature (K) = 493; reaction time (h) = 20. BA = Benzoic anhydride; 4-HBP = 4-hydroxybenzophenone; 2-HBP = 2-hydroxybenzophenone; 4-/2-HBP = 4-/2-hydroxybenzophenone.

The yield of 4-HBP slowly but steadily increases from 11.1 wt% to 23.0 wt% and simultaneously the yield of PB decrease from 79.0 wt% to 63.6 wt% when reaction time was increased from 4 h to 20 h, respectively. The results suggest that mostly increase in the yield of 4-HBP with reaction time takes place by the transformation (intramolecular reaction) of PB into 4-HBP and the reaction of phenol with PB (intermolecular reaction). However, a small increase in the yield of 2-HBP (from 8.5 wt% 10.2 wt%) could not be avoided when the reaction time was increased from 4 h to 20 h, respectively. In addition an increase in the ratio of 4-HBP/2-HBP with the increase in the reaction time may be attributed to the transformation of higher amount of PB into 4-HBP.

3.3.3.3 Influence of the SiO_2/Al_2O_3 ratio

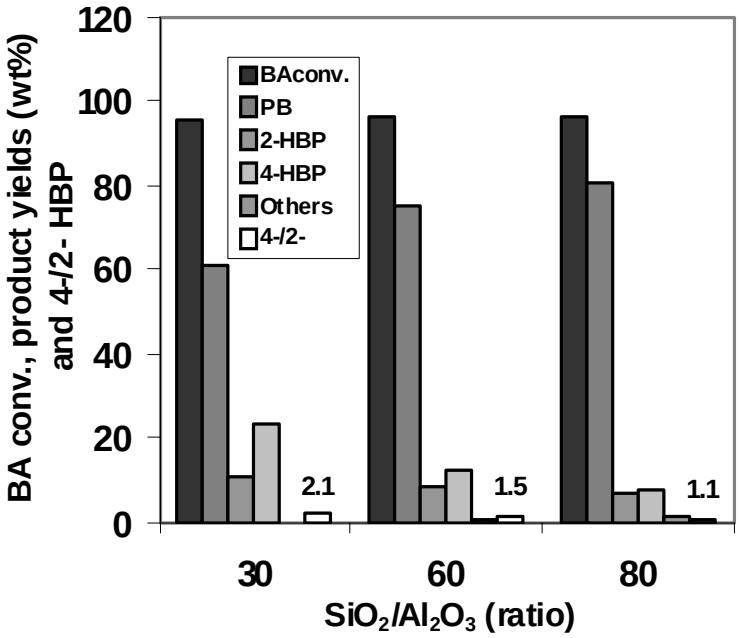

Figure.3.14. Influence of SiO_2/Al_2O_3 ratio of H-beta on the conversion of BA, product Yields and 4-/2- isomer ratio; Reaction conditions: Catalyst (g) = 0.5; phenol (mol) = 0.21; BA (mol) =0.01; phenol/BA (molar ratio) = 20; reaction temperature (K) = 493; reaction time (h) = 20. BA = Benzoic anhydride; 4-HBP = 4-hydroxybenzophenone ; 2-HBP = 2-hydroxybenzophenone; 4-/2-HBP = 4-/2-hydroxybenzophenone, Other = consecutive products.

Figure 3.14 shows the influence of SiO_2/Al_2O_3 ratio of H-beta on the yield of 2-HBP, 4-HBP and 4-/2- ratio in the benzoylation of phenol as a function of aluminium content of the H-beta. Increasing the SiO_2/Al_2O_3 ratio from 30 to 60 decreases the yield of 2-HBP and 4-HBP formations. In addition, the yield of 4-HBP decreases with a faster rate compared to the yield of 2-HBP and as a result, the 4-HBP/2-HBP ratio in the product mixture is significantly decreased from 2.1 to 1.1 when SiO_2/Al_2O_3 ratio of H-beta is increased from 30 to 80, respectively It appears that the transformation of phenol is catalysed by both weak and stronger acid sites, so the higher is the acid site density (lower SiO_2/Al_2O_3 ratio), the higher is the catalytic activity of H-beta.

3.3.3.4 Influence of Phenol/BA molar ratio

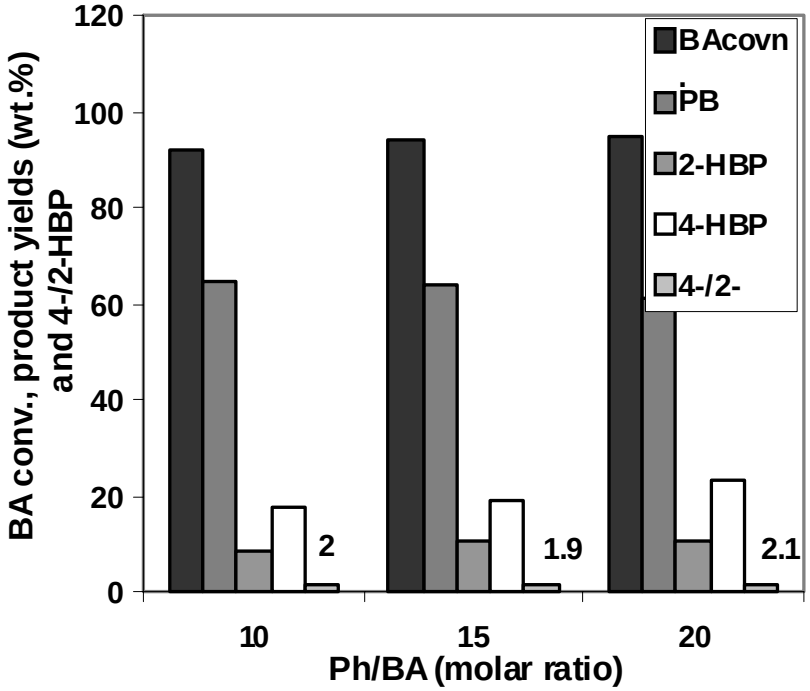

Figure.3.15. Influence of Ph/BA molar ratio on the conversion of BA, product yields and 4-/2-isomer ratio; Reaction conditions: Catalyst (g) = 0.5; phenol (mol) = 0.21; BA (mol) =0.01; phenol/BA (molar ratio) = 20; reaction temperature (K) = 493; reaction time (h) = 20; BA = Benzoic anhydride; 4-HBP = 4-hydroxybenzophenone ; 2-HBP = 2-hydroxybenzophenone; 4-/2-HBP = 4-/2-hydroxybenzophenone.

A series of catalytic activity test were performed to investigate the effect of Ph/BA ratio on the 2-HBP and 4-HBP formations. The Ph/BA ratio was varied in the (by keeping the amount of phenol constant) range of 10 to 20. Figure 3.15 clearly shows that the gradual increase in the Ph/BA molar ratio causes a progressive but small increase in the 2-HBP and 4-HBP formation and the PB transformation. The 4-HBP/2-HBP ratios are not significantly affected by the increase in the Ph/BA molar ration from 10 to 20.

3.3.3.5 Recycle

In order to check the stability and reusability of the catalyst, two reaction cycles were carried out using the same catalyst. After completion of the reaction on fresh catalyst, it was separated from the reaction mixture via sedimentation, filtration and subsequent washing with the acetone, further the catalyst was dried at 383 K for 2 h and calcined in air at 773 K for 16 h then the next run was carried out and shown in Figure 3.16. The reaction was

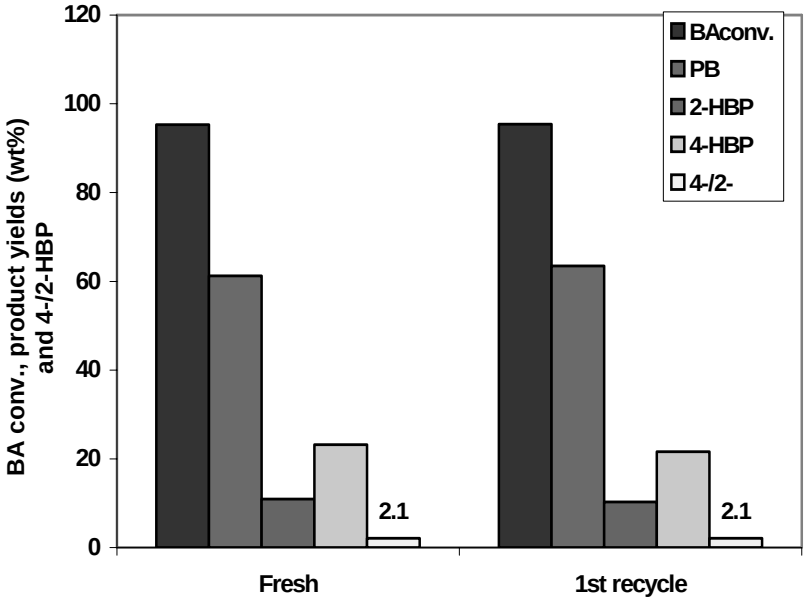

Figure.3.16. Influence of recycle of catalyst H-beta on the conversion of BA, product yields and 4-/2- isomer ratio; Reaction conditions: Catalyst (g) = 0.5; phenol (mol) = 0.21; BA (mol) =0.01; phenol/BA (molar ratio) = 20; reaction temperature (K) = 493; reaction time (h) = 20. BA = Benzoic anhydride; 4-HBP = 4-hydroxybenzophenone ; 2-HBP = 2-hydroxybenzophenone; 4-/2-HBP = 4-/2-hydroxybenzophenone

performed for 20 h at 493 K. It was found that the activity of the catalyst in the formation of 2-HBP and 4-HBP does not distinctly decreases when catalyst was used from fresh to first recycle and the product selectivity (4-HBP/2-HBP) seemed to remain unchanged. In order to study the structure change of the catalyst after reactions, X-ray powder

diffraction patterns were recorded after the last run, XRD measurement indicated that the catalyst retained its structure, which suggests that the catalyst was stable in structure.

3.3.4. CONCLUSIONS

Catalytic behaviour of the zeolite catalysts in the benzoylation of phenol was studied. Results showed that only H-beta has higher selectivity (4-HBP/2-HBP = 2.1) and reasonable stable catalytic performance for the formation of 2-HBP and 4-HBP in the reaction. The activity of the catalyst increases with the increase in the number of acid site whereas the selectivity for 4-HBP (4-HBP/2-HBP) was found to increase with the increase in acid strength of acid sites. The yield of 2-HBP and 4-HBP are mainly dependent on the duration of the run, SiO_2/Al_2O_3 ratio of H-beta and Phenol to BA molar ratio. The yield of 2-HBP and 4-HBP increases with the increase in the number of acid sites, duration of run and phenol to BA molar ratio whereas it decreases with the increase of SiO_2/Al_2O_3 ratio of H-beta. Recycle of H-beta does not appreciably decreases its activity and selectivity in the benzoylation of phenol. Phenol debenzoylation to 2-HBP and 4-HBP can occurs through several pathways: The reaction of Phenol with BA rapidly forms the PB through O-acylation. The benzoylation of PB leads to the formation of phenol, which further reacts with PB by an intermolecular reaction and produces 2-HBP and 4-HBP. Direct C-acylation of phenol with BA and Fries Rearrangement of PB also results in the formation 2-HBP and 4-HBP.

3.4 REFERENCES

1. G. A. Olah, *Friedel Crafts and Related Reactions*, Vol.III, 1964.
2. *Ullamas encyclopedia* vol. A1. P.209.
3. K. W. Rosenmund, W. Schurr, Justus, *Liebigs.Ann.Chem*. 460 (1928) 56.
4. **J. Kassner, H. Zimmer.in, F. Korte (ed).** ***Methodicum Chimicum, Thieme.Verlag,***

   Stultgart Vol.5 (1975) p.432.
5. B. Chiche, A. Finiels, C. Gauthier, P. Geneste, *J. Org.Chem*.51 (1986) 2128.
6. A. Corma, M. J. Climent, H. Garcia, P. Primo**,** *Appl. Catal.* 49 (1989) 109.
7. I. Neves, F. Jayat, P. Magnoux, G. Perot, F. R. Ribeiro, M. Gubelman, M. Guisnet, *J. Chem. Soc. Chem. Commun.* (1994) 717.
8. F. Richard, H. Carreyre, G. Perot**,** *J. Catal.* 159 (1996) 427.
9. R. Fang, H. W. Kouwenhoven, R. Prins, *Stud.surf.Sci.Catal.* 83 (1994) 1441.
10. H. Van Bekkum, A. J. Hoefnagel, M.A.Vankoten, E.A.Gunnewegh, A.H.G.Vog, H.W. Kouwenhoven, *Stud.Surf.Sci.Catal.* 83 (1994) 379
11. E.A.Gunnewegh, S.S.Gopie, H.Van Bekkum, *J.Mol.Catal. A* 106 (1996) 5.
12. A. P. Singh, D. Bhattacharya and S. Sharma, *J. Mol. Catal. A* 102 (1996) 139.
13. A. P. Singh and D. Bhattacharya, *Catal. Lett.* 32 (1995) 327.
14. A. K. Pandey and A. P. Singh, *Catal. Lett.* 44 (1997) 129.
15. A. P. Singh and A. K. Pandey, J. *Mol. Catal.* 123 (1997) 141.
16. A. P. Singh, D. Bhattacharya and S. Sharma, *Appl. Catal. A* 150 (1997) 53.
17. B. Jacob, S. Sugunan and A. P. Singh, *J.Mol. Catal. A* 139 (1999) 43.
18. Michel Guisnet, Dmitri B.Lukyanov, Francois Jayat, Patrick Magnoux, and

Isabel Neves. *Ind. Eng. Chem. Res.* 34 (1995) 1624.

19. I.Neves, F.Jayat, P.Magnoux, G.Perot,F.R.Ribeiro,M.Gubelmann,M.Guisnet, *J. Mol. Cata.* 93 (1994) 169.
20. **Y.V.Subba Rao, S.J.Kulkarni, M.Subrahmanyam, A.V.Rama Rao, *Appl. Catal.A*: 33 (1995) L1.**
21. **Alfred. Heidekum, Mark. A. Harmer, and Wolfgang. F. Hoelderich, *J. Catal.* 176 (1998) 260.**
22. F.Jayat, M.J. Sabater Picot. M. Guisnet, *Catal. Lett.* 41 (1996) 181.
23. Gupta, B. B.G. *U.S.Patent* 4,668, 826, (1987).
24. Nicolau. I, Aguilo.A, *U.S.Patent* 4,652,683, (1987).
25. I. Neves, F. Jayat, P. Magnoux, G. Perot, F. R. Ribeiro, M. Gubelman, M. Guisnet, *J. Mol. Catal.* 93 (1994) 169.
26. I. Neves, F. Jayat, P. Magnoux, G. Perot, F. R. Ribeiro, M. Gubelman, M Guisnet, *J. Chem. Soc., Chem. Commun*. (1994) 717.
27. R.J. Argaurer, G.R. Landolt**,** *US Patent* 3,702,886 (1972).
28. M.A. Chambler, J.Perze Pariente, *Zeolites* 11 (1991) 202.
29. M.Chamumi, D. Brunel, F. Fajula, P. Geneste, P. Moreau, J. Solof, *Zeolites* 14 (1994) 283.
30. J.M. Newsam, M.M.J. Teracy, W.T. Koestier, C.B. DeGruyter, *Proc. E. Soc. London A* 420 (1988) 375.
31. T. Abe, T. Kimura, Y. Ayabe, T. Shiomi, *J. Pat.* 85-123831 (1985).
32. N. Fukuoka, M. Suzuki**,** *J. Pat*. 87 –228021 (1987).

33. U. Eichenauer, P. Neumann *DE* 3831092 (1988).

34. V.D. Chaube, P. Moreau, A. Finiel, A.V. Ramaswamy, A.P.Singh, *J. Mol. Catal. A.*174 (1-2), (2001) 255.

35. M.M.J. Treacy, J.M. Newsam , *Nature* 332 (1988) 249.

36. M. Windholz, ed., Merck Index, *An Encylopedia of Chemical, Drugs and Biochemicals,* (Merck, NJ, 1983) p.1107.

CHAPTER 4

ALKYLATION REACTION OF BENZENE

4. BENZYLATION OF BENZENE TO DIPHENYLMETHANE USING ZEOLITE CATALYSTS

4.1. INTRODUCTION

Diphenylmethane is used in the fragrance industry both as a fixative and in scenting soap [1]. It can serve as a synergist for pyrethrin in pesticides and insecticides. Diphenylmethane is recommended as a plasticizer to improve the dying properties, as solvents for the dyes and as a dyes carrier printing with disperse dyes. The addition of diphenylmethane to saturated linear polyesters improves their thermal stability and its addition to jet fuels increases their stability and lubricating properties. Industrially, the diphenylmethane is synthesized by the Friedel-craft reaction of benzyl chloride with benzene in presence of a Lewis acid catalyst i.e. $AlCl_3$ [1, 2]. Liquid phase alkylation of aromatic compounds, using homogenous acid catalyst is commonly practiced by Friedel-crafts type reaction in organic synthesis [3]. However, the commonly used homogeneous acid catalysts (viz. $AlCl_3$, BF_3 and H_2SO_4) pose several problems, such as difficulty in separation and recovery, disposal of the spent catalyst, corrosion, high toxicity, etc. Hence, development of reusable solid acid catalyst is required. Zeolite catalysts, due to their shape selectivity, thermal stability and easy separation from the products and possibility of regeneration of deactivated catalysts have been widely used in the field of petrochemistry [1, 3]. Further, there are some more reports to replace the homogeneous acid catalysts by heterogeneous solid acid catalysts, such as heteropoly acids, Ga or Fe substituted H-ZSM-5, Ga-containing MCM-41 and $GaCl_3$, $FeCl_3$ and $ZnCl_2$ supported on clay and Si-MCM-41 for the alkylation of aromatic compounds [4-7]. The main purpose of this study is to replace the homogeneous Lewis acid catalyst by the environmentally

friendly solid recyclable catalyst and to enhance the selectivity for diphenylmethane using zeolites as catalyst and benzyl chloride as alkylating agent (Scheme. 4.1).

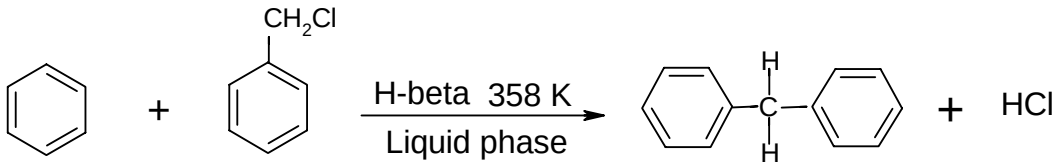

Scheme 4.1

4.2. EXPERIMENTAL

4.2.1. Materials

Zeolites Na-Y was obtained from Laporte Inorganics, Cheshire, U.K. Zeolites ZSM-5 and beta were prepared using the methods described in the literature [8,9]. The synthesized zeolites were washed with deionized water, dried and calcined at 813 K for 16 h in the presence of air to eliminate the organic templates from the zeolite channels. The resultant samples were thrice NH_4^+-exchanged for 8 h at 353 K. The NH_4^+-exchanged samples were again calcined at 823 K for 8 h to get their protonic forms.

4.2.2. Characterization

The SiO_2/Al_2O_3 ratio of various zeolites and degree of ion- exchange were determined by a combination of wet and atomic absorption methods (Hitachi 800). X-ray powder diffraction (XRD) was carried out on a Rigaku, D-Max/III-VC model using the CuK_α radiation and was used to evaluate the peak positions of various zeolite samples. The surface area of the catalysts was measured by nitrogen BET method using an area meter. The size and morphology of the zeolite catalysts were estimated by scanning electron microscope (Cambridge Stereoscan 400).

4.2.3. Acidity measurements

Temperature programmed desorption measurements were carried out to measure the acid strength of the zeolite catalysts using ammonia as an adsorbate (Table 2.1a, b) [9, 10]. In a typical run, 1.0 g of a calcined sample was placed in a quartz tubular reactor and heated at 773 K under a nitrogen flow of 50 mL / min, for 4 h. The reactor was then cooled to 303 K and adsorption conducted at that temperature by exposing the sample to ammonia for 30 min. Physically adsorbed ammonia was removed by purging the sample with a nitrogen stream flowing at 50 mL /min, for 15 h at 303 K. Acid strength distribution was obtained by raising the catalyst temperature (10 ^{0}C/min) from 303 K to 773 K in a number of steps in a flow of nitrogen (10 mL/min). The NH_3 evolved was trapped in an HCl solution and titrated with a standard NaOH solution (Table 2.1a, b).

4.2.4 Catalytic reactions

The liquid phase catalytic runs were carried out Batch wise in a mechanically stirred, closed 50 mL glass reactor fitted with a reflux condenser, a thermometer and a septum for withdrawing the product samples. The temperature of the reaction vessel was maintained using an oil bath .In a typical run, appropriate amounts of benzene and benzyl chloride (3:1 molar ratio) were charged in the reactor along with 0.5g catalyst. The reaction mixture was heated to 358 K under stirring. Samples were withdrawn periodically and analyzed with a

gas chromatograph (HP 6890) fitted with a flame ionization detector and a capillary column (50m*0.2mm) with methyl silicon gum. The identification of the product was done by comparing their gas chromatograph with those of authentic samples and GC-MS.

Table .4.1. Benzylation of Benzene.[a]

Catalyst	Conv.[b] BC (wt%)	Rate of BC Conv. (ROBC) ($mmolg^{-1}h^{-1}$)	Product yields (wt%)[c]	
			DPM	Others
H-beta	33.3	4.7	89.1	10.9
H-Y	64.1	9.1	64.8	35.2
H-ZSM-5	2.8	0.4	2.8	0
$AlCl_3$	100	170	58	42

[a] Reaction conditions: Catalyst (g) = 0.5 ; Benzene (mol) = 0.12 ; BC (mol) = 0.04 ; Benzene/BC (molar ratio) = 3; reaction temperature (K) = 358 ; reaction time (h) = 6 for $AlCl_3$ reaction time (h) = 0.5. [b] BC = Benzyl chloride [c] DPM = diphenylmethane ; Others = Polyalkylated products.

Finally, the percentage conversion (wt. %) of benzyl chloride is defined as a total percentage of BC transformed. The rate of BC conversion ($mmolg^{-1}\ h^{-1}$) was calculated as the amount of BC (mmol) converted per hour per gram of catalyst. The selectivity to the product is expressed as the amount of particular product divided by amount of total products and multiplied by 100.

4.3 RESULTS AND DISCUSSION

4.3.1. Catalyst characterization

Table 1 lists the SiO_2/Al_2O_3 ratios, H^+ - exchange (%), crystal size and surface areas of the zeolites used in this work. These data reveal that zeolite samples are highly crystalline. No reflections of a dense phase or any other zeolite phase are found. Table

2.1a,b also illustrates the amount of NH_3 desorbed from zeolites in different temperature steps equivalent to the concentration of Bronsted acid sites.

4.3.2. Catalytic activity of various catalysts

The results of the catalytic activities of various catalysts such as H-beta, H-Y and H-ZMS-5 in the benzylation of benzene with benzyl chloride are depicted in Table 4.1. The results with Lewis acid catalyst, $AlCl_3$, are compared under the identical reaction conditions. The main product of the reaction is diphenylmethane (DPM). A small amount of higher molecular weight polybenzylated products (others) are also observed, however, the concentration of polybenzylated products depends on the reaction conditions and the type of the catalyst used. The formation of DPM results from the aromatic substitution of the benzene by parallel reactions while the ployalkylated products are obtained by the consecutive reactions of DPM. The activities of the catalysts are compared using data after an initial 1h run.

As can be seen from the Table 4.1, zeolites H-beta is found to be less active (33.3 wt. % BC conv.) compared to the H-Y (64.1 wt. % BC conv.). However, in terms of selectivity, H-beta is found to be more selective (89.1wt. %) than H-Y (64.8wt.%) in the benzylation of benzene. The higher selectivity of H-beta might be explained on the basis of its strong acidity and smaller pore opening (7.5-5.5 Å) than H-Y. (7.4 Å). The result presented in the Table 2.1a, b show that geometrical constraints produced by H- beta did not allow the formation of bulkier polybenzylated products in the small channels of H-beta and, hence a higher selectivity to DPM is achieved over H-beta rather than H-Y zeolite. H-ZSM-5, in spite of its strong acidity as indicated in (Table.2.1a, b) it is found to be less active in the reaction. The lower activity of H-ZSM-5 may be attributed to its small pore openings than the size of the product (DPM) to diffuse out. $AlCl_3$ found to be

more active (100 wt. % BC conv.) compared to all zeolite catalysts, however, a higher amount of consecutive products (42 wt.%) is obtained due to its non-shape-selective character. The activities of various catalysts at 358 K after 6h of the reaction time are found to be in the following decreasing order: $AlCl_3$ > H-Y >H-beta > H-ZSM-5.

The reaction appears to proceed via an electrophile intermediate, which involves the reaction of benzyl chloride with the acidic zeolite catalyst. The Bronsted acid site of the zeolite polarizes the benzylating agent and in turn produces an electrophile ($C_6H_5CH_2^+$). Thus the generated electrophilic species attack the benzene ring, resulting in the formation of DPM [11, 12].

The influence of various other parameters on the conversion of BC and selectivity to DPM are discussed using H-beta in the section 4.3.3.

4.3.3. Duration of the run

Figure. 4.1 shows the conversion of BC and product distribution at 358 K using zeolite H beta as a function of reaction time. The conversion of BC increased almost linearly up to 6 h of reaction time. The conversion of the BC leads mainly to DPM up to 2 h of the reaction time and then decreases marginally with the reaction time. The results show that the reaction time influences the conversion of BC but did not affect selectivity of DPM to a greater extend.

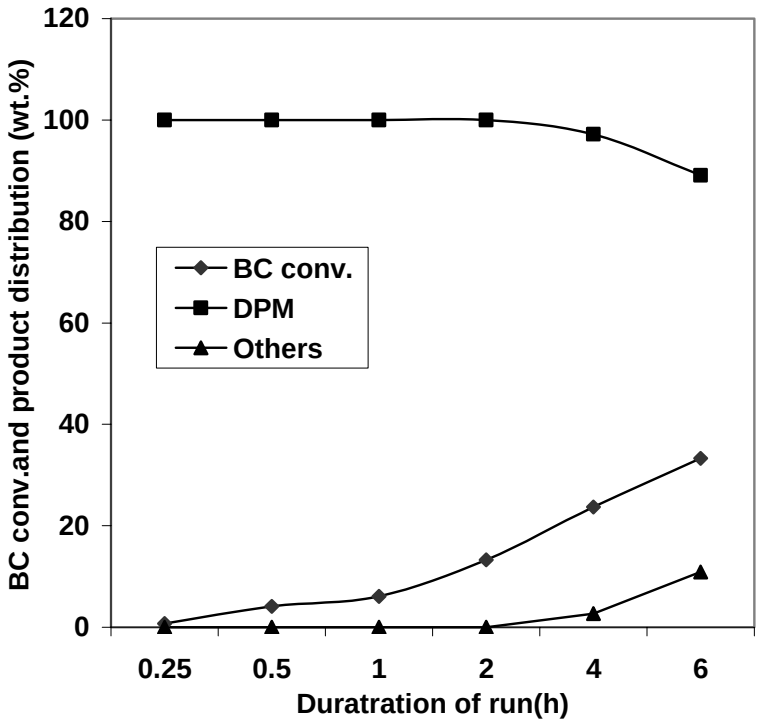

Figure 4.1. Duration of the run on the conversion of the benzylchloride, rate of conversion of BC and product distribution; [a] Reaction conditions: Catalyst H-beta (g) = 0.5; Benzene (mol) = 0.12 ; BC (mol) = 0.04 ; Benzene/BC (molar ratio) = 3; reaction temperature (K) = 358 ; reaction time (h) = 6 for $AlCl_3$ reaction time (h) = 0.5. [c] BC = Benzyl chloride [d] DPM = diphenylmethane ; Others = Polyalkylated products.

4.3.4. Influence of catalyst concentration (H-beta / BC wt./wt.)

Figure. 4.2 displays the conversion of BC and product distribution after 6 h of the reaction time as a function of H-beta to BC (wt./wt.) ratio. The different H-beta to BC ratios are obtained by varying the amount of the H-beta zeolite and keeping the concentration of BC constant. An initial steep increase in the conversion of BC is observed when the catalyst to BC ratio is increased up to 0.13. Beyond this ratio, the conversion of BC and even the selectivity for DPM are leveled off in the reaction mixture. These results indicate that a small amount of catalyst is efficient for catalyzing the reaction.

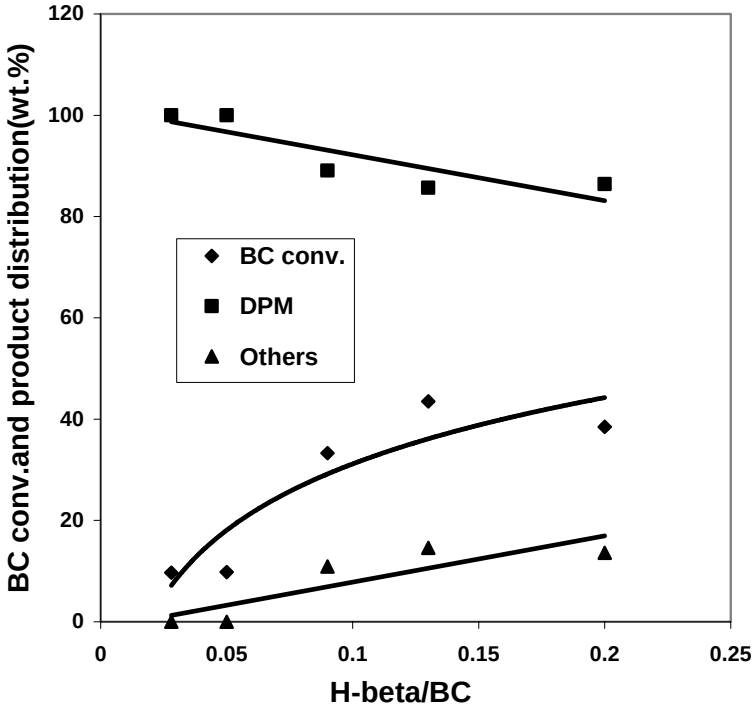

Figure 4.2. Influence of H-beta/Benzene (wt./wt.) ratio on the conversion of BC, product distribution. [a] Reaction conditions: Catalyst (g) = 0.5 ; Benzene (mol) = 0.12 ; BC (mol) = 0.04 ; Benzene/BC (molar ratio) = 3; reaction temperature (K) = 358 ; reaction time (h) = 6 for $AlCl_3$ reaction time (h) = 0.5. [c] BC = Benzyl chloride [d] DPM = diphenylmethane ; Others = Polyalkylated products.

4.3.5. Influence of SiO_2/Al_2O_3 molar ratio

The influence of SiO_2/Al_2O_3 ratio of H-beta on its catalytic activity in the benzylation of benzene is investigated at 358 K (Figure. 4.3). It is shown that conversion of BC in the benzylation of benzene is markedly affected by the SiO_2/Al_2O_3 molar ratio of H-beta. The higher the SiO_2/Al_2O_3 molar ratio of H-beta lowers the BC conversion. The results are in agreement with the earlier reports of Friedel-Crafts reactions [13, 14]. Furthermore, it is observed that the selectivity to DPM is affected significantly by the SiO_2/Al_2O_3 ratio of H-beta. The conversion of BC over 26 and 60 SiO_2/Al_2O_3 ratio of H-beta is found to be 33.3 and 16.8 wt. %, respectively. The corresponding selectivity to DPM was 89.1 wt.%

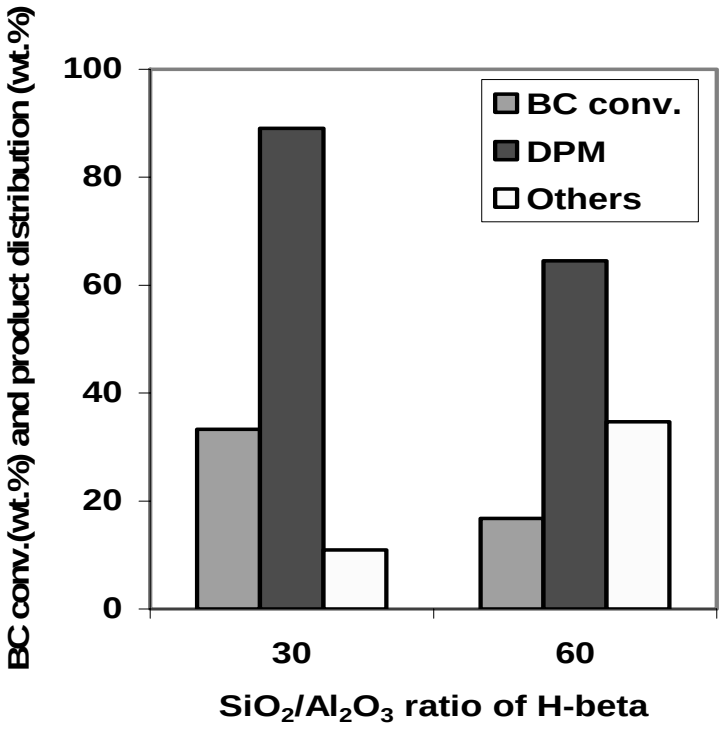

Figure 4.3. Influence of SiO_2/Al_2O_3 ratio of H-beta on the conversion of BC, product distribution; [a] Reaction conditions: Catalyst (g) = 0.5; Benzene (mol) = 0.12; BC (mol) = 0.04; Benzene/BC (molar ratio) = 3; reaction temperature (K) = 358; reaction time (h) = 6 for $AlCl_3$ reaction time (h) = 0.5. [c] BC = Benzyl chloride [d] DPM = diphenylmethane; Others = Polyalkylated products.

and 64.5 wt.% respectively. Higher SiO_2/Al_2O_3 ratio decreases the density of acid sites. Hence, the lower selectivity to DPM at higher SiO_2/Al_2O_3 ratio may be attributed to the residual Bronsted acid sites, which are mainly responsible for catalyzing the consecutive reactions in the benzylation of benzene.

4.3.6. Influence of reaction temperature

The dependence of the conversion of BC (wt. %), rate of BC conversion (mmolg $^{-1}h^{-1}$) and product distribution (wt. %) on the reaction temperature is investigated in the range of 368 to 348 K using zeolites H-beta as catalyst (Figure.4.4). The conversion of BC and rate

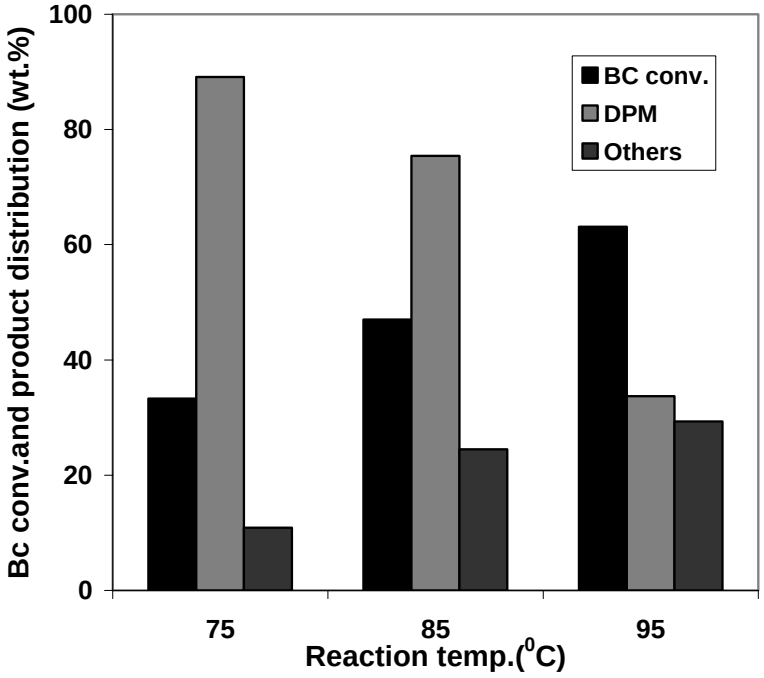

Figure 4.4. Influence of reaction temperature on the conversion of BC, product distribution Reaction conditions; catalyst = H-beta: [a] Reaction conditions: Catalyst (g) = 0.5 ; Benzene (mol) = 0.12 ; BC (mol) = 0.04 ; Benzene/BC (molar ratio) = 3; reaction temperature (K) = 358 ; reaction time (h) = 6 for $AlCl_3$ reaction time (h) = 0.5. [c] BC = Benzyl chloride [d] DPM = diphenylmethane ; Others = Polyalkylated products.

of conversion are found to increase with the increase in reaction temperature. The conversion of BC and rate of BC conversion increase from 33.3 to 63.1 wt % and 4.73 * 10^{-3} to 8.9 * 10^{-3} $mmolg^{-1}h^{-1}$, respectively, when temperature is raised from 348 to 368 K. However, the selectivity for DPM decreases with the increase in the reaction temperature as shown in the Figure. 4.4. A maximum in DPM selectivity (89.1 wt. %) is observed at 348 K. At higher temperatures (368 K), the decrease in DPM selectivity may be attributed to the formation of consecutive products.

4.3.7. Influence of benzene to BC molar ratio

Figure 4.5 exhibit the effect of the benzene/BC molar ratio on the catalytic activity of H-beta.

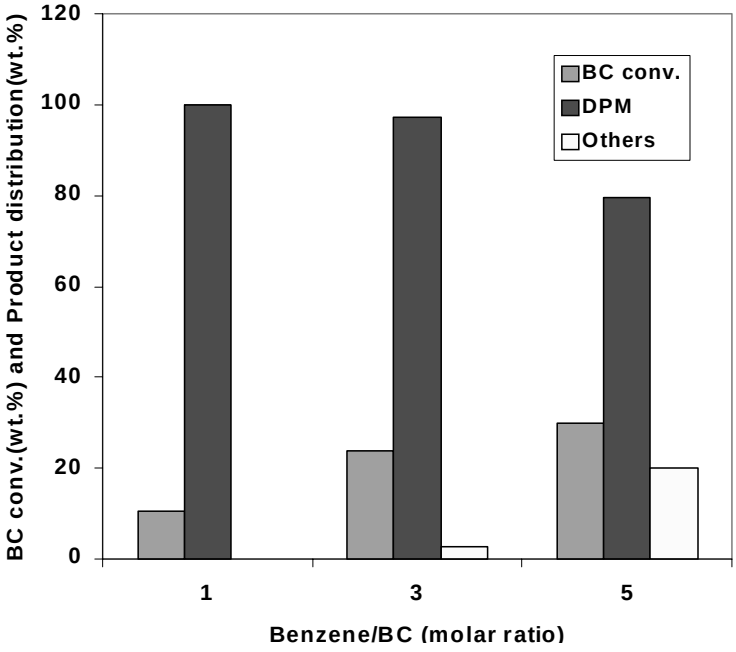

Figure 4.5. Influence of Benzene/BC molar ratio on the conversion of BC, product distribution. Reaction conditions: reaction time (h) = 4; catalyst = H-beta [a] Reaction conditions: Catalyst (g) = 0.5 ; Benzene (mol) = 0.12 ; BC (mol) = 0.04 ; Benzene/BC (molar ratio) = 3; reaction temperature (K) = 358 ; reaction time (h) = 6 for $AlCl_3$ reaction time (h) = 0.5.

The ratios are changed by keeping the amount of benzene constant. The data at 358 K shows that as the benzene/BC molar ratio is increased up to 5, the conversion of BC increased linearly. The results are in agreement with the earlier reported data in the benzylation of toluene and o-xylene over zeolite H-Y and H-beta [12]. In addition, the selectivity to DPM is found to be affected over this range of benzene to BC ratio [15-21].

4.3.8. Recycling of the catalyst

H-beta used in the benzylation of benzene is recycled two times in order to check the activity, stability and reusability of the catalyst. The results are shown in Table 4.2. After completion the reaction on fresh catalyst, the catalyst was separated from the reaction mixture via sedimentation or filtration, washed with acetone and calcined at 773 K for 16 h in the presence air. The activity of H-beta decreases progressively but slightly after each cycle when catalyst was used from fresh to second recycle. Moreover, the selectivity to DPM is also affected to a small extent compared with that of fresh catalyst. X-ray diffraction patterns are recorded after each recycle and indicate that the catalyst retains the H-beta structure. The results of chemical composition and the XRD of the catalysts show that the loss of activity may be correlated to the minor dealumination of zeolite H-beta by HCl, which is produced during the reaction as a by-product. These results are consistent with the earlier results [11-14, 22, 23].

Table 4.2. Recycling of H-beta[a]:

Run	Change in SiO_2/Al_2O_3	Conversion of BC(wt %)[b]	Rate of BC conversion[c] ($mmolg^{-1}h^{-1}$)	Product distribution (wt %)[d]		Crystallinity of H-beta (%)
				DPM	Others	
Fresh catalyst	26.0	23.7	3.37	93.2	6.5	100
1st	24.7	22.4	3.18	91.1	9.7	86.7
2nd	23.1	22	3.13	87. 3	12.7	79.2

[a] Reaction conditions: Catalyst (g) = 0.5 ; Benzene (mol) = 0.12 ; BC (mol) = 0.04 ; Benzene/BC (molar ratio) = 3; reaction temperature (K) = 358 ; reaction time (h) = 6 for $AlCl_3$ reaction time (h) = 0.5.

[b] Surface area (m^2/g), degree of ion exchange (%) and crystal size (μm) = H-beta = 745, 98, 0.5 ; H-Y = 615, 98, 1.0; H-ZSM-5 = 413, 98, 0.4, respectively.

[c] BC = Benzyl chloride

[d] DPM = diphenylmethane ; Others = Polyalkylated products.

4.4. CONCLUSIONS

It is demonstrated that the H-beta zeolite catalyses the benzylation of benzene with benzylchloride efficiently, which leads to the formation of DPM in high selectivity compared to the other zeolite catalysts. The conventional homogeneous catalyst, $AlCl_3$, does not possess shape selectivity and favor the formation of large amount of polybenzylated products. A selectivity of the order of 89.1 wt.% to DPM is achieved at 33.3 wt.% conversion of BC over H- beta, whereas, $AlCl_3$ gave lower selectivity to DPM (58 wt.%)

and higher amount of polyalkylated products (42 wt. %) under certain reaction conditions. The conversion, rate of BC conversion and product distribution largely depends on the experimental conditions. The conversion of BC increases with the increase in reaction time, catalyst concentration, reaction temperature and benzene to BC molar ratio, whereas it decreases with the increase in SiO_2/Al_2O_3 ratio of H-beta. Recycling of the catalyst progressively decreases the BC conversion. The presence of strong, as well as weak, acid sites in the zeolite catalysts appear to be very important for the polarization of the benzyl chloride into an electrophile ($C_6H_5CH_2^+$) which attack the benzene ring resulting in the formation of diphenylmethane.

4.4 REFERENCES

1. U. Beck, A.G.Bayer, in: *Ullmann's Encyclopedia of industrial chemistry* Vol. A13, Eds. W. Gerhartz, Y. S. Yamamoto, F. T. Campbell, Weinheim, New York (1985) p.260.
2. M. Grayson, Kirk-Othmer, *Encyclopedia of chemical Technology*, Vol. 5, Wiley, New York (1979) p. 686, 830; Vol. 11, Wiley, New York (1980) p. 275.
3. G.A. Olah: *Friedel-crafts and Related Reactions*, Wiley-Interscience, New York (1963).
4. V. R. Choudhary, S. K. Jana, B. P. Kiran**,** *Catal. Lett*. 59 (2–4) (1999) 217.
5. V. R. Choudhary, S. K. Jana, *Appl. Catal. A*. 224 (1-2) (2002) 51.
6. K. Okumura, K. Nishigaki, M. Niwa, *Microporous and Mesoporous Mater*. 44 (2001) 509.
7. V. R. Choudhary, S. K. Jana, *J. Mol. Catal. A- Chemical* 180 (1-2) (2002) 267.
8. R. J. Argauer, G. R. Landolt, *US Pat*. 3 702 886 (1972).
9. M. A. Camblor, J. P. Pariente, *Zeolites* 11(1991).
10. M. Chamoumi, D. Brunel, F. Fajula, P. Geneste, P. Moreau, J. Solof, *Zeolite* 14 (1994) 283.
11. A. P. Singh, D. Bhattarchaya, S. Sharma*, J. Mol. Catal.* 102 (1995) 139.
12. B. Coq, V. Gourves, F. Figueras, *Appl. Catal. A*.100 (1993) 69.
13. K. Arata, K. Sato, I. Toyoshima, *J.Catal*. 42 (1976) 221.
14. A. P. Singh, A. K. Pandey, J. *Mol. Catal*. 123 (1997) 141
15. R. Commandeur, N. Berger, P. Jay, J. Kervennal, *EP* 0 442 986 (1991).
16. G. A.Olah, S. J. Kuhn, S. Flood, *J. Am. Chem. Soc*. 84 (1962) 1688.

17. G. A. Olah, *Friedel-Crafts Chemistry*, Wiley, NewYork 1973.

18. P. Ratnaswamy, A. P. Singh, S. Sharma, *Appl. Cata. A.*135 (1996) 25.

19. Y. Izumi, N. Natsume, H. Takamine, J. Tamaoki, K. Urabe, *Bull. Chem. Soc. Jpn.* 62 (1989) 2159.

20. J. H. Clark, A. P. Kybett, D. J. Macquarrie, S. J. Barlow, P. Landon, *J. Chem. Soc. Chem. Commun.* (1989) 1353.

21. J. M. Lalancette*, US. Pat*. 3880944 (1975).

22. Corma, M. J. Ciment, H. Garcia, P. Primo**,** *Appl. Catal*. 49(1989)109.

23. D. Bhattacharya, S. Sharma, A. P. Singh, *Appl.Catal.A.*150 (1997) 53.

CHAPTER 5

MESOPOROUS ALUMINA AND

MODIFIED MESOPOROUS ALUMINA

5. SYNTHESIS, CHARACTERIZATION AND CATALYTIC ACTIVITY OF Co (II) AND Mn (III) SALEN COMPLEXES IMMOBILIZED OVER MESOPOROUS ALUMINA

5.1. INTRODUCTION

After the discovery of silica based ordered mesoporous materials of M41S family by Mobil researchers [1], much attention had been focused in the synthesis of non-siliceous mesoporous materials due to its potential applications in the field of separation science, nano science, catalysis, etc. Huo et al. [2] and Sayari et al. [3] demonstrated the synthesis of a variety of non-siliceous mesoporous materials, among them only a few exhibit better stability and increased meso structural ordering after the removal of the structure directors which limits its use as a catalyst or catalyst support. Hence, the synthesis of nonsiliceous mesoporous materials with better stability remains a challenge because compared to its oxide form, the mesoporous materials possesses high surface areas and variable pore sizes and hence can be finely tuned for specific applications like selective adsorption process by the suitable anchoring of various organic pendant groups [4]. Thus the synthesis of various organic-inorganic hybrid mesoporous materials emerges as a potential tool to anchor various homogeneous metal salts/complexes and it is interesting to probe the stability of such materials during various modification processes.

Heterogenization of homogeneous catalysts has been an interesting area of research in an academic and an industrial point of view, as this method can provide an ideal way for combining the advantages of homogeneous catalysts and simultaneously avoiding its disadvantages like handling and reusability [5, 6]. Mn/Co (salen) complexes have been reported as efficient catalysts for the epoxidation of various olefins [7-9]. The increasing interest towards this reaction brought some authors to develop the heterogeneous form of Mn (III)/Co (II) salen catalysts and to date three kinds of approaches have been generally adopted [10-16]. First, Mn salen complexes were supported on polymers for a better reusability of the materials. For instance, Janssen

et al. have synthesized a dimeric form of (salen) Mn (III) ligand and retained this complex in the cross-linked polymer membrane and used as a catalyst for epoxidation reactions [17] while Minutolo et al. synthesized the polymer-bound salen Mn (III) complex by copolymerization of salen complex with styrene and divinylbenzene [18]. Secondly, the encapsulation of salen complex was performed by using the so-called, 'ship in a bottle' technique. Sabater et al. synthesized Mn (III) salen complex of simple structure inside the supercage of Y-zeolites, and showed that the catalytic activity was similar to that of chloride complexes in the homogeneous phase [19]. Alternatively, Mn (III) salen ligands were immobilized by an ion exchange mechanism like the embedding of selective homogeneous Mn (III) cationic salen complexes into the pores of mesoporous MCM-41 materials [20]. Hence, novel routes for the anchoring of these metal complexes over various supports having good stability and open channels rely as a potential way to extend their applicability and reusability. The present work deals with the synthesis and characterization of metal (salen) complexes immobilized mesoporous alumina, performed by the chemical anchoring of the complex to the support surface *via* suitable modifications. The heterogenity of the developed materials were verified in the epoxidation reaction of various olefins and the performance was compared with the homogeneous counterparts. To the best of our knowledge, this is the first report detailing the immobilization of salen-ligated metals *via* condensation procedure over mesoporous alumina.

5.2. EXPERIMENTAL

5.2.1 Synthesis

The materials used for the synthesis were: aluminium isopropoxide (Aldrich), lauric acid (Loba Chemie), 1-propanol (Merck), 3-amino propyl triethoxy silane (3-APTES, Lancaster), salicyl aldehyde (Merck), cobalt (II) acetate and manganese (III) acetate (Aldrich).

5.2.2. Preparation of mesoporous alumina (MA)

Non-siliceous mesoporous alumina was synthesized according to the following procedure at a temperature of 110 °C using carboxylic acid (Lauric acid) as surfactant [21]. The composition of gel mixture is Al-isopropoxide: Lauric acid: 1-propanol as 1: 0.03: 26. Typically, an aluminum hydroxide suspension was prepared by the hydrolysis of 43.8 g of Al-isopropoxide with 10.3 g of deionised water in 275 g of 1-propanol (99

%). After stirring for 1 h, 10.8 g of lauric acid (99.5 %) was added slowly to the gel mixture. The mixture was aged for 24 h at room temperature and then heated under static conditions at 110 °C in 1 L glass jar for two days. The solid material obtained was then filtered, washed with ethanol and dried at 100 °C for 4-5 h. Finally, the material was calcined at a temperature of 450 °C with a temperature ramp of 1°C/min from room temperature to the final temperature. The calcination atmosphere was nitrogen during the earlier stages (<200 °C) and air at final temperatures.

5.2.3. Preparation of 3-APTES functionalized mesoporous alumina (NH_2-MA)

To a suspension of 10 g of calcined mesoporous alumina in 50 mL dry toluene, 2.68 g of 3-aminopropyl triethoxy silane (3-APTES) was added slowly and heated to reflux with continuous stirring for 8 h under nitrogen atmospheres (Scheme 5.1). The powdery sample containing amino groups was filtered, washed with acetone and then soxhlet extracted using a solution mixture of diethyl ether and dichloromethane (1:1) for 24 h and dried under vacuum. Elemental analysis shows that 0.89 % of nitrogen gets introduced into the mesoporous support, which indicates that ~52 % of 3-APTES was immobilized per gram of mesoporous alumina.

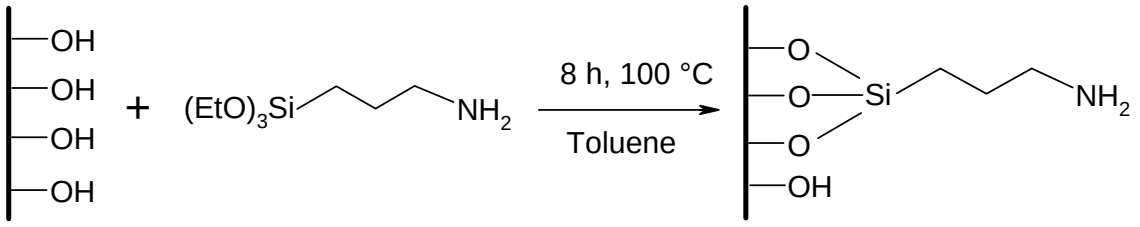

Scheme 5.1

5.2.4. Preparation of neat Co (II) and Mn (III) complexes

Cobalt and manganese (salen) precursors were prepared according to the following procedure. The appropriate metal (cobaltous and manganese) acetate hydrate (6.0 mmol) in ethanol (10 mL) was added slowly to a solution of salicylaldehyde (2.94 g,

24.0 mmol) in ethanol (40 mL). The solutions were stirred at room temperature for 24 h and their subsequent concentration leads to precipitation of the corresponding metal (salen) precursor (Scheme 5.2). The solid product obtained was washed with copious amounts of chloroform and dried in vacuum at 100 °C for 24 h. Elemental analysis datas obtained after purification are as follows; theoretical value (actual value) of C (%) 56.56 (58.18), H (%) 3.36 (4.11) for Mn-complex, while Co-complex shows C (%) 58.18 (56.49) and H (%) 3.32 (3.01).

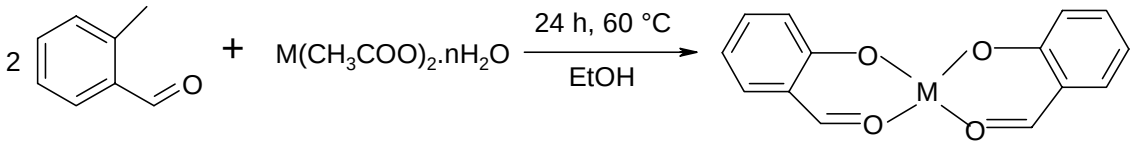

Where, M=Mn, Co

Scheme 5.2

5.2.5. Preparation of salen Co (II) and salen Mn (III) complexes immobilized on modified mesoporous alumina (Co/Mn-S-NH_2-MA)

The synthesized neat complex, *viz.,* (bis-salicyl aldehyde) M, has been chemically anchored to the aminopropyl modified alumina support, using a procedure as shown in the Scheme 5.3 [22]. The material was then soxhlet extracted, using a mixture of $CHCl_3$-EtOH mixture for 12 h to remove the unreacted organic residue from the mixture.

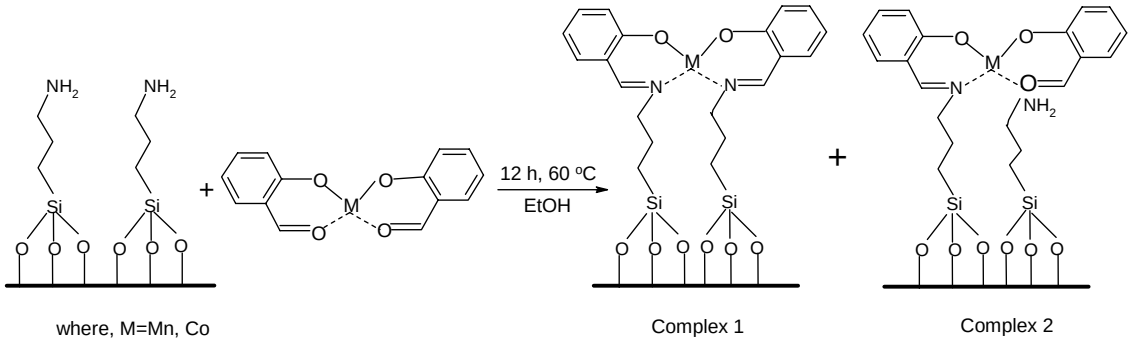

Scheme 5.3

5.2.6 Characterization

Analysis of the organic material incorporated on the solid mesoporous material was carried out by using EA1108 Elemental Analyzer (Carlo Erba Instruments). X-ray diffraction measurements were carried out on a Rigaku Miniflex diffractometer using Cu K_α radiation, at a scan rate of 3 °/min from 1.5-50 °. FTIR spectra of the solid samples were taken in the range of 4000 to 400 cm^{-1} on a Shimadzu FTIR 8201 instrument by diffuse reflectance scanning disc technique. The specific surface area, total pore volume and average pore diameter were measured by N_2 adsorption-desorption method using NOVA 1200 (Quanta chrome). The samples were activated at 200 °C for 3 h under vacuum and then the adsorption-desorption was conducted by passing nitrogen into the sample, which was kept under liquid nitrogen. Pore size distribution (PSD) was obtained by applying the BJH pore analysis applied to the adsorption branch of the nitrogen adsorption-desorption isotherm. Thermo gravimetric and differential thermogravimetric (TG-DTA) analysis of the neat and immobilized Co and Mn-salen complexes was recorded on a Rheometric Scientific (STA 1500) analyzer. Diffuse reflectance UV-Vis spectra were recorded in the range 200-600 nm with a Shimadzu UV-2101 PC spectrometer equipped with a diffuse reflectance attachment, using $BaSO_4$ as reference.

XPS spectra were recorded on a VG micortech multilab-ESCA 3000 spectrometer equipped with a twin anode of Al and Mg. All the measurements are made on powder samples using Mg K. X-ray at room temperature. Base pressure in the analysis chamber was 4×10^{-10} torr. The overall energy resolution of the instrument is better than 0.7 eV, determined from the full width at half maximum of the $4f^{7/2}$ core level of the gold surface. The error in all the binding energy (B.E) values was within ± 0.1 eV. The correction of binding energy was performed by using the C1s peak of carbon at 284.9 eV, as reference.

5.2.7. Catalytic measurements

In a typical reaction, TBHP (0.45 g, 5 mmol) was added to a solution of styrene (0.52 g, 5 mmol) in acetonitrile (6 g) containing 0.2 g of catalyst (pre-activated at 100 °C for 2 h). The reaction mixture was magnetically stirred at 60 °C in a silicone oil bath. Samples of the reaction mixture were taken periodically and analyzed by gas chromatograph (HP 6890) equipped with a flame ionization detector (FID) and a capillary column (5 μm thick cross-linked methyl silicone gum, 0.2 × 50 m). The products were further identified by GC-MS analysis (Shimadzu 2000 A).

5.3. RESULTS AND DISCUSSION

Figure. 5.1 depicts the XRD patterns of as-synthesized, calcined, aminopropyl modified and complex functionalized mesoporous alumina. The diffraction patterns of as synthesized and calcined forms of mesoporous alumina shows a broad reflection at a 2 theta value of 2.6, assigned to the (100) reflection of the hexagonal lattice. Even though

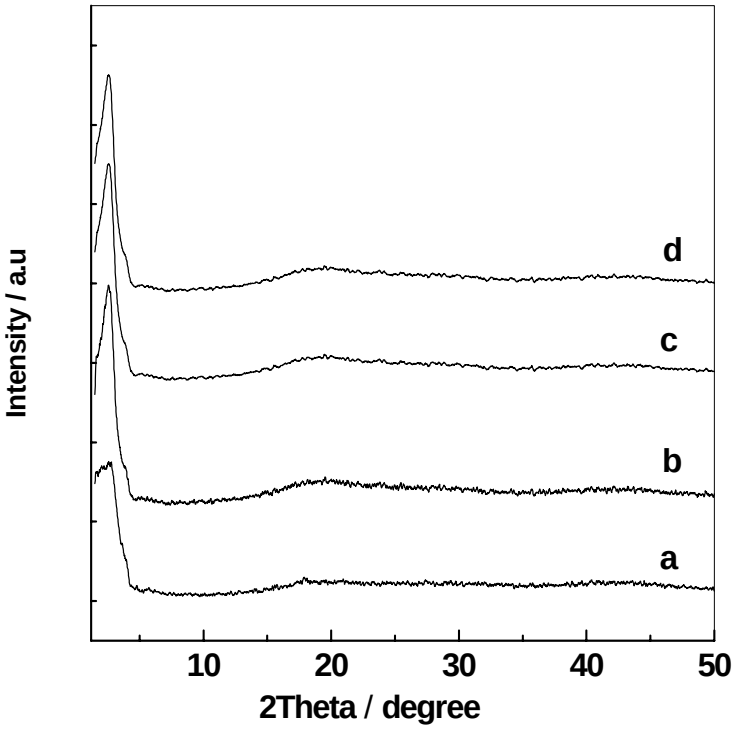

Figure 5.1. XRD patterns of (a) as synthesized mesoporous alumina; (b) calcined mesoporous alumina; (c) aminopropyl modified mesoporous alumina; (d) Co-salen immobilized mesoporous alumina.

the XRD patterns are devoid from any higher order reflections, the intensity of the characteristic d_{100} peak of calcined mesoporous alumina is quite pronounced and is similar to earlier reports over non-siliceous mesoporous materials [23, 24]. The absence of higher order reflections indicates that the pore walls are amorphous or there is a lack of correlation between the structures of adjacent pores. Further, after modifications the intensity of the characteristic d_{100} reflection gets decreased while the mesostructure remains intact. These results show that the anchoring of the functionalized moieties (3-APTES and further anchoring of salen complexes), inside the pore channels of mesoporous alumina, had not damaged the overall structure of the support material.

The IR spectra of as-synthesized, calcined, 3-APTES modified and Co (II) and Mn (III) salen immobilized mesoporous alumina in the 4000-400 cm^{-1} range are presented in Figure. 5.2 (A and B). The as-synthesized samples exhibit bands at 2930 and 2870 cm^{-1} corresponding to C-H vibrations of the surfactant molecules, but in the case of calcined samples, the peaks disappeared due to removal of the template molecules. In detail, the spectra of calcined alumina show peaks in the range of 3600-3200 cm^{-1}, attributed to the hydroxyl stretching of the hydrogen bonded internal alumina groups. However, after amine functionalization, new bands appeared at 2939 and 2879 cm^{-1} which are assigned to the asymmetric and symmetric stretching vibrations of $-CH_2$ groups and thus the presence of these bands on NH_2-MA sample shows that amino propyl groups get anchored on the inner wall surface of mesoporous alumina [25, 26]. Further, the presence of band at 3300 cm^{-1} in the NH_2-MA sample, assigned to the N-H stretching vibrations of the propyl amino groups, confirms the successful functionalization of 3-APTES groups on the alumina surface (Figure. 5.2C). After complex immobilization, the band due to N-H vibration gets disappeared with the formation of a new band at 1630 cm^{-1}, which is the characteristic stretching vibration of C=N band [27, 28]. These two results clearly indicate the anchoring of Co and Mn complexes over the amino groups of modified mesoporous alumina surface, as shown in Scheme 3. Further, the immobilized complex materials show all the characteristic peaks of the neat complexes and thereby confirm that the complex species gets anchored on the pendant organic groups of the mesoporous support.

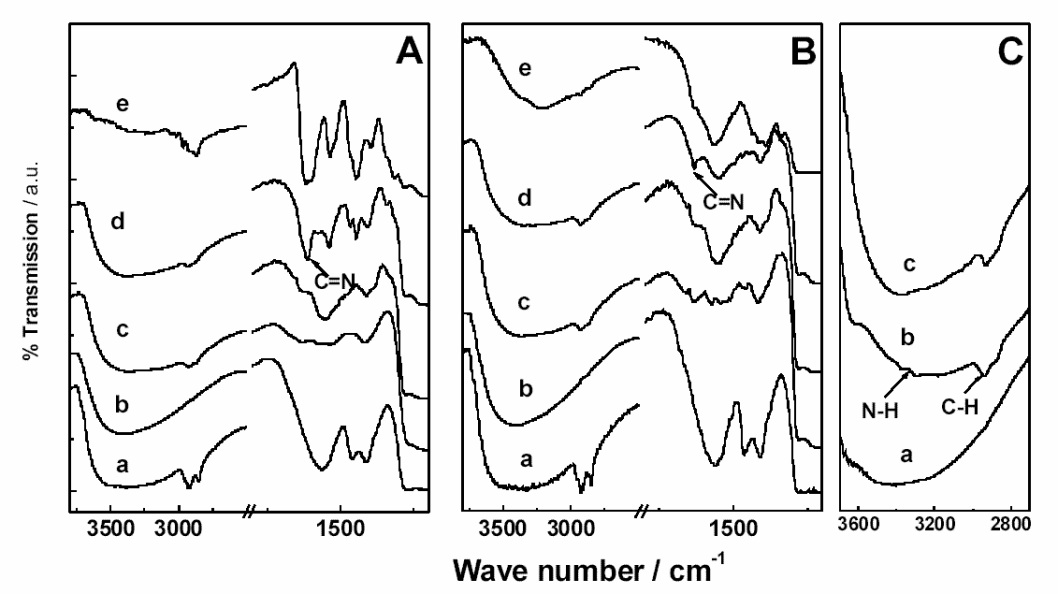

Figure 5.2. FTIR spectra of (A) Co-salen containing mesoporous alumina, (B) Mn-salen containing mesoporous alumina, where (a) as synthesized mesoporous alumina, (b) calcined mesoporous alumina, (c) aminopropyl modified mesoporous alumina, (d) metal salen immobilized mesoporous alumina, (e) neat metal complex, while (C) shows the zoom over 2700-3700 cm^{-1} region of (a) calcined mesoporous alumina, (b) aminopropyl modified mesoporous alumina and (c) metal-salen immobilized mesoporous alumina.

It is well known that the introduction of homogeneous catalysts or metals on porous supports shows a decrease in the specific surface area and pore volume. The support, mesoporous alumina, shows a high surface area of 450 m^2g^{-1} and pore volume of 0.4212 ccg^{-1}; after metal complex functionalization the surface area gets reduced to 223 m^2g^{-1} for Co-S-NH_2-MA and 234 m^2g^{-1} for Mn-S-NH_2-MA. Thus the decrease in mesoporous volume (~52 %) and surface area (~48 %) after metal immobilization is indicative of the grafting of complex inside the channels of mesoporous alumina and a detailed list of surface area, pore volume and pore diameter of support and modified samples are given in Table 5.1. It is clear from table that, even though silylation procedures changed the textural properties of the mesoporous material, the decrease is

more prominent after complex immobilization and is due to the presence of bulkier organic moieties inside the pore channel of the support. These results reveal that the anchoring of complex groups had occurred inside the pore channels of mesoporous alumina. Further the adsorption-desorption isotherms of mesoporous alumina and metal complex immobilized mesoporous alumina are of Type IV, according to the IUPAC classification, and its steep condensation behavior indicates the existence of uniformly sized mesopores (Figure. 5.3). In detail, the alumina support shows an inflection in the P/P° ~0.5 range while after complex immobilization the P/P° value changed to a lower value of ~0.45, indicative of some sort of structural damage to the material after modifications, and are consistent with the XRD results. Moreover, the BJH pore size distribution analysis shows that the material posses uniformly sized mesopores (see inset of figure 3) centered at ca ~44 Å (Figure. 5.3A) for alumina support and ca ~38 Å (Figure. 5.3B) for the metal complex functionalized samples.

Table 5.1.

Textural properties of mesoporous alumina and functionalized samples

Sample	d_{100} (nm)	S_{BET} (m^2 /g)	Pore volume (ml/g)	Pore diameter (nm)
MA	3.17	450	0.4212	4.43
NH_2-MA	3.23	359	0.2311	n.d.
Mn-S-NH_2-MA	3.20	234	0.1821	3.76
Co-S-NH_2-MA	3.33	223	0.1710	3.89

n.d. = not determined

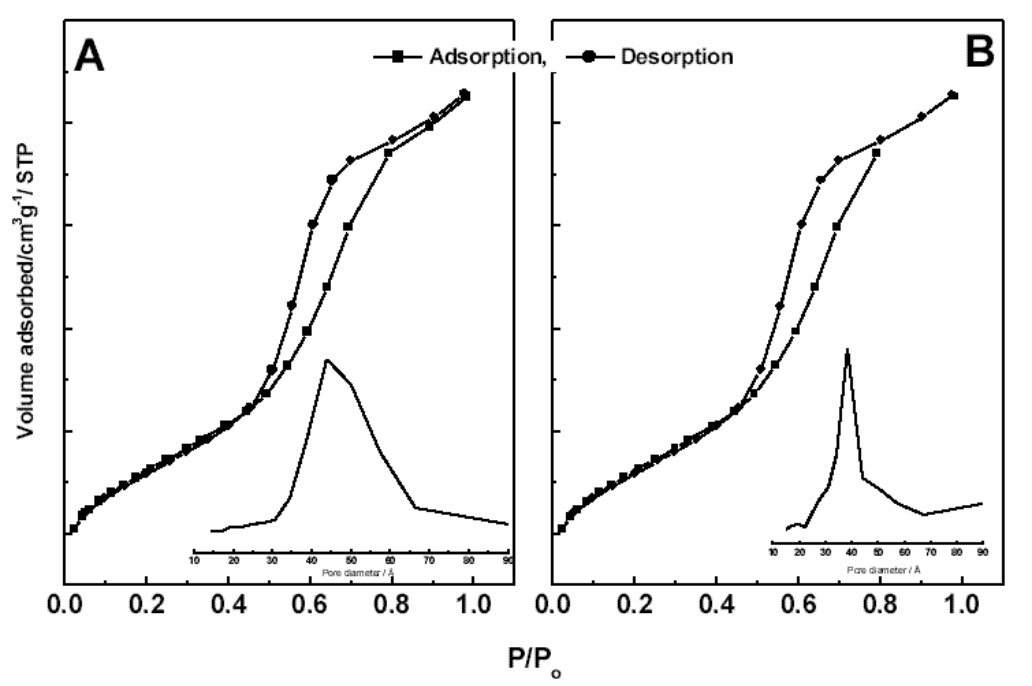

Figure 5.3. N_2 adsorption-desorption isotherms and pore size distributions (inset) of (A) calcined mesoporous alumina; (B) Co-salen immobilized mesoporous alumina.

Thermal analysis had been used to monitor the decomposition profiles of the neat as well as anchored metal complexes and the results obtained are depicted in Fig. 5.4. The spectrum of as-synthesized mesoporous alumina shows two steps of weight loss, when heated under airflow, one at ~100 °C and the other at ~400 °C. The former weight

loss is usually attributed to the loss of physisorbed water molecules while the latter loss attributes to the decomposition of template molecules from the pore channels. A complete decomposition of the surfactant groups below 400 °C indicates that the calcination procedure opted for the removal of structure directors was optimum (see experimental section). In accordance with that, the DTG spectrum of calcined alumina shows only a sharp weight loss below ~100 °C, without any template decompositions at higher temperature regions. On the contrary, the TG/DTG spectrum of NH_2-MA shows two steps of weight loss, one below ~100 °C and the other in the region of 340-380 °C. As mentioned, the former weight loss is due to desorption of physisorbed water, while the second weight loss is attributed to the loss of organo propyl amino fragments [26]. The DTA results further confirm the above results that a strong exothermic peak is observed around ~360 °C, for the decomposition of the propyl groups from the alumina surface (figure not shown). The decomposition profiles of homogenous metal complexes get completed at ~468 °C and ~423 °C for Co and Mn salen complexes, respectively, with the residues amounting to cobaltous and manganese oxides. Interestingly, after immobilization, the final decomposition temperatures gets increased up to ~626 and ~619 °C for Co-S-NH_2-MA and Mn-S-NH_2-MA complexes, respectively, due to the mutual stabilization of propyl amino groups and the complexes and are indirect proofs for the entrapment of complex moieties inside the pore channels of mesoporous alumina [29].

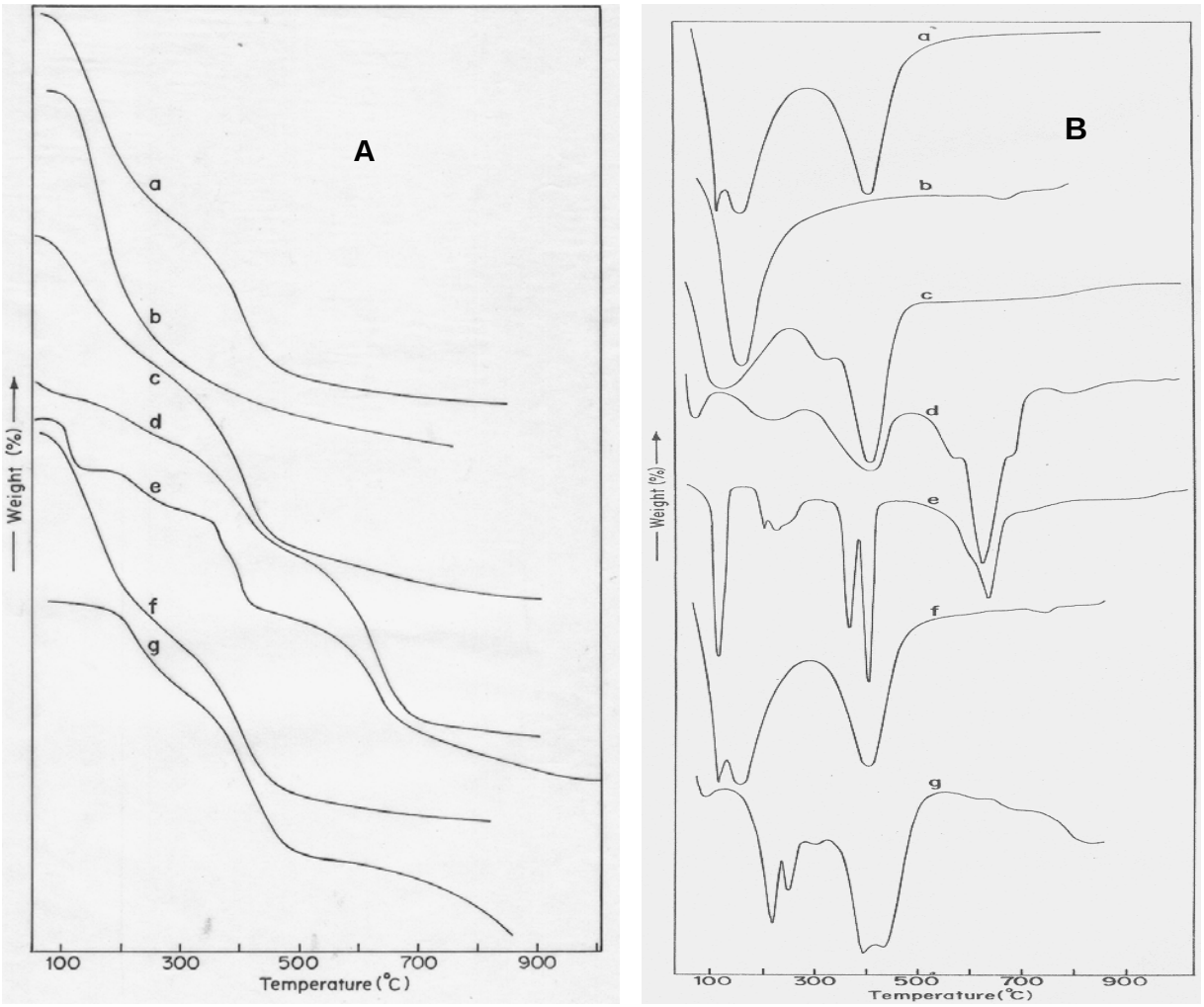

Figure 5.4. Thermogravimetric (A) and differential thermo gravimetric (B) results of (a) assynthesized mesoporous alumina, (b) calcined mesoporous alumina, (c) aminopropyl modified alumina, (d) Mn immobilized mesoporous alumina, (e) Co immobilized mesoporous alumina, (f) neat Mn complex, (g) neat Co complex.

The UV-Vis electronic spectra of mesoporous alumina (MA), 3-APTES modified mesoporous alumina (NH_2-MA), Co (II)/Mn (III) salen immobilized mesoporous alumina (Co-S-NH_2-MA and Mn-S-NH_2-MA) and homogenous adducts were presented in Figure. 5.5 A&B. The UV-Vis spectra of neat Co-complex exhibits two broad bands at ~280 and

~390 nm, while Mn-complex exhibits a broad band at ~415 nm ascribed to the ligand to metal charge transfer transition bands, akin to related metal (salen) compounds described in the literature [29-31]. After immobilization, for Co (salen) sample the two distinct bands observed in the neat complex gets overlapped to form a broad band centered around ~425 nm, whereas for Mn (salen) sample the spectrum exhibits multiple bands at ~280, ~320, ~430 nm. Even though a proper comparison between the neat and immobilized complex is inappropriate, due to the different coordination spheres, as an indirect evidence it can be concluded that the occurrence of the band at higher wave numbers and its splitting may be due to the different environment and donor sites of the heterogenized metal complexes than the neat complexes. These results are complementary to the datas obtained from IR spectra that the immobilization of Co (II)/Mn (III) complexes occurred through schiff base condensation with the amino propyl groups.

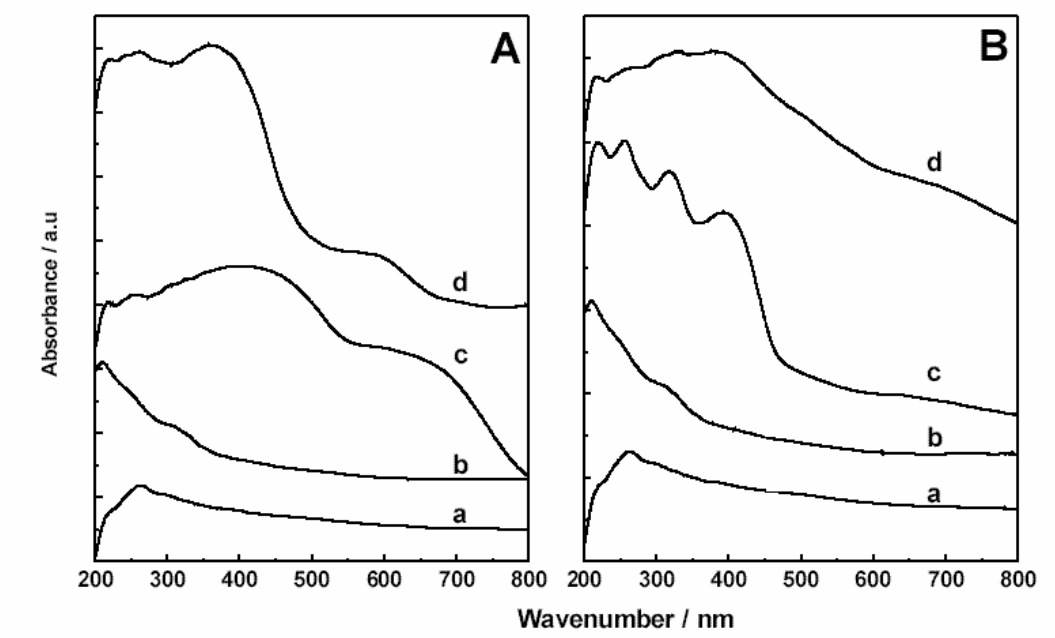

Figure 5.5. DRUV-Vis spectra of (A) Co-Salen containing mesoporous alumina and (B) Mn-Salen containing mesoporous alumina, where (a) calcined mesoporous alumina; (b) aminopropyl

modified mesoporous alumina; (c) metal-salen immobilized mesoporous alumina; (d) neat metal complex.

X-ray photoelectron spectroscopy (XPS) is a powerful technique used to investigate the electronic properties of the species formed on the surface. As the electronic environment e.g. oxidation state and/or spin multiplicity influences the binding energy (B.E.) of the core electrons of the metal, XPS is extensively used to attain detailed information about the state of metal species on the surfaces. Figure 5.6 (A and B) shows the XPS spectra obtained for pure homogeneous adduct and Co (II) and Mn (III)-

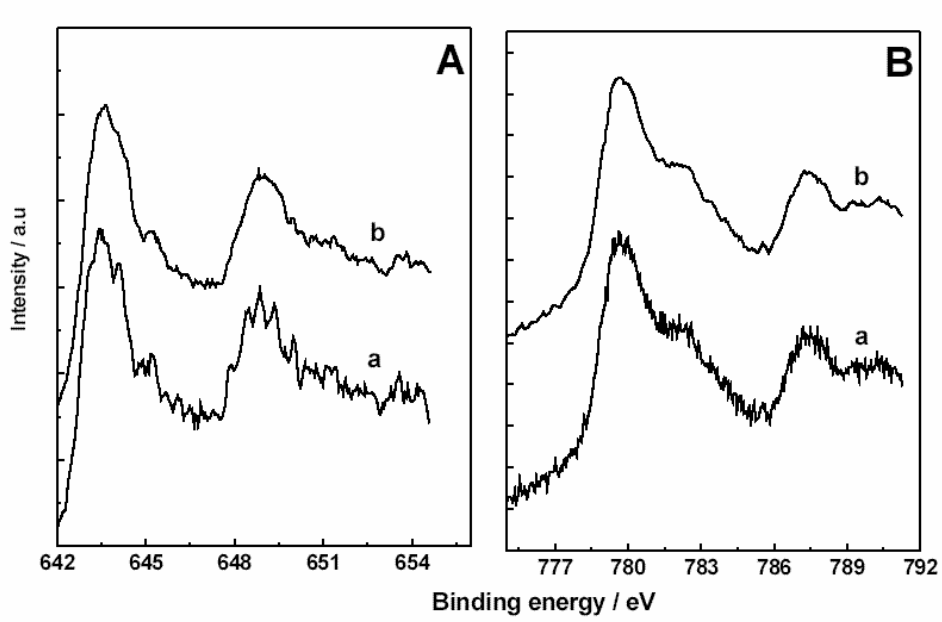

Figure 5.6. XPS spectra of (A) Mn-Salen containing mesoporous alumina and (B) Co-salen containing mesoporous alumina, where (a) neat metal complex; (b) immobilized metal complex.

salen immobilized mesoporous alumina. Briggs and Seah [32] proposed that the intensity ratio and the energy difference between the two signals obtained for electron ejected from the $p^{1/2}$ and $p^{3/2}$ levels can be used as a tool to investigate the spin multiplicity and

therefore to the electronic properties of the cobalt and manganese compounds [33]. The neat manganese complex exhibits Mn $2p^{3/2}$ core level peak at a binding energy of ~642.5 eV, while the immobilized Mn salen complex shows a binding energy at ~643.3 eV, and are in accordance with earlier literature datas [34]. The observed increased chemical shift of ~1 eV for the immobilized salen complex than the neat complex attributes to the differences in the coordination environment of metal inside the confined pore channels of mesoporous alumina than under neat conditions. Similarly, cobalt complex also shows an experimental trend as in Mn complexes and matches well with the reported binding energy values of Co $2p^{3/2}$ peak, viz. 779.1 eV for neat cobalt complex and 779.9 eV for immobilized Co-salen complex [35].

5.4. Catalytic reactions

Structural characterization results show that the metal complex is firmly held inside the pore channels of mesoporous alumina and hence the present materials are applied in the liquid phase epoxidation reaction of styrene and cyclohexene. The results obtained from the epoxidation reaction of neat as well as immobilized complexes are

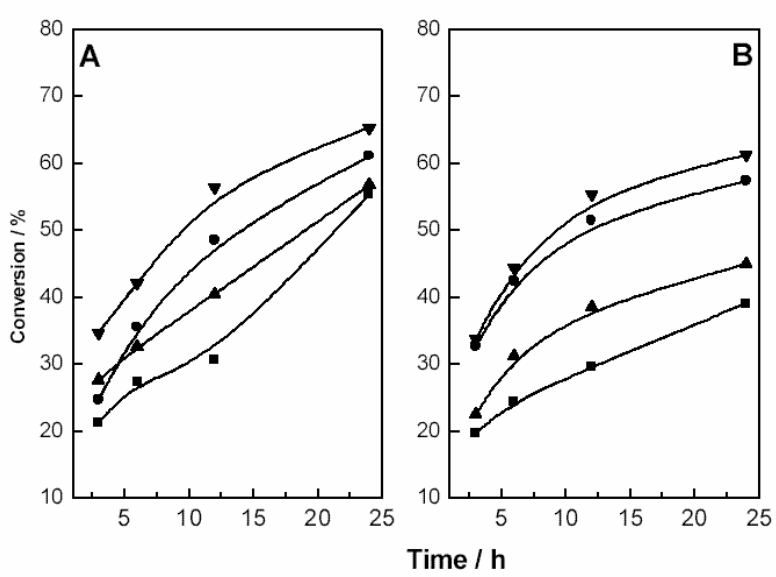

Figure 5.7. Reaction kinetic profiles of neat and immobilized Co and Mn-salen complex in the oxidation reaction of (A) Cyclohexene and (B) Styrene.

presented in Table 5.2 and 5.3 and the kinetic profiles for the activity of neat and immobilized complexes under both reactions are further shown in Figure. 5.7.

Table 5.2.

Oxidation of olefins by neat and immobilized metal-salen catalysts

Catalyst	Substrate Used	Conversion (wt%)	Epoxide Yield (wt%)	TON[a]
Neat Mn(salen)	Cyclohexene Styrene	26.7 29.5	13.5 11.8	25.2 24.8
Mn-S-NH_2-MA	Cyclohexene Styrene	48.5 51.4	19.5 27.2	56.8 47.6
Neat Co(salen)	Cyclohexene Styrene	40.4 38.4	20.2 9.8	33.0 32.1
Co-S-NH_2-MA	Cyclohexene Styrene	56.3 55.3	27.6 28.2	63.3 50.0

Reaction conditions: styrene: 0. 52 g / cyclohexene: 0.41 g, TBHP (70%): 0.45 g, CH_3CN: 6 g, T: 60 ^oC, t: 12 h, Catalyst amount: 0.2 g.

[a]TON: Turn over number, moles of substrate converted per mole of metal.

Table 5.3.

Oxidation of cyclohexene by neat and immobilized metal-salen catalysts.

Catalyst	M (%)[a]	Conversion (wt%)	Selectivity (%)			TON[c]
			Epoxide	One[b]	Others	
MA	-	5.7	12.6	47.1	40.3	25.2
Neat Mn(salen)	0.69	26.7	13.5	70.5	16	25.2
Mn-S-NH_2-MA	0.57	48.5	19.5	69.8	10.7	56.8
Neat Co(salen)	0.87	40.4	20.2	65.2	14.6	33.0
Co-S-NH_2-MA	0.63	56.3	27.6	58.8	13.6	63.3

Reaction conditions: cyclohexene: 0.41 g, TBHP (70%): 0.45 g, CH_3CN: 6 g, T: 60 ^oC, t: 12 h, Catalyst amount: 0.2 g.

[a]M : metal content determined from ICP analysis.

[b]one : cyclohexenone, [c]TON: Turn over number, moles of substrate converted per mole of metal.

From Table 5.2 and Figure 5.7, it is clear that mesoporous alumina functionalized metal complexes show an enhanced activity (calculated in terms of turn over number, TON) and selectivity towards the desired epoxide product than the neat metal complexes. Since the support alumina had a high surface area and moderate pore size, we believe that the confined environment of the metal complex avoids undesirable side reactions like the over oxidation process, as observed with the neat complexes, leading to better activity as well as selectivity to epoxides [25, 31]. However, as mentioned earlier, it is inappropriate to compare the catalytic results under neat as well the heterogenized conditions, since the coordination sphere of both complexes is different. Among olefins, styrene conversion is higher than cyclohexene, which may be due the comparatively easier side chain oxidation than the reactions in the aromatic ring. Interestingly, even though benzaldehyde was the major product obtained during styrene epoxidation, kinetic studies revealed that the formation of phenyl acetaldehyde, an isomerized product of styrene epoxide, is not formed over immobilized catalysts while under neat catalysts a significant amount of its formation is noted. Hence, it is reasonable to assume that the reaction proceeds under different mechanisms over the homogenous complexes and heterogeneous catalysts. Further, in order to ascertain whether the activity of the immobilized catalysts arise from true heterogeneous catalysts, the stability of metal complexes were probed by performing typical leaching studies. For that, the catalyst was separated from the reaction mixture after a definite period of time (viz. 2 h) and the hot filtrate was probed for further

reactions. Interestingly, it was found that the conversion rate essentially gets terminated after the removal of the catalyst sample, which confirms that the present anchored metal complexes are stable in the reaction medium and are not prone for leaching. Hence considering the increased stability of the materials, it is reasonable that between the two complex species shown in Scheme 5.3, complex 1 may be the major species formed. Moreover the catalyst, Mn-S-NH_2-MA, was reused three times in the reaction of styrene without significant differences in the conversion (51.4 % changed to 46.4 %) and selectivity (27.2 % changed to 25.1 % after third run), and thereby relies as novel heterogeneous catalysts for various (ep) oxidation reactions.

5.5. CONCLUSION

The immobilization of manganese and cobalt complexes over mesoporous alumina, modified previously by 3-APTES, has been achieved by schiff base condensation reaction. Different characterizations techniques such as XRD, FTIR, TGDTG, UV-Vis and XPS reveal that the complex is attached firmly over the modified alumina surfaces. The molecular dispersion of the complex with sufficient space and hydrophobic surface are appropriate for activation of hydrocarbons as evidenced by the higher TON over immobilized catalysts in the selected epoxidation reactions. Moreover, these new catalysts did not leach its active sites during reactions and are reusable which indicates that the immobilization of neat complexes are effective by the present synthesis protocols over mesoporous alumina.

5.6 REFERENCE:

1. C. T. Kresge, M. E. Leonowicz, W. J. Roth, J. C. Vartuli, J. S. Beck, *Nature* 359 (1992) 710.
2. Q. Huo, D. I. Margolese, V. Ciesla, P. Feng, T. E. Gier, P. Sieger, R. Leon, P. M. Petroff, F. Schuth, G. D. Stucky, *Nature* 368 (1994) 317.
3. A. Sayari, P. Liu, *Microporous Mater.* 12 (1997) 149.
4. M. Chidambaram, D. C-Ferre, A. P. Singh, B. G. Anderson, *J. Catal.* 220 (2003) 442
5. Y. Iwasawa, *Tailored Metal Catalysts*, Reidel, Holand, 1986.
6. A. Kozlov, K. Asakura, Y. Iwasawa, *Microporous Mesoporous Mater.* 21 (1998) 579.
7. E. N. Jacobson, W. Zhang, A. R. Muci, J. R. Ecker, L. Deng, *J. Am. Chem. Soc.* 113 (1991) 7063.
8. M. Palucki, P. J. Pospisil, W. Zhang, E. N. Jacobson, *J. Am. Chem. Soc*.116 (1994) 9333
9. R. Irie, K. Noda, Y. Ito, N. Matsumoto, T. Katsuki, *Tetrahedron Lett*.31 (1990) 7345.
10. B. M. Choudary, M. L. Kantam, B. Bharathi, P. Sreekanth, F. Figueras, *J. Mol. Catal.A. Chem.* 159 (2000) 417.
11. C. Baleizao, B. Cignate, H. Garcia, A. Corma, *J. Catal*. 215 (2003) 199.
12. S. R. Cicco, M. Latronico, P. Mastrorilli, G. P. Suranna, C. F. Nobile, *J. Mol. Catal. A. Chem.* 165 (2001) 135.

13. C. Bowers, P. K. Dutta, *J. Catal*. 122 (1990) 271.

14. P. P. Knops-Gerrits, M. L. Abbe, P. A. Jacobs, *Stud. Surf. Sci. Catal.* 108 (1997) 445.

15. P. P. Knops-Gerrits, D. E. de Vos, P. A. Jacobs, *J. Mol. Catal.* 117 (1997) 57.

16. J. Zhao, J. Han, Y. Zhang, *J. Mol. Catal. A. Chem*. 231 (2005) 129.

17. K. B. M. Janssen, I. Laquiere, W. Dehaen, R. F. Parton, I. F. J. Vankelecom, P. A. Jacobs, *Tetrahedron Asym*. 8 (1997) 3481.

18. F. Mintolo, D. Pini, P. Salvadori, *Tetrahedron Lett*. 37 (1996) 3375.

19. M. J. Sabater, A. Corma, A. Domenech, V. Fornes, H. Garcia, *J. Chem. Soc. Chem. Commun.* (1997) 1285

20. P. Piaggio, P. McMorn, C. Langham, D. Bethell, P. C. Bulman-Page, F. E. Hancock, G. J. Hutchings, *New. J. Chem*. 22 (1998) 1167.

21. L. Frunza, H. Kosslick, H. Landmesser, K. Hoft, R. Fricke, *J. Mol. Catal. A. Chem.*123 (1997) 179.

22. E. F. Murphy, A. Baiker, *J. Mol. Catal. A. Chem*. 179 (2002) 233.

23. F. Vaudry, S. Khodabandeh, M. E. Davis, *Chem. Mater*. 8 (1996) 1451.

24. M. J. Hudson, J. A. Knowles, *J. Mater. Chem*. 6 (1996) 89.

25. S. Shylesh, A. P. Singh, J. Catal. 228 (2004) 333.

26. S. Shylesh, S. Sharma, S. P. Mirajkar, A. P. Singh, *J. Mol. Catal. A. Chem*. 212 (2004) 219.

27. P. Karandikar, M. Agashe, K. Vijaymohanam, A. J. Chandwadkar, *Appl. Catal. A. Gen.* 257 (2004) 133

28. X. G. Zhou, X. Q. Yu, J. S. Huang, S. G. Li, L-.S. Li, C. M. Che, *Chem.*

Commun. (1999) 1789.

29. T. Joseph, S. B. Halligudi, C. V. V. Satyanarayana, D. P. Sawant, S. Gopinathan, *J. Mol. Catal. A. Chem*.168 (2001) 8797
30. S. B. Halligudi, K. N. Kalaraj, S. S. Despande, S. Gopinathan**,** *J. Mol. Catal.* 154 (2000) 25.
31. T. Joseph, D. P. Sawant, C. S. Gopinath, S. B. Halligudi, *J. Mol. Catal. A. Chem. 1*84 (2002) 289.
32. D. Briggs, M. P. Seah, *Practical Surface Analysis*, Auger and X-Ray Photoelectron Spectroscopy, Vol. 1, II Ed., Wiley, London 1996, p. 129.
33. D. Briggs, V. A. Gibson, *Chem. Phys. Lett*. 25 (1974) 493.
34. A. R. Silva, J. L. Figueiredo, C. Freire, B. D. Castro. *Microp. and Mesop. Mater.* 68 (2004) 83.
35. L. Guezi, R. Sundararajan, Zs. Koppany, Z. Zsoldos, Z. Schay, F. Mizukami, S. Niwa, *J. Catal*. 167 (1997) 482.

CHAPTER 6

SUMMARY AND CONCLUSIONS

6. CONCLUSIONS

The present work reports the synthesis, modification and characterization of synthesized or commercially available zeolite catalysts, mesoporous alumina and organo functionalized materials such as 3-aminopropyltriethoxysilyl functionalized mesoporous alumina. The catalytic activity of these catalysts in the selective acylation (benzoylation and Propionylation of phenol and Propionylation of chlorophenol), alkylation (benzylation of benzene) and oxidation of styrene and cyclohexene is investigated for producing industrially important products in high selectivity.

The work is presented in six chapters

A review on the published and patented literature on the synthesis, characterization and utility of zeolites and salen complex immobilized mesoporous alumina in the synthesis of fine chemicals, particularly in the acylation, alkylation, oxidation reactions of styrene and cyclohexene with shape selective characteristics is reported in **Chapter 1**.

Chapter 2 describes the synthesis, modification and characterization of different zeolites, mesoporous alumina and Organo functionalized mesoporous alumina. It contains the hydrothermal synthesis zeolite, beta and ZSM-5 and reflux method synthesis of mesoporous materials. Organo functionalized mesoporous material has been synthesized by in-situ co-condensation of coupling agent with Organo-silane with required proportions. The modification of various synthesized as well as commercial zeolites in protonic H+ and RE+ forms is also included here. Characterization of these zeolites, and

mesoporous materials with various physico-chemical methods such as chemical analysis, XRD, FT-IR, elemental analysis, thermal studies, surface area measurements as well as acidity measurements using TPD of ammonia is also discussed. In addition the chapter includes procedure for the experimental set up for the evaluation of catalytic activity, product identification and product analysis.

Chapter 3 deals with the catalytic applications of the different zeolites for the liquid phase selective acylation reactions particularly in propionylation of phenol, chlorophenol and benzoylation of phenol.

The catalytic results indicated the advantages of Zeolite H-beta catalysts for the production of desired ring products (ortho and para) compared to the ZSM-5, RE-Y and H-Mordenite etc. The conventional catalyst, $AlCl_3$, is less active and selective in all the cases, under investigation. The higher activity of H-beta in the formation of 2-and 4- could be related to the presence of very strong acid sites than other zeolite catalysts. The higher yields of ring products (2- and 4-) could be achieved by increasing the values of reaction time, H-beta to PC ratio (wt./wt.) and reaction temperature. The H-beta was recycled and the decrease in yields of 2- and 4- was observed after each cycle in the acylation of phenol. The plausible reaction pathways for the formation of products were confirmed by the additional experiments such as Fries rearrangement of PP and propionylation of phenol with PP using zeolite H-beta as catalyst. The PP results from the rapid o-propionylation of phenol with PC, 2-HPP is produced through the intramolecular rearrangement of PP, propionylation of phenol with PP and direct C-propionylation of phenol with PC, 4-HPP is produced by the reaction of 4-PXPP with zeolite hydroxyl groups.

Chapter 4 deals with the alkylation reaction i.e. Benzylation of benzene.

It is demonstrated that the H-beta zeolite catalyses the benzylation of benzene with benzyl chloride efficiently, which leads to the formation of DPM in high selectivity compared to the other zeolite catalysts. The conventional homogeneous catalyst, $AlCl_3$, does not possess shape selectivity and favour the formation of large amount of polybenzylated products. A selectivity of the order of 89.1 wt. % to DPM is achieved at 33.3 wt. % conversion of BC over H- beta, whereas, $AlCl_3$ gave lower selectivity to DPM (58 wt. %) and higher amount of polyalkylated products (42 wt. %) under certain reaction conditions. The conversion, rate of BC conversion and product distribution largely depends on the experimental conditions. The conversion of BC increases with the increase in reaction time, catalyst concentration, reaction temperature and benzene to BC molar ratio, whereas it decreases with the increase in SiO_2/Al_2O_3 ratio of H-beta. Recycling of the catalyst progressively decreases the BC conversion. The presence of strong, as well as weak, acid sites in the zeolite catalysts appears to be very important for the polarization of the benzyl chloride into an electrophile ($C_6H_5CH_2^+$) which attack the benzene ring resulting in the formation of diphenylmethane.

Chapter 5 deals with the synthesis, characterization of mesoporous alumina and Mn and Co salen immobilized mesoporous alumina and their application in oxidation reactions.

The immobilization of manganese and cobalt complexes over mesoporous alumina, modified previously by 3-APTES, has been achieved by schiff base condensation reaction. Different characterizations techniques such as XRD, FT-IR,

TGDTG, UV-Vis and XPS reveal that the complex is attached firmly over the modified alumina surfaces. The molecular dispersion of the complex with sufficient space and hydrophobic surface are appropriate for activation of hydrocarbons as evidenced by the higher TON over immobilized catalysts in the selected epoxidation reactions. Moreover, these new catalysts did not leach its active sites during reactions and are reusable which indicates that the immobilization of neat complexes are effective by the present synthesis protocols over mesoporous alumina. Finally, the **CHAPTER SIX** summarizes all the major conclusions of the present study and the future outlook. The major theme of this study is to pave the way for other advanced industrial application by tuning and tailoring of different synthetic methodologies and catalytic reaction parameters.

LIST OF PUBLICATIONS AND PATENT

PAPERS

1 V. D. Chaube, P. Moreau, A. Finiels, A.V. Ramaswamy and A.P. Singh*

Propionylation of phenol to 4-hydroxypropiophenone over zeolite H-beta. **J.Mol. Catal. A Chemical** 174 (2001) 255 –264.

2 V. D. Chaube, P. Moreau, A. Finiels, A.V. Ramaswamy and A.P. Singh*

Novel single step synthesis of 4-hydroxybenzophenone (4-HBP) using zeolite H-beta. **Catal. Lett** 79,1-4(2002) 89-94

3 V. D. Chaube*

Benzylation of benzene to diphenylmethane using zeolite catalysts. **Cata. Commun.** 5 (2004) 321 – 326.

4 V. D. Chaube and A.P. Singh*

Synthesis and characterization and catalytic activity of Co (II) and Mn(III) salen Complexes immobilized over mesoporous alumina. **J. Mol. Catal. A: Chemical** 241 (2005) 79

5 V. D. Chaube and A.P. Singh*

Synthesis of 4-hydroxy 3-chloropropiophenone using zeolite H-beta. (**Communicated**).

6 S. R. Dhaga, Vandana D. Chaube, V. Ravi

Non-linear I-V characteristics of doped SnO_2. **Material Science & Engineering B** 110 (2004) 168-171.

7 S. R. Dhage, Vandana D. Chaube, Violet Samuel, V. Ravi.

Synthesis of Non-crystalline TiO_2 at 100°C. **Material lett**.*58 (2004)* 2310-2313.

PATENT

1 An improvement process for the production of Hydroxy Phenyl Ketones
U. S. Patent No. (Filed NCL- 32)

Conference Participated:

1. CATSYMP-15/IPCAT-2 held at National Chemical Laboratory, Pune India in Jan 2001. Presented poster on "Benzylation of benzene to diphenylmethane using zeolite catalysts,"
2. 4th National Symposium in chemistry held at National Chemical Laboratory, Pune India on Feb 2002. Presented a Poster Presentation on "Novel single step synthesis of 4-hydroxybenzophenone (4-HBP) using zeolite H-beta."
3. 'Catalysis: Concepts to practice' held from 26 to 27 June 2002 at National Chemical Laboratory, Pune India conference in honour of Dr. Paul Ratnaswamy on his 60th birth anniversary. Presented a poster entitle "Selective acylation of Phenol to 4-hydroxyphenylketons.
4. 'Catalysis Research in India-Some Highlights' held on 30th May 20003 at National Chemical Laboratory, Pune India. A symposium in honor of Dr. A. V. Ramaswamy on his 60th birth anniversary. Presented a poster on "selective acylation of aromatic using solid acid catalysts".
5. National Workshop on Catalysis: Forays into Non-traditional Areas (Catworkshop, 2000) the Catalysis Society of India. Held during 7-8 January 2000 at IICT, Hydrabad and achieved First Prize for the poster presentation on "Propionylation of phenol to 4-hydroxypropiophenone using zeolite catalyts".